Identifying Erosional Hotspots in Streams Along the North Shore of Lake Superior, Minnesota using High-Resolution Elevation and Soils Data

A Thesis
SUBMITTED TO THE FACULTY OF
UNIVERSITY OF MINNESOTA
BY

Molly J. Wick

IN PARTIAL FULFILLMENT OF THE REQUIREMENTS
FOR THE DEGREE OF
MASTER OF SCIENCE, Water Resource Science

Karen Gran

September 2013

Acknowledgements

The funding for this project came from the USGS through a grant from the Water Resources Center at the University of Minnesota. Thank you to the Department of Geological Sciences at University of Minnesota-Duluth for the teaching assistantship and additional summer and travel stipends that supported me through this thesis project.

I would like to extend my gratitude to my advisor Karen Gran for her support and assistance in the completion of this thesis. I would also like to thank my committee members, Rich Axler, George Host, and Stacey Starke, who helped me on many different aspects of this project. Thank you to Kirk Stueve for teaching me how to use Feature Analyst. Thank you to everyone who helped me in the field or on GIS work in the lab: Ryan Peterson, Tessa Schneider, Martin Bevis, and Dan Titze. I would also like to thank Jenny Jasperson, Martin Bevis, Grant Neitzel, and all the other graduate students who helped me think through different aspects of my thesis project. Lastly, I would also like to thank my parents, Norm and Diane, who have provided so much love and support me throughout my entire education.

Abstract

Many streams on the North Shore of Lake Superior, Minnesota, USA, are impaired for turbidity driven by excess fine sediment loading. The goal of this project was to develop a GIS-based model using new, openly-available, high-resolution remote datasets to predict erosional hotspots at a reach scale, based on three study watersheds: Amity Creek, the Talmadge River, and the French River. The ability to identify erosional hotspots, or locations that are highly susceptible to erosion, using remote data would be helpful for watershed managers in implementing practices to reduce turbidity in these streams.

Erosion in streams is a balance between driving forces, largely controlled by topography; and resisting forces, controlled by the materials that make up a channel's bed and banks. New high-resolution topography and soils datasets for the North Shore provide the opportunity to extract these driving and resisting forces from remote datasets and possibly predict erosion potential and identify erosional hotspots. We used 3-meter LiDAR-derived DEMs to calculate a stream power-based erosion index, to identify stream reaches with high radius of curvature, and to identify stream reaches proximal to high bluffs. We used the Soil Survey Geographic (SSURGO) Database to investigate changes in erodibility along the channel. Because bedrock exposure significantly limits erodibility, we investigated bedrock exposure using bedrock outcrop maps made available by the Minnesota Geological Survey (MGS, Hobbs, 2002; Hobbs, 2009), and by using a feature extraction tool to remotely map bedrock exposure using high-resolution air photos and LiDAR data.

Predictions based on remote data were compared with two datasets. Bank Erosion Hazard Index surveys, which are surveys designed to evaluate erosion susceptibility of banks, were collected along the three streams. In addition, a 500-year flood event during our field season gave us the opportunity to collect erosion data after a major event and validate our erosion hotspot predictions.

Regressions between predictors and field datasets indicate that the most significant variables are bedrock exposure, the stream power-based erosion index, and

bluff proximity. A logistic model developed using the three successful predictors for Amity Creek watershed was largely unsuccessful. A threshold-based model including the three successful predictors (stream power-based erosion index, bluff proximity, and bedrock exposure) was 70% accurate for predicting erosion hotspots along Amity Creek. The limited predictive power of the models stemmed in part from differences in locations of erosion hotspots in a single large-scale flood event and long-term erosion hotspots. The inability to predict site-specific characteristics like large woody debris or vegetation patterns makes predicting erosion hotspots in a given event very difficult. A field dataset including long-term erosion data may improve the model significantly. This model also requires high resolution bedrock exposure data which may limit its application to other North Shore streams.

Table of Contents

List of Tables

List of Figures

Introduction

Streams along the North Shore of Lake Superior drain the Arrowhead region of northeastern Minnesota and provide habitat for a wide range of animals, including the native brook trout. These streams are valued by locals and tourists alike for their natural beauty and recreational opportunities. However, several of these streams have been listed as impaired for turbidity according to section 303d of the EPA's Clean Water Act by the Minnesota Pollution Control Agency (MPCA). Elevated turbidity has been found to cause gill damage and reduce foraging success and growth rates in many fish types rates, including salmonids like trout (e.g. Weithman et al., 1977; Sigler et al., 1984; Barrett et al., 1992; Sweka & Hartman, 2001). In order to develop ways to deal with the impairment, an understanding of where fine sediment is derived is required.

Natural characteristics in the channel corridor such as topography, planform geometry, and bank and bed material can result in erosion hotspots. Erosion hotspots are segments of a stream that are highly susceptible to erosion and could contribute significantly to turbidity. These areas tend to facilitate geomorphic change in the stream over time and can shift through time. Hotspots can be of special concern since high banks or bluffs have the potential to contribute large amounts of sediment to the stream. Erosion hotspots in the channel corridor may be caused by natural characteristics alone, and may be exacerbated by land use trends or hydrologic changes caused by humans on the landscape. These areas are highly sensitive to future changes in hydrologic regime or land use. The ability to identify these hotspots and understand what causes them would be valuable for watershed managers in order to identify areas that would benefit from restoration or bank stabilization or protection efforts.

Because the most significant driver of erosion is water flowing over the landscape, if we have a good representation of the topography, we should be able to predict the locations of most erosion hotspots at a reach scale. New openly-available LiDAR data offer us the opportunity to test if we can predict erosion hotspots using remotely-collected data. LiDAR stands for light detection and ranging and is a form of remote sensing that provides a dense sampling of elevation points that can then be processed into bare earth digital elevation models (DEMs) of the landscape. The

collection of the high-resolution LiDAR data along the North Shore of Lake Superior in 2011 was part of a publicly-funded statewide initiative.

Along with topographic drivers of erosion, the resistance of the material at a given site determines if the site can erode or not. In North Shore watersheds, channel materials can range from erodible clay banks to nonerodible bedrock channels. Newly-released Soil Survey Geographic (SSURGO) Database soils data have erodiblity data at a much finer resolution than previous datasets provided.

The goal of this project was to develop a GIS-based model using these new, openly-available, high-resolution remote datasets to predict erosional hotspots at a reach scale. We used the LiDAR-derived DEMs, SSURGO data, and other bedrock exposure datasets, including remote bedrock exposure mapping techniques, to develop erosion potential predictors for three streams along the North Shore of Lake Superior. We validated our erosion potential predictions using field surveys, and evaluated the ability of these remote datasets to predict erosion potential remotely.

Background

What Controls Fluvial Erosion

Stream networks are dynamic systems that react to changes in the prevailing climate, geology, topography, vegetation, and base level. These changes result in channel adjustments such as changes to the geometry, slope, and dimensions of a stream. These can occur at a timescale of a single flood or over the course of thousands of years. Channel adjustments occur via erosion and deposition of sediment or incision into bedrock. The relative magnitude of the down-slope gravity force and the friction resisting down-slope motion determines if water has the ability to erode and move sediment. In other words, the ability of a stream to erode is a function of the stream power and the shear strength of the sediment. Stream power is defined as the rate of potential energy expenditure per unit length of channel (Knighton, 1984). Erosion by water action occurs primarily during peak flows, when stream power is greatest. The opposing frictional force depends on the erodibility of the sediment. In non-cohesive sediments, friction resistance to particle movement depends on the particle's size, shape, and density. In cohesive

sediments, the resistance to erosion also depends on the strength of the cohesive bonds between the particles. In order for erosion to occur, the down-slope force must be greater than the frictional force.

Sediment in streams can result from stream incision, bank erosion, or overland flow. Here, we focus on bank erosion because it is the dominant process providing sediment in North Shore streams (Nieber et al., 2008). Banks can be composed of bedrock, which has extremely low erodibility at the time scales of interest, or of sediments, which can be very erodible. Most bank cohesion is due to the presence of finer material, as well as vegetation, which both greatly reduce bank erodibility (e.g. Hickin, 1984; Abernathy & Rutherfurd, 2000; Easson & Yarbrough, 2002; Wynn & Mostaghimi, 2006).

There are three central bank erosion processes: frost action, slumping, and direct action of water. Frost action is an important factor for conditioning the banks for erosion by loosening cracks and disaggregating pore spaces. These processes lower the strength of the material and make it more susceptible to erosion (e.g. Walker and Arnborg, 1966, Gatto, 1995).

Slumping refers to the failures of banks by gravity-driven movement of blocks of sediment downslope. Slumps on stream banks are related to soil moisture conditions and the undercutting of the toe, or the lower bank, due to direct hydraulic action (Hooke, 1979; ASCE, 1998). Saturation of clays results in a reduction in cohesion, and can lead to slumping (e.g. Day and Axten, 1989). Cohesive banks are also particularly susceptible to sapping, or seepage and piping of water through the bank, which reduces the internal resistance of the material and can cause bank failure. Bank failures often occur after the peak flow has receded when banks are still saturated leading to high pore pressure (e.g. ASCE, 1998). Slumping can result in the delivery of a large amount of sediment to the stream at one time.

Direct hydraulic action refers to the direct erosion of the banks by flowing water and is a function of shear stress or stream power. However, because slumping and frost action are working in conjunction with hydraulic action, the amount of bank erosion is not a simple function of stream power. The effectiveness of these three processes all

depend on the saturation of the sediments, so repeated precipitation events and repeated peak flow events can be more effective at bank erosion than one peak flow event of greater magnitude (e.g. Knighton, 1973, Hooke, 1979). Because of the importance of repeat precipitation events and saturated sediments for bank erosion, on North Shore streams the greatest amount of erosion should occur during the spring and early summer when there are repeat precipitation events and peak flow events.

Typically lower banks are cut by hydraulic action while upper banks are eroded by slumping due to undercutting of the lower bank. In meander bends, secondary flow is directed towards the outer bank at the surface and towards the inner bank at the bed. This can result in undercutting of the bank at the water level (Knighton, 1998). The upper bank slump blocks can fall in front of the lower banks, temporarily prohibiting further undercutting until the blocks themselves are eroded away (e.g. Thorne & Tovey, 1981; Simon et al., 2003).

The processes described above can operate at multiple temporal scales. We are interested in the processes operating at the temporal scale that will contribute the most sediment to the stream and contribute to the most geomorphic change in a channel over time. The term "effective discharge" is used to describe a discharge that moves the largest amount of sediment over time and thus contributes most significantly to long-term geomorphic change. The effective discharge is a product of a high transport rate of the stream and a high frequency of occurrence, so the maximum amount of sediment is moved over time (Wolman and Miller, 1960). The effective discharge is the discharge that sets the channel geometry and channel size. This discharge is also referred to as the bankfull discharge, because it is approximated to be the discharge that fills the bankfull height (Wolman and Miller, 1960; Leopold and Wolman, 1957). The bankfull height is the height at which a stream begins to flood onto its floodplain.

The effective discharge is not the same for every stream. The ability to find an exact interval of an effective discharge, and what the value of that exact recurrence interval, is highly debated. Williams (1978) found that for 28 streams, the average recurrence interval for a bankfull discharge is 1.5 years. However, the bankfull discharge recurrence intervals for different streams ranged from 1 - 32 years, so there is wide

variability in the recurrence interval of the bankfull discharge from stream to stream. Generally, effective discharge is approximated to be a 1 to 2 year event unless information is available to suggest otherwise. (Knighton, 1998).

Predicting Erosion in North Shore Streams

Several streams along the North Shore have been listed by the Minnesota Pollution Control Agency as impaired for turbidity due to elevated sediment loads under Section 319 of the Clean Water Act: the Little Knife, Talmadge, Big Sucker, Poplar, Amity, Lester, Knife, French, and the Beaver (MPCA, 2012; Figure 1). To be removed from the impaired waters list, best management practices must be implemented to reduce turbidity or higher turbidity limits must be justified if natural causes are responsible for the high sediment loads in these systems. In order to do this, researchers model sediment inputs from various sources and conduct Total Maximum Daily Load (TMDL) studies. For example, Nieber et al. (2008) modeled and predicted relative sediment contributions to the main stem of the Knife River from bluff, bank and tributary sources and compared the predicted results to the observed results. These studies are time-intensive and require a great deal of background research and field data collection. On the other hand, an accurate GIS-based erosion potential model based on openly-available data could give resource managers the opportunity to learn more about watersheds easily and at little cost. These models can also help managers choose locations for detailed studies or for bank restoration or stabilization efforts.

As discussed above, there are many interdependent factors that determine if and where erosion occurs in streams. Historic and modern land use changes have impacted water quality in many North Shore streams. A better understanding of natural drivers of erosion in North Shore streams is necessary to distinguish natural effects from land use effects. Previous studies have hypothesized that land use is the central driver in water quality impairments in Lake Superior streams (Detenbeck et al., 2003, Detenbeck et al., 2004, Crouse, 2013). However, correlations between land use variables and turbidity and TSS measurements are poor, suggesting that it is not simply land use variables that drive high turbidity in North Shore streams (Crouse, 2013). We hypothesize that natural drivers

like topography, soils, and hydrology are the main variables that control erosion potential and sediment loads in North Shore streams, and land use change tends to exacerbate areas already prone to erosion based on natural drivers.

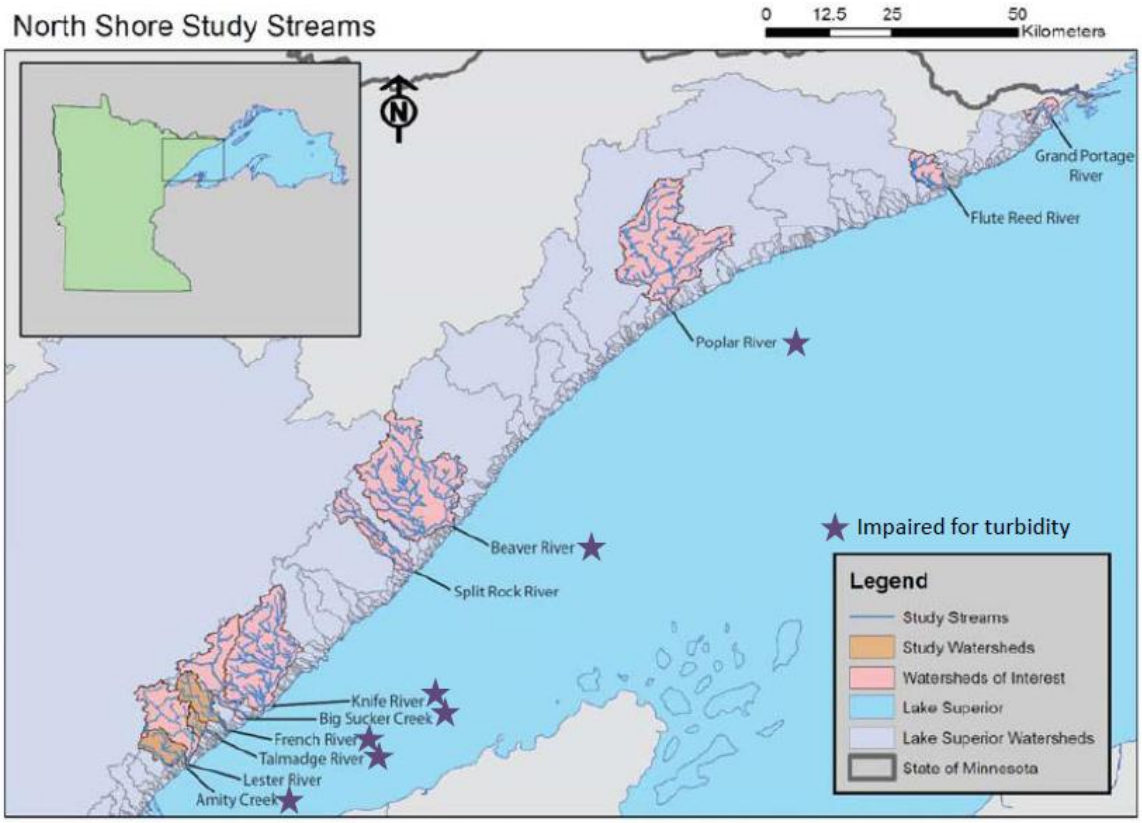

Figure 1. Map of North Shore watersheds of interest (yellow), and the study watersheds that we focus on in this thesis: Amity Creek, Talmadge River, and French River (pink). The inset shows the area shown in the main map relative to the state of Minnesota and Lake Superior. All of the streams and watersheds shown, except the Beaver River, were delineated using new 3-meter LiDAR data according to the methods described in this thesis. The Beaver River stream delineation shown here was derived from 1:24,000 scale USGS topographic maps.

Analysis of digital elevation models has previously proven to be useful in identifying areas with high rates of channel incision (e.g. Zeitler et al., 2001; Finlayson et al., 2002; Snyder et al., 2000). Gran et al. (2007) used GIS analysis of 30-meter DEMs to identify erosional hotspots at a reach scale in the Little Fork River in Northeastern Minnesota. Brown et al. (2011) used 10- and 20-meter Digital Elevation Models, along with STATSGO soils data and land use data to calculate an erosion index for Lake

Superior watersheds and subwatersheds. Their study was limited by the low resolution of the State Soil Geographic (STATSGO) database, which does not provide detailed soils information, and by the DEM resolution. In addition, neither study included validation of the erosion indices with field data.

The limitations of available datasets for topography and soils previously restricted the development of fine-scale erosion prediction models for North Shore streams. However, recently-released DEMs for the entire Arrowhead region of Minnesota have 3-meter resolution. These DEMs were produced using airborne LiDAR. Airborne LiDAR is collected by planes that fly swaths over the landscape. The survey hits the surface with up to 150,000 discreet laser pulses (or returns) per second. The returns are collected along with GPS positions. The product produced is a point cloud, which includes the returns generated at each surface the laser pulse encounters (e.g. canopy top, foliage, bare earth, etc). From the point cloud, several layers can be derived. The bare earth layer contains just the last returns, or the points that are representative of the landscape itself. The first returns contain the dataset representative of the top of the vegetation, or the first material that the laser pulse encounters. The airborne LiDAR for the Arrowhead Region in Minnesota was collected in spring 2011. The LiDAR datasets available for download from the Minnesota Geospatial Information Office include the point clouds, the bare earth layer, and the intensity, which is the amount of energy reflected for each return, and is representative of different types of surfaces (e.g. vegetation, concrete, water). The 3-meter resolution DEM is generated from the bare earth layer and corrected for errors.

Previously the only available digital soils data were in the STATSGO dataset, which has a large coverage extent but provides only low-resolution, aggregated data. The SSURGO dataset was recently released for St. Louis County. SSURGO is a soil survey that was based on County Soil Surveys by the Natural Resource Conservation Service (NRCS) and released at a 1:24,000 scale. For comparison, for the 41.7 km^2 Amity Creek watershed, the STATSGO dataset contains three distinct mapping units, while the SSURGO dataset contains 47.

The availability of these new datasets gives us the opportunity to develop a GIS model to identify erosional hotspots in North Shore Rivers. As discussed above, initiation

of erosion depends on having larger driving forces than resisting forces. We can derive information about both driving forces and resisting forces from these newly available datasets.

Stream power is a measure of a driving force, and is based on upstream area and channel slope. Elevated shear stress resulting from high stream power has been used previously to predict erosion potential in both bedrock and alluvial systems with success. Stream power was developed to model incision in bedrock systems (e.g. Sklar & Dietrich, 1998; Whipple and Tucker, 1999; Stock and Montgomery 1999; Finlayson et al., 2002), but it has also proven useful in alluvial systems to highlight areas with high erosion potential (e.g. Lecce, 1997, Talling and Sowter, 1998; Gran et al., 2007). Unit stream power (ω) is the product of the specific weight of water (density times gravity, or (ρ· g)), the slope (S) and the unit discharge (total discharge divided by channel width, or (Q/w)).

$$\omega \propto \rho g(Q/w)S \tag{1}$$

Some of the early work by Leopold and Maddock (1953) established important empirical hydraulic geometry relationships including that channel width varies as a power function of discharge, $w = c_1 Q^b$. Channel width is a function of sediment type (accounted for by c_1) and discharge, but in a stream with constant erodibility, the width is primarily a function of discharge (Knighton, 1974; Leopold and Maddock, 1953). Discharge itself varies linearly as a function of area (A), $Q = c_2 A$ (Leopold and Maddock, 1953). Because of these two relationships, we can substitute area for both Q and W. This gives a stream power-based erosion index (SP) in terms of drainage area:

$$SP = jA^{(1-b)}S \tag{2}$$

where j is a coefficient accounting for the specific weight of water and the coefficients c_1 and c_2, and incorporates the effects of varying bedrock and substrate erodibility. Because

the other parameters can be determined remotely from topography alone, we can use the high-resolution LiDAR data to calculate *SP* along the stream network.

Channel geometry should also influence erosion rates. Along the outside of meander bends, secondary flow vectors are directed towards the outer bank at the surface and towards the inner bank at the bed, resulting in increased shear stress and direct hydraulic action on the outer bank. This secondary flow along with the main downstream component of flow gives a downstream spiral motion to the overall flow. Nanson and Hickin (1986) studied channel migration rate along meander bends on 18 rivers. They compared migration rates to bend curvature, which is defined as the radius of curvature divided by the channel width. They found maximum channel migration rates at a bend curvature of 2 to 3, above and below which migration rates decreased. However, Furbish (1988, 1991) found that migration rates increase continually as bend curvature decreases when bend length is accounted for. At bend curvatures below 2 - 3, the force on the bank itself may be reduced resulting in lower shear stress and slower migration rates (Begin, 1981). The maximum boundary shear stress, and thus maximum erosion rate in a bend, tends to be located on the outer bank just downstream of the apex of the meander (Knighton, 1998).

In order to identify areas that might have elevated shear stress, and thus elevated erosion potential, related to bend curvature, we can use the channel networks delineated from high-resolution LiDAR data to calculate an angle of impingement. When channel width is constant, then the angle of impingement is a proxy for bend curvature with high values of angle of impingement wherever the bend curvature is low. Angle of impingement (*AOI*) is calculated as:

$$AOI(a_i) = | Va_{i-1} - Va_i | \quad (3)$$

where Va_i is the vector direction of the main channel at point *i.* Angle of impingement approximates areas in streams where the radius of curvature is low and thus migration rates and erosion rates should be higher, but is highly dependent on the "ruler" length used, or the distance between points a_i and a_{i-1} (see Discussion).

Initiation of erosion depends also on the resisting forces, or how erodible the substrate is. In bedrock channels, the substrate has very low erodibility, so erosion potential would be expected to be very low. For streams that flow through sediments like glacial till or alluvium, erodibility can be much greater. We can account for erodibility of the channel using the SSURGO dataset, which includes the K factor, the erodibility factor from the Revised Universal Soil Loss equation (RUSLE). K factor data incorporate characteristics such as texture, structure, organic matter, and permeability of the soil. The K factor is a rating of the susceptibility of soil particles to be removed and transported away by water, and ranges from 0.01 to 0.55 (Renard et al., 1991). K factor values only apply to soils, and do not include data on bedrock erodibility. The SSURGO dataset does not include depth to bedrock or locations of bedrock outcrops. Given the importance of bedrock outcrops on erosion, we used other data sources to identify the locations of bedrock outcrops along the river corridor. One source that is available over the lower end of most of the rivers along the North Shore comes from Minnesota Geological Survey (MGS) geological and surficical geology maps that contain generalized outcrop exposure locations (Hobbs, 2002; Hobbs 2009). Alternatively, we can use high-resolution LiDAR data and air photo data in GIS to identify repeated patterns and map bedrock exposure remotely.

The balance of driving forces and resisting forces determines if hydraulic action will result in bank erosion or not. If erosion is initiated, some areas may contribute significantly more sediment than others due to the physical characteristics. If a bluff composed of sediment is present and the stream interacts with it during a high flow event, undercutting can occur, resulting in slumping or in some cases complete scouring of the bluff. In North Shore streams, these bluffs can be terraces or valley walls, and if they erode, they contribute significant amounts of sediment to the stream (Neitzel, in prep). We account for bluff erosion by using 3-meter DEMs to delineate high bluffs proximal to the stream network.

Using the five predictors discussed above: stream power-based erosion index, angle of impingement, K factor, bedrock exposure, and bluff proximity, we developed a GIS-based model to identify erosion hotspots on North Shore streams. We developed our

model using primarily the Amity Creek Watershed, but also completed GIS analyses on the Talmadge River and French River watersheds (See Figure 2). We collected field data on these watersheds to validate our erosion potential predictions. This thesis presents the results of our GIS-based erosion potential predictive model, and field validation thereof, and a discussion of the benefits and limitations of using these high-resolution remote datasets to predict erosion potential along the North Shore of Lake Superior.

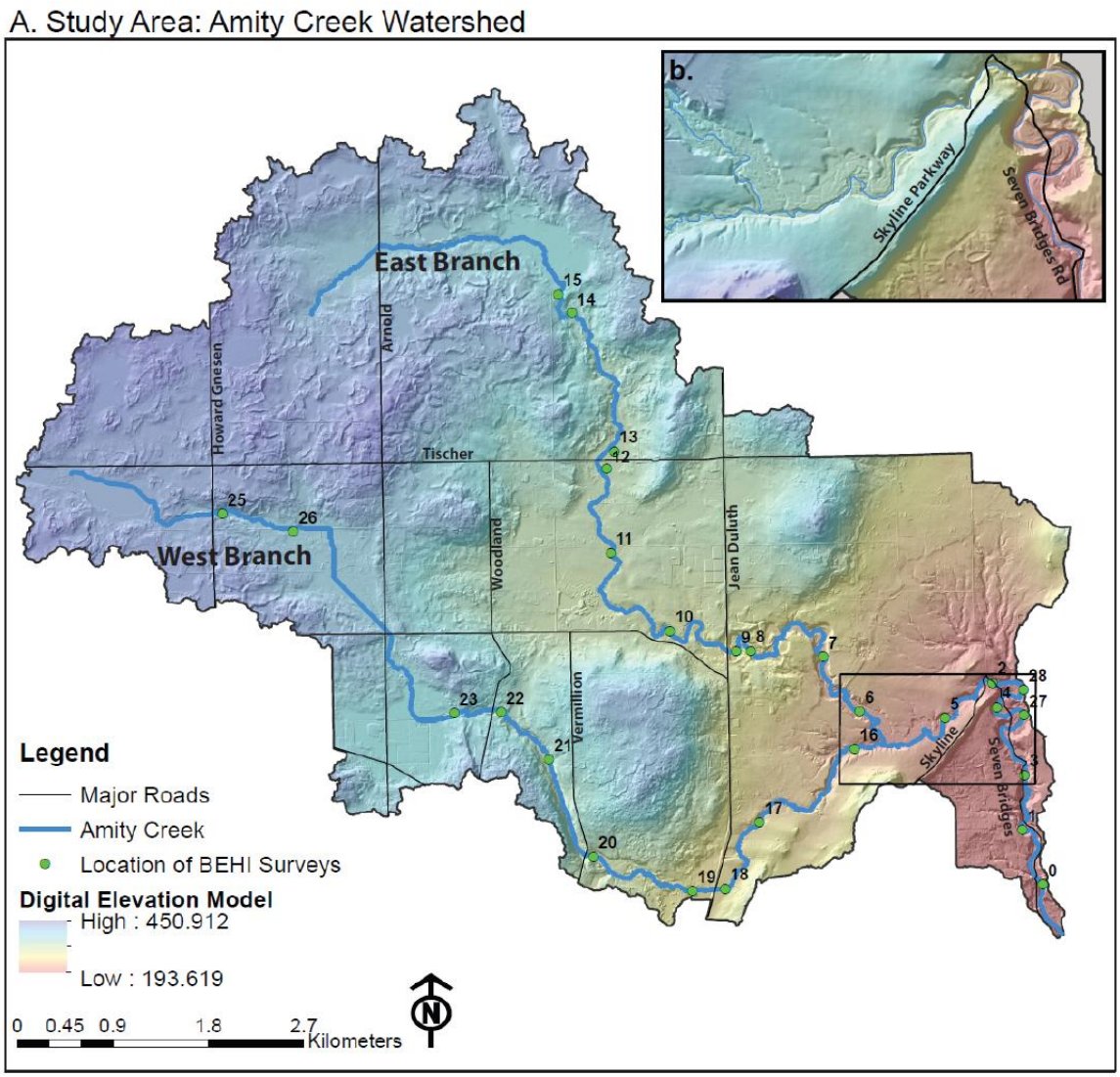

Figure 2. Study watersheds. A. Amity Creek Watershed. Network shown has an accumulation threshold of 100,000 m^2 and was delineated using ArcMap tools as described in the methods. Green points are locations of the Bank Erosion Hazard Index (BEHI) surveys. The outlined box denotes the area shown in Figure 5. Figure is continued on next page.

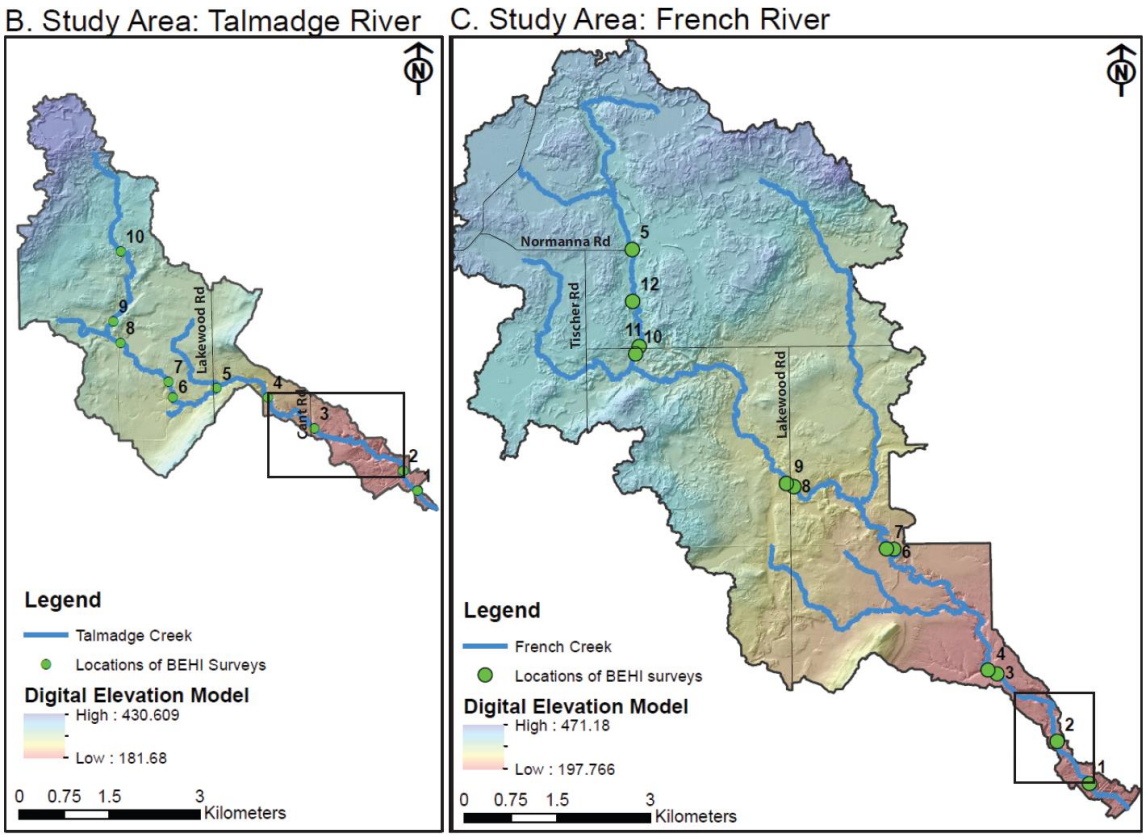

Figure 2, ctd. Three study watersheds. B. Talmadge River Watershed. C. French River Watershed. Networks shown have an accumulation threshold of 100,000 km^2 and were delineated using ArcMap tools as described in the methods. Green points are locations of the Bank Erosion Hazard Index (BEHI) surveys. The boxes outlined in each watershed denote the areas shown in Figures 6 and 7.

Study Area

Characteristics of North Shore Watersheds

Watershed and site characteristics can influence bank erosion, and are intimately linked with the geologic history of an area. In North Shore streams, the surficial and bedrock geologic history have a large impact on the location of sediment sources. That geologic history starts when the Lake Superior Basin was created 1.1 billion years ago by a Midcontinent Rift system. The bedrock geology along the North Shore of Lake Superior is predominantly stacked basalt flows and igneous intrusions formed during the Midcontinent Rift (Sims & Morey, 1972). These are the dominant rock units that outcrop

along many streams today, with stacked lava flows sometimes creating steps in the river long profiles.

During the last glacial maximum about 18,000 years ago, the Superior Lobe of the Laurentide ice sheet occupied the Lake Superior basin and extended to the southwest as far as the St. Croix terminal moraine in southeastern Minnesota, depositing clay-rich glacial tills in its path (Wright, 1971). This clay-rich glacial till forms many of the banks of North Shore streams that are not bedrock or alluvium. By 11,500 years ago, the Superior Lobe was retreating to the northeast and glacial Lake Duluth had formed from meltwater in the Lake Superior basin (Wright, 1971). Glacial Lake Duluth, which at its highest level reached to 335 meters (1100 feet) above sea level, deposited red lacustrine sediments along its bed, found today in a narrow band along the shores of Lake Superior. During the highest levels of glacial Lake Duluth, the lake interacted with and reworked the glacial tills that were deposited by the ice sheet. Glacial Lake Duluth drained to the south until the Superior Lobe retreated far enough for the lake to drain to the east, about 9500 years ago (Wright, 1971; Farrand, 1969). After the lake was able to drain to the east through Sault St. Marie, the lake level in glacial Lake Duluth fell to its minimum level of ~122 meters (400 feet) above sea level (Farrand, 1969). Subsequent to the retreat of the Laurentide ice sheet, isostatic uplift of the North Shore began, and continues to take place today (Farrand, 1969). This uplift caused a rise in lake level of the glacial lake to the present-day level of Lake Superior at 183 meters (601 feet) above sea level, which it reached about 5000 years ago (Farrand, 1969). This is the current base level for North Shore streams.

North Shore streams have similar fluvial environments to those found in typical mountain streams, including similar reach classifications, slope regimes, and bed roughness. Mountain streams typically have steep headwaters flowing over bedrock or cascade reaches with boulder-sized sediment. As they flow downstream, slope is reduced and streams form step-pool or plane-bed channels with boulder, cobble, and gravel beds. Further downstream, slopes continue to decline and pool-riffle channels form with gravel beds, then sandy dune-riffle channels (Montgomery & Buffington, 1998). In these streams, the sediment size, slope, and valley confinement are continually decreasing.

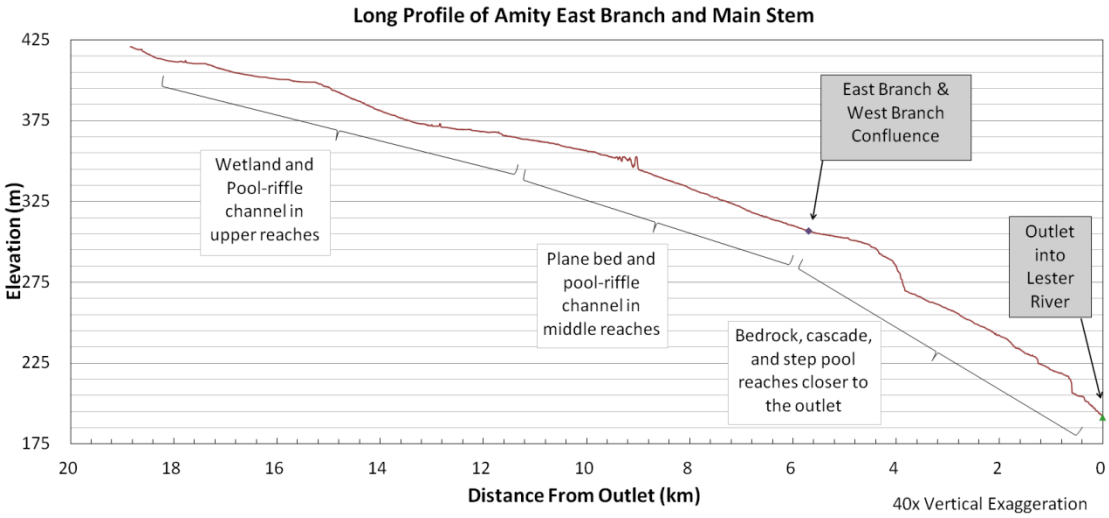

Figure 3. Annotated longitudinal profile of Amity Creek. As is typical of North Shore streams, the long profile has a concave-down shape, with increasing slope towards the outlet.

However, North Shore streams have fundamentally different long profiles from typical mountain streams. Isostatic rebound from the most recent glaciation, which continues today, is fastest where the ice was thickest to the north. This rebound causes the land surface to tip up to the north, and forces water towards the south shore of Lake Superior. This rebound has resulted in a very slow but continual drop in base level for North Shore streams and continuing incision of those streams. North Shore streams have long profiles that are typically flat near the headwaters, steepening closer to the outlet (See Figure 3). Fitzpatrick et al. (2006) studied the geomorphology of Duluth-area streams in particular. While Duluth-area stream watersheds are in general more urbanized than streams further up the shore, most North Shore streams follow a similar geomorphic pattern, which is shown for Amity Creek in an annotated long profile in Figure 3. As Duluth streams flow towards Lake Superior, they typically begin in flat, wetland channels that run through glacial till. They then steepen towards the lake, encountering pool-riffle and plane-bed channels. In the Lester River for example, this is the area where tributaries begin delivering more significant amounts of sediment into the main stem, and Fitzpatrick et al. (2006) found evidence for valley side failure, landslides, and bank erosion. Close to Lake Superior, channels typically steepen further and transition into step-pool, cascade and bedrock reaches (Fitzpatrick et al, 2006).

Overall, the most important drivers for erosion in North Shore streams appear to be the erodibility of the channel material (bedrock, lacustrine sediments, or clay till), and the location within the network, which determines the slope, stream power, and the valley confinement, or how much the stream interacts with the valley walls. In Duluth-area streams, Fitzpatrick et al. (2006) concluded that the highest potential for erosion in these streams occurs in main-stem at the contact of glacial sediments and bedrock, because they have narrow valleys, moderate slopes and clay banks. These are the drivers that we consider in detail in our study.

Other watershed characteristics that affect the hydrology of the stream and thus affect in-channel erosion, albeit in a secondary way, include upland vegetation type and storage capacity. Although upland vegetation can affect how much sediment is delivered to the stream via overland flow, it also affects the amount of water that reaches the channel network, thereby affecting peak flows and the hydrologic regime of the stream. Detenbeck et al. (2004) found that for both second- and third-order streams along the North Shore, higher turbidity is correlated with areas with less than 50% mature forest coverage. Likewise, upland storage capacity can also affect peak flows (Detenbeck et al. 2004). Along reaches with large amounts of storage capacity upstream, despite other factors, erosion may be reduced due to the reduced flows and therefore reduced stream power.

Other land use changes can also influence sediment loads. Alterations to flow direction and intensity like storm drains and ditches can concentrate flow and deliver sediment more quickly to a stream, especially if water is concentrated in areas with steep slopes and erodible soils. Logging or removal of forest cover can lower evapotranspiration, increase surface runoff and increase the size of floods (Verry, 1987). Impervious surfaces such as roads, parking lots, or roofs increase the surface runoff and aid in the delivery of sediment to rivers. Research done for the process of determining the Total Maximum Daily Load (TMDL) for the Poplar River on the North Shore identified eight different sources of sediment: channel incision; bluff erosion on a feature known as “the megaslump”; other landslides; golf courses; developed areas; ski runs, trails and roads; forest; and gullies/ravines. Among these, the largest contributors to the sediment

load were the megaslump; and ski runs, trails, and roads (Hansen et al., 2001). Overall, development in this watershed contributed 36% of the sediment load, while natural sources contributed 64%, showing the potential effects development can have on sediment loads (Hansen et al., 2010).

While land use trends like vegetation cover, storm drains and ditching, and impervious surfaces are no doubt significant contributors to stream turbidity, here, we focus on natural drivers of erosion in the channel corridor to identify topographically-driven erosion hotspots that might be exacerbated by land use change.

Individual storm events may provide insight into potential long-term erosion hotspots in North Shore streams. Erosion in an individual flood may be influenced by additional variables besides the general hydrologic regime and surficial geology of the watershed, like fine-scale vegetation patchiness and large woody debris (LWD). However, in a large-scale flood event, all erosion hotspots would be expected to erode. The Duluth area experienced such an event June 19 – 20th, 2012, when the region received 6 – 10 inches of rain within a 24 hour period (Huttner, 2012). Duluth streams are very "flashy", meaning water levels in Duluth streams rose very quickly and then fell very rapidly after the event. Many stream gages were lost during the event, but peak discharge rates have been estimated for several area streams based on flow observations. Peak discharge at the Knife River gauge near Two Harbors, Minnesota, was estimated to be 25,000 ft^3/s, over three times larger than the previous peak flow record, 7,440 ft^3/s, set May 10, 1979 (Czuba et al., 2012). The recurrence interval of the flood, calculated based on five area stream gauges including the Knife River gauge, was greater than 500 years (Czuba et al., 2012). The flood resulted in substantial geomorphic changes to Duluth streams. Erosion during the flood event was likely also influenced by rain events prior to June 19 that resulted in saturated soils and high pore pressure leading to bank failure. The historic flood event offered us the opportunity to collect post-storm data on erosion that actually occurred in a large event, and compare it to erosion predictions.

Methods: Developing Erosion Potential Predictor Variables

Data Sources

The primary data used in this project are DEMs derived from LiDAR data and provided by the Minnesota Geospatial Information Office. These DEMs are currently available in 1.5-meter resolution for the Duluth area and 3-meter resolution for the entire Arrowhead region. Our analyses were completed using the 3-meter DEMs because these are available for the entire North Shore. This dataset was collected May 3 - June 2, 2011. The LiDAR data were tested to meet a vertical accuracy of 50 mm Root Mean Squared Error (RMSE).

SSURGO soils data are made available by the NRCS Soil Data Mart. The dataset consists of digital soil surveys completed by the NRCS, and include individual map units of aggregated soils data at a 1:24,000 scale. The dataset includes information like available water capacity, soil reaction, electrical conductivity, frequency of flooding, cropland, rangeland, pastureland, and woodland yields, and information about site development and engineering uses. The accuracy of map unit boundaries varies based on boundaries observed in the field, but is generally within ±6 meters. The SSURGO soils data are currently available for St. Louis County, but not yet available for Lake and Cook counties. Because they were available for the three main watersheds of interest, we used them here to investigate soil erodibility.

In order to map bedrock exposure, we used The National Map Large Scale Imagery Overlay air photos from the U.S. Geological Survey National Geospatial Program. These are 0.3-meter 4-band orthoimagery collected in spring 2009 and available for download at the USGS National Map Viewer (http://viewer.nationalmap.gov/viewer/). For comparison, we also used bedrock outcrop maps that are available at 1:24,000 for the Duluth, French River, and Lakewood Quadrangle surficial geology maps as a part of the supplementary GIS files on the Minnesota Geological Survey (MGS) website (Hobbs, 2002; Hobbs, 2009).

We used the Minnesota DNR 24K Stream file for comparison during channel delineation. These data are derived from USGS 1:24,000 scale topographic maps, and are

available for download at the Minnesota DNR Data Deli (http://deli.dnr.state.mn.us/data_search.html).

Defining stream network and delineating watersheds

Because the focus of this project was bank erosion, producing an accurate stream network was imperative. Currently-available stream network layers, like the DNR 100K and DNR 24K stream files, are not highly accurate as they were defined based on USGS 1:100,000 scale and 1:24,000 scale topographic maps instead of high-resolution LiDAR-derived DEMs. To create a more accurate stream network, we delineated channel networks from the 3-meter DEMs. Because DEMs show the elevation of the surface and are not three-dimensional, pixels at bridges and culverts typically are assigned the elevation of the top of the bridge and not the stream itself. During QA/QC, some large bridges are "burned", which means the elevations at large bridges are replaced with the elevation of the stream below it, prior to release to the public. However the majority of road crossings and bridges are not corrected. During automated stream network delineation, flow routes are determined by routing flow down slope and identifying the amount of area that is upstream (referred to as flow accumulation) of each pixel. When the flow reaches a road crossing, it becomes a barrier to the flow, or a "digital dam", and results in the delineation of an erroneous stream network.

In order to correct for this problem, we tried two methods. We used the Hydrology toolbox in ArcMap, as well as a program called GeoNet (Passalacqua et al., 2010a,b). In order to use the Hydrology toolbox in ArcMap, road crossings must be manually burned to prevent errors in network extraction, which can be time consuming and requires multiple iterations until an acceptable network is produced. Alternatively, we can use GeoNet, which is run in MatLab. GeoNet uses nonlinear filtering to remove noise in low-gradient areas while enhancing edges in high-gradient areas. Ideally, filtering smoothes out potential flow barriers such as road crossings and prevents errors in network extraction due to the nature of the high-resolution data. GeoNet then extracts the channel based on the flow accumulation and curvature.

We used both the GeoNet and ArcMap methods for delineating the Amity Creek watershed and got similar resultant networks. Errors in delineated networks were identified by comparing the produced networks to the DEM and DEM hillshade layers and to high-resolution air photos. Both networks were significantly more accurate than the DNR stream files, however they both contained errors in the very flat upper reaches of stream networks. The ArcMap-generated network was more accurate in lower reaches. Figure 4 shows an area along the East Branch of Amity that illustrates the difference between the two networks. The ArcMap network follows the actual meanders very closely while the GeoNet network cuts off meanders. In addition we found the ArcMap Hydrology toolbox to be more user-friendly. GeoNet required a significant amount of computing power and time to run. Therefore we delineated all further networks using the ArcMap hydrology toolbox, using an accumulation threshold of 100,000 m^3 to define the headwaters. Errors in the network were corrected only if essential for the identification of erosion hotspots. For example, if errors were located in upper reaches and wetlands where erosion potential is known to be low or where the stream is intermittent, they were disregarded.

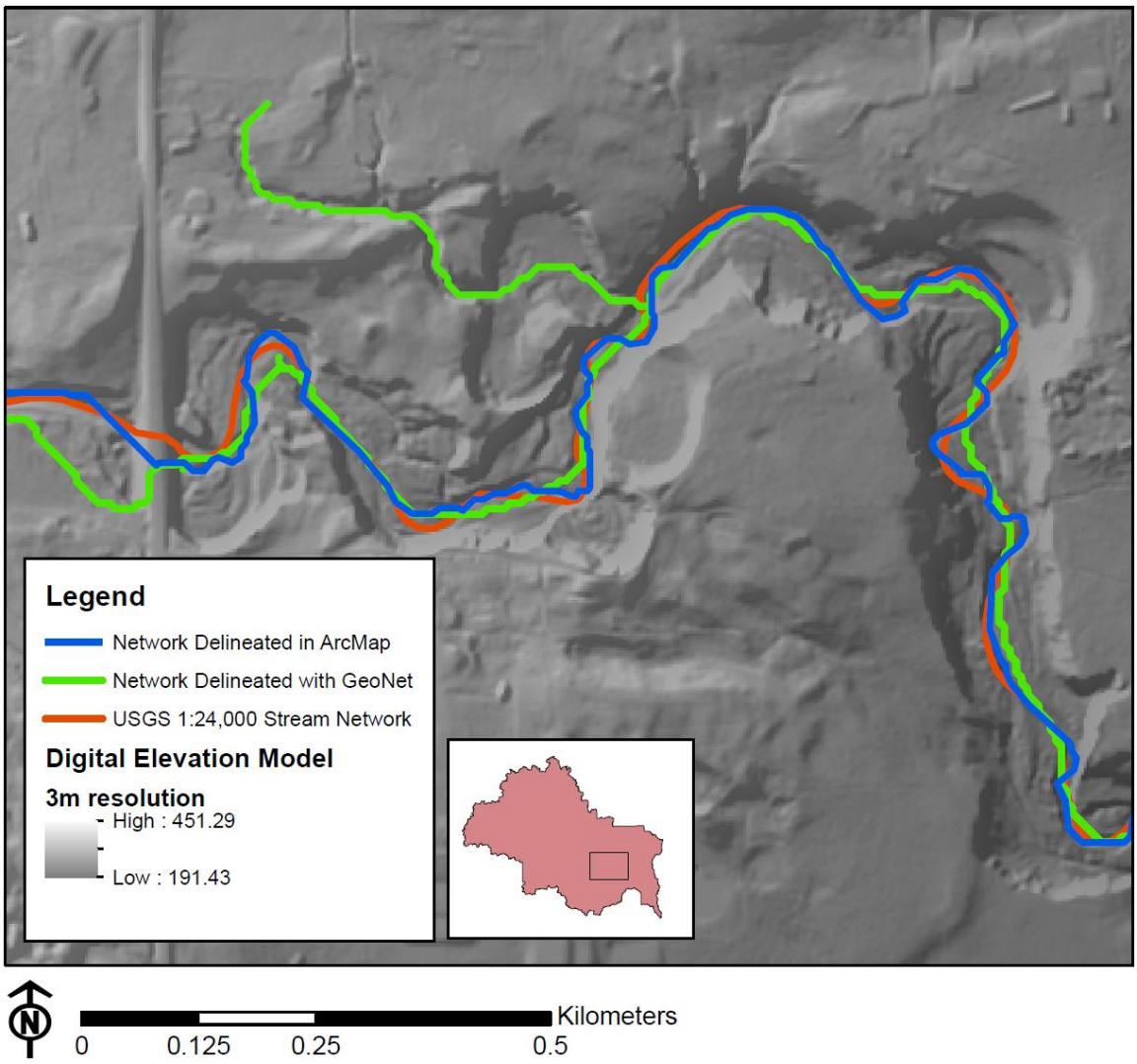

Figure 4. Comparison of GeoNet-derived and ArcMap-derived stream networks, along the East Branch of Amity Creek. Channel heads for the ArcMap network are defined by a thresholds for accumulation (100,000 m^3), and for the GeoNet network, channels are defined by a cost function based on curvature and accumulation (Passalacqua et al., 2009).

Predictor Variable Development

After the stream network and watershed were delineated, spatial analyses were conducted in ArcGIS. We completed five predictor analyses: the stream power-based erosion index, angle of impingement, bluff proximity, soil erodibility from SSURGO, and bedrock exposure. The rationale and basis for each analysis is described above, while detailed methods are described here. Detailed procedures for the analyses described below are located in Appendix A.

We calculated the stream power-based erosion index using equation (2) described above: $SP = jA^{(1-b)}S$. Although we have both till and bedrock in these channels, we assign a constant value to *j*, because we account for differences in erodibility separately, using the SSURGO dataset and bedrock exposure mapping. The value *b*, the exponent in the width-discharge relation, was assigned a value of 0.5. Width-discharge relationships in North Shore streams are poor, but Leopold & Maddock (1953) found that 0.5 was appropriate in alluvial channels, and Montgomery & Gran (2001) found values of 0.3 – 0.5 are appropriate for bedrock channels. We extracted elevation data every 25 meters on Amity Creek, the Talmadge River, and the French River. These data were then used to calculate the average slope over 100 meter reaches on all streams. The upstream area at each point along the streams was extracted from the flow accumulation raster created using the Hydrology toolbox.

In order to identify high bluffs along streams, we used the LiDAR data to delineate two bluff heights. To do this, we used the focal statistics tool in ArcMap using the "range" function, which used a 4-cell by 4-cell moving window to calculate relief. Because the resolution of the DEM is 3 meters, this means the window was 12 meters by 12 meters. We then identified areas with relief greater than 4 meters, and areas with relief greater than 2 meters. We then identified the bluffs along the stream that were within a 14-meter buffer of the channel. The channel itself is typically less than 7 meter wide, so this analysis identifies all bluffs within twice a channel-width from the stream centerline. During bankfull, the stream would interact with these bluffs.

Using the delineated stream network as a centerline, we used the Planform Statistics Toolbox (Lauer, 2006) to calculate angle of impingement. The angle of impingement was calculated according to equation (3) above. We tested ruler lengths of 5 meters, 10 meters, 20 meters, and 30 meters. The longer the ruler length is, the more likely it is that very tight bends fall in between points and go unidentified (see discussion). Therefore, we chose to use a ruler length of 5 meters in our analyses unless stated otherwise. We then converted this to a raster file to sample at the prediction points.

We investigated soil erodibility using K factor, the erodibility factor from the Revised Universal Soil Loss Equation. K values are reported in the SSURGO dataset for

each horizon in each map unit. We extracted the values for K at the prediction points along stream networks, using the K value of the major component, for all soil horizons.

To identify bedrock exposure, we used three datasets. First, we used bedrock outcrop data that are part of MGS bedrock and surficial geology maps for both Amity Creek and Talmadge River watersheds. For comparison, we also used a manually-digitized bedrock exposure file based on our own field data (referred to as the manual bedrock map). Lastly, we mapped bedrock exposure remotely for Amity Creek using the Feature Analyst extension for ArcGIS, distributed by Visual Learning Systems Inc. The user inputs "training" polygons that the tool uses to identify areas with similar patterns based on input datasets. Typically, training polygons are drawn by the user based solely on visual inspection of remote data. Because of the limits of our datasets (see Discussion), we used records of outcrop exposure from our field data as well as MGS outcrop maps to verify outcrop locations for our training polygons. We mapped bedrock within a stream corridor of 300 meters wide, and ran the program only on Amity Creek below Jean Duluth Road, as we know that bedrock outcrop interaction with the creek is very limited along the creek upstream of Jean Duluth Road (Figure 2). The input datasets included 4-band air photos (0.3m resolution, obtained from the USGS); LiDAR first returns (vegetation height), last returns (bare earth), and intensity (all 1m resolution); and the Normalized Difference Vegetation Index (NDVI). The NDVI is calculated as (Band 4 - Band 3)/(Band 4 + Band 3), where Band 4 is the near-infrared region and Band 3 is the visible region (red).

We obtained the LiDAR point cloud data from the Minnesota Geospatial Information Office, and the LiDAR Analyst tool (also distributed by Visual Learning Systems Inc.) to calculate first returns, last returns and intensity from the point cloud data. After the Feature Analyst identifies similar polygons to the training polygons, the user then inputs correctly and incorrectly identified polygons and reiterates the program, until a satisfactory map is produced.

Methods: Field Surveys

Field work was completed during the summer of 2012. We completed Bank Erosion Hazard Index (BEHI) surveys and Field Erosion Index (FEI) surveys in order to validate our erosion potential predictions. BEHI survey sites were completed along Amity, Talmadge and French main stems throughout the stream network. Field Erosion Index surveys were conducted on Amity Creek and the Talmadge River on a range of different channel types covering approximately the lower third of the main stem channels in each watershed. FEI surveys were conducted after the June 2012 flood while BEHI surveys were conducted both before and after the flood event.

Bank Erosion Hazard Index Surveys

Bank Erosion Hazard Index (BEHI) surveys are a pre-established protocol for assessing erosion potential, giving a rating of very low to extreme bank erosion hazard, for each bank (Pfankuch, 1975, see Table 1). These surveys are commonly used in state and federal protocols (e.g. Clar et al., 1999; Hansen et al., 2010; Van Eps et al., 2004). The survey is based on field observations of the near-channel zone, including bank height, material, angle, channel area, and signs of erosion. We used a modified BEHI survey, adding a component to account for stream interaction with till valley walls. Details of the calculation of BEHI scores are described in Appendix B. BEHI surveys were completed on main stems only. We completed 28 sites on Amity Creek, 10 sites on the Talmadge River, and 12 sites on the French River. The sites are all located in the lower non-wetland reaches of the main stems. This corresponds to approximately 1 site per km of stream for Amity Creek and the Talmadge River and 1 site every 2 km for the French River. Site locations were chosen based on accessibility. Typically they were located 100m upstream or downstream of road crossings, in order to facilitate access but also prevent influence from bridges or culverts. For the Talmadge and French Rivers, these surveys were completed following the June 2012 flood (See Study Area), however on Amity Creek, surveys at 17 sites were completed before the flood and surveys at 11 sites were completed after the flood.

Table 1: Field Survey Scoring Systems for Estimating Erosion

Field Erosion Index (FEI)		**Bank Erosion Hazard Index (BEHI)**		
Score	Description	Score	Level	Description
0	Bedrock, Little or No Erosion	<10.15	1	Very Low
1	Little or No Erosion	10.15 - 20.65	2	Low
2	Bank Erosion/Undercutting, one bank	20.65 - 34.65	3	Moderate
3	Bank Erosion/Undercutting, both banks	34.65 - 48.65	4	High
4	Slump, one bank	48.65 - 59.50	5	Very High
5	Slump, both banks, or on bank >4m	59.50 - 70	6	Extreme
6	Complete scour, one bank			
7	Complete scour, both banks, or one bank > 4m			

FEI Surveys

We completed what we called Field Erosion Index surveys (FEI) to evaluate erosion after the June 2012 flood and help assess the validity of our predictive model. The June 2012 flood caused extensive geomorphic change and erosion along North Shore streams. We assumed that the degree of erosion that occurred during this flood should be proportional to the erosion potential along the streams during a typical annual flood. We created a protocol for these surveys based on the rating system shown in Table 1. Values of 0 denoted bedrock exposure and indicate erosion potential is very low. Because we recorded values of 0 as bedrock, the FEI surveys included the data we needed to create the manual bedrock exposure map. Values of 1 indicate little to no erosion in reaches with sediment banks. Higher values indicate increasingly erosion. We walked the streams and used the rating system to collect a running assessment of field erosion due to the flood event based on field observations. On Amity Creek, we completed these FEI surveys from the outlet (the confluence with Lester River) to Jean Duluth Road, 3.35 km upstream of confluence on East Branch and 3.08 km upstream of confluence on West Branch (Figure 2). On the Talmadge, we completed the surveys from the outlet at Lake Superior to Lakewood Road (5.48 km upstream from outlet, Figure 2). For each stream, the survey included a range of FEI values, from very high at tall, scoured bluffs to little or no erosion on bedrock and wetland reaches.

Methods: Development of Predictive Model

Logistic Model

In order to identify which variables are statistically significant predictors for erosion potential, we used JMP software (SAS Institute, Inc.) to fit our predictor variables and our FEI data with linear regressions. We also fit linear regressions to the predictor variables and the BEHI field data. For each regression we calculated r^2 values to understand how well the regression fit the data, and p-values to know the level of significance of each regression.

We then developed a nominal logistic model to predict the probability of erosion along Amity Creek using the significant variables identified in the linear regressions. We fit the model using JMP software. A nominal logistic model fits nominal *Y* responses to a linear model of *X* predictors. The model fits probabilities (*P*) for the response levels (r_1 and r_2), in this case FEI ≥ 2 (erosion) or FEI <2 (no erosion), using a logistic function:

$$P(Y = r_1) = (1 + e^{-Xb})^{-1} \quad (4)$$

where *b* is a coefficient for each predictor. The model can then be used as a measure of erosion potential.

We tested a range of predictors (*X*) in the model including the predictors that were identified as significant in our single variable linear regressions. The predictor variables tested were: *SP*; log *SP*; proximity to 2 meter and 4 meter bluffs; a bluff index (defined below); angle of impingement with a ruler length of 5 meters, 10 meters, 20 meters, and 30 meters; angle of impingement scaled to *SP*; and points adjacent to bedrock including the Feature Analyst bedrock exposure, the MGS bedrock exposure, and the manual bedrock exposure maps in the model. The bluff index assigns a value of 5 to each point if it is within 7 meters of a 2 meter or taller bluff, and a value of 10 to each point if it is within 7 meters of a 4 meter or taller bluff, and was calculated because the individual bluff proximity predictors alone were not significant in the model. We applied the logistic model to the entire Amity Creek dataset, as well as to subdatasets including just data from the main stem, West Branch, and East Branch of Amity Creek. Below we show the

most successful model based on significant predictors with high r^2 values for Amity's entire stream dataset.

Threshold Model

The major limitation of the logistic model is its inability to incorporate specific knowledge of stream processes. For example, it is difficult to incorporate the fact that if bedrock is present, then other factors do not matter because the erodibility is so low that essentially no erosion occurs. An alternative approach is to develop a predictive model based on our qualitative understanding of the physical processes occurring in the streams. We can define thresholds in our predictors above which a given reach is more prone to erode. We know that above a certain threshold of *SP*, the critical shear stress is high enough to entrain and transport sediment. We also know that reaches that interact with tall, erodible bluffs can contribute significant fine sediment to the stream. And lastly, we know that regardless of *SP* or bluff proximity, bedrock channels have very low erodibility, so they will not be erosion hotspots. In a threshold-based model, we can set a threshold for *SP*, include only reaches that interact with tall bluffs, and exclude all bedrock reaches from hotspot predictions. In this way, the true meaning of each predictor can be incorporated in the model, unlike with the logistic model.

We developed a threshold-based model for Amity creek using three significant predictors (See Results) and FEI data. Reaches that have values above the threshold for each predictor are identified as erosion hotspots. In order to develop this model, we first ran single-predictor models, or models with only one predictor. The first single-predictor model was for *SP*. We ran the model several times, each with a different threshold in order to identify the most effective threshold. We set thresholds at 10,000, 15,000, 20,000, 25,000, and 30,000 kg/ms^2, based on a visual comparison of stream power and high FEI areas. If a given 25 m stream reach had *SP* greater than the threshold, then it was designated a hotspot (1). If *SP* was less than the threshold, it was designated not to be a hotspot (0). Each model run with a different *SP* threshold was compared with the FEI data. For this comparison, we extracted data at points spaced 2 meters apart in order to extract the most data possible. Although *SP* data were only calculated every 25 meters,

the FEI data along the stream changed more frequently than that. For each point, the FEI value indicates if it eroded (1), or if it did not erode (0). Thus, each point along the stream had a value for *SP* (0, 1) and for FEI (0, 1).

We calculated several statistics to evaluate the most effective single-predictor model and its *SP* threshold. We found the ***percent accuracy for all points***, or the percent of all the points that had *SP* greater than the threshold and FEI ≥ 2; or had *SP* below the threshold and FEI < 2. We also calculated the ***percent accuracy for FEI*** $\geq$ ***2***, or the percent of all of the points with FEI ≥ 2 that also had *SP* greater than the threshold. Lastly, we found the ***percent of points over-predicted*** (false positives, or the percent of all points that had *SP* greater than the threshold but FEI < 2), and the ***percent of points under-predicted*** (false negatives, or the percent of all points that had *SP* less than the threshold but FEI ≥ 2).

Generally, if the threshold is set at a lower value, the accuracy of the model increases, while the percent of points over-predicted also increases. A lower threshold results in more points being designated a hotspot. With more points being designated as hotspots, the accuracy of the model improves because the probability that points with FEI ≥ 2 will be designated a hotspot increases. However, the percent of points over-predicted also increases. Because we are most interested in predicting the actual erosion hotspots (FEI≥ 2), while minimizing the number of points over-predicted, we used a *threshold index* defined as the percent accuracy for FEI ≥ 2 divided by the percent of points over-predicted to determine the most effective *SP* threshold. The threshold with the maximum threshold index maximizes the percent accuracy for FEI ≥ 2 while minimizing the percent of points over-predicted. This maximum threshold index value was at a *SP* of 15,000 kg/ms^2. Because North Shore watersheds vary in size, in order to apply this threshold to other watersheds, we calculated the threshold value as a fraction of highest *SP* value in watershed (1.89%) and used that fraction for the application of the model to the Talmadge.

We also used single-predictor models to determine the most effective bedrock exposure dataset for Amity Creek. At each predictor point along the stream, we extracted FEI data indicating if it eroded (1), or if it did not erode (0). Likewise, at each data point

we extracted bedrock data from each bedrock exposure dataset: Feature Analyst, MGS, and manual bedrock exposure. Because we are interested in areas that will erode, we compared points that are *not* within 5m of bedrock to the FEI dataset and have FEI ≥ 2, using the same statistics described above. We found that the highest value for our threshold index, was for the manual bedrock exposure map (3.24), but the Feature Analyst map was very similar (3.19).

In order to determine the best bluff threshold, we visually compared the > 2 meter bluffs within 7 meter of the centerline with the > 4 meter bluffs within 7 meter of the centerline. Because the 2 meter bluff map was more inclusive, we used all points within 7m of 2 meter and greater bluffs in our threshold model.

In order to verify the accuracy of our single-predictor models, we also compared single-predictor models for *SP*, bedrock, and bluff proximity to a random-number generator. At each point along the stream, we generated a random number with the same data distribution as the FEI dataset, and compared it to the FEI dataset. The three single-predictor models for *SP* (threshold = 15,000 kg/ms^2), bluff proximity (2m and greater bluffs within 7m of centerline), and bedrock exposure (manual) all had higher accuracy (59 - 65% accuracy for all points) than the random model (43% accuracy for all points).

Based on our evaluations of each of the single-predictor models, we developed three multi-predictor models. Model 1 includes *SP*, bluffs, and bedrock. For this model, the reaches that fit all of the following qualifications were identified as hotspots: had *SP* > 15,000 kg/ms^2, were within 7 meters from bluffs > 2 meters tall, and were not within 5m from manual bedrock exposure. Model 2 included the same thresholds but for bluffs and bedrock only. Model three included the same thresholds but for *SP* and bedrock only. For each of these models, we calculated the same statistics as described above for the single-predictor models to determine their accuracy.

After developing the threshold-based models described above, we applied the model to the Talmadge River. The Talmadge River watershed is significantly smaller (area: 1,516,241 m^2) than the Amity Creek watershed (area: 4,174,166 m^2). In order to account for variations among North Shore watersheds in size and in order, we used the *SP* threshold for Amity (15,000 kg/ms^2), normalized to the highest *SP* value for the

watershed (794,311 kg/ms^2) to determine a *SP* threshold ratio (1.89%). We used this ratio to calculate a *SP* threshold for other watersheds, including the Talmadge. A *SP* threshold of 2.7 kg/ms^2 was used in the model for the Talmadge River. For the Talmadge River threshold model, we used the only bedrock data available, the MGS bedrock exposure maps.

Results: Erosion Hotspot Predictors

We calculated five erosion potential predictors: the stream power-based erosion index, bluff proximity, angle of impingement, soils, and bedrock exposure, for each watershed: Amity Creek, Talmadge River, and French River watersheds. Figure 2 shows each of these three watersheds, and results for each analysis are shown in Figures 5, 6, and 7.

We calculated *SP* along the stream networks (Figures 5a, 6a, and 7a) and as expected, generally *SP* is lowest in the upper reaches of the stream network where drainage area is small and slopes are very low. A long profile of Amity (Figure 3) is representative of most North Shore streams. Both the slope and the drainage area increase towards the outlet, resulting in a rapid increase in *SP* toward the outlet. For Amity Creek, the average *SP* was 25671 kg/ms^2, and the values ranged from 0 to 794311 kg/ms^2.

We delineated bluffs of two sizes along the stream network, both shown for each watershed in Figures 5b, 6b, and 7b. Bluffs > 2 meters and bluffs > 4 meters, within 7 meters from the channel centerline are shown. These bluffs can be observed along the entire length of the channels, but have a greater density in middle reaches and closer to the outlet, for all the streams. These bluffs include all types of substrate including glacial till and bedrock.

The results for the angle of impingement are shown in Figures 5c, 6c, and 7c. The angle of impingement is the greatest at sharp, tight curves in the stream network. The possible values for the angle of impingement range from 0 to 6.28 radians, and the highest observed values for each creek were 1.57 rad along Amity Creek and the French River, and 1.18 rad along the Talmadge River.

Soil erodibility data (RUSLE K factor) are shown for the three watersheds in Figures 5d, 6d, and 7d. The values of the erodibility factor along the stream network varied minimally in all three watersheds. The value of K at individual sites can vary from the K value assigned for the map unit because data are aggregated over the map unit. The average polygon area of the SSURGO data in the Amity Creek is large, 139,994 m^2. Any variation within a given polygon is lost, even in this high-resolution dataset. For example, the lower 7.8 km of Amity Creek main stem/west branch, and the lower 7.0 km of the Talmadge River main stem all flow through only K values of 0.49. Although SSURGO is a high-resolution dataset, the resolution is far coarser than the resolution of the LiDAR datasets used here and appears to be inadequate for identifying erosion hotspots associated with soil variability.

Bedrock exposure for a 300 m corridor along the channel, from Jean Duluth to the outlet, was mapped using the feature extraction methods for Amity Creek only, and is shown in Figure 5e, compared to bedrock outcrop mapped on the surficial maps completed by the MGS (Hobbs, 2002; Hobbs, 2009). In Amity Creek, most bedrock outcrops are located along Seven Bridges Road, especially in the vicinity of the uppermost three bridges (Figure 5e). This method resulted in identification of the large obvious outcrops which were visually confirmed on the air photos, but also small polygons (~1 to 10m^2) along the creek that may be erroneous.

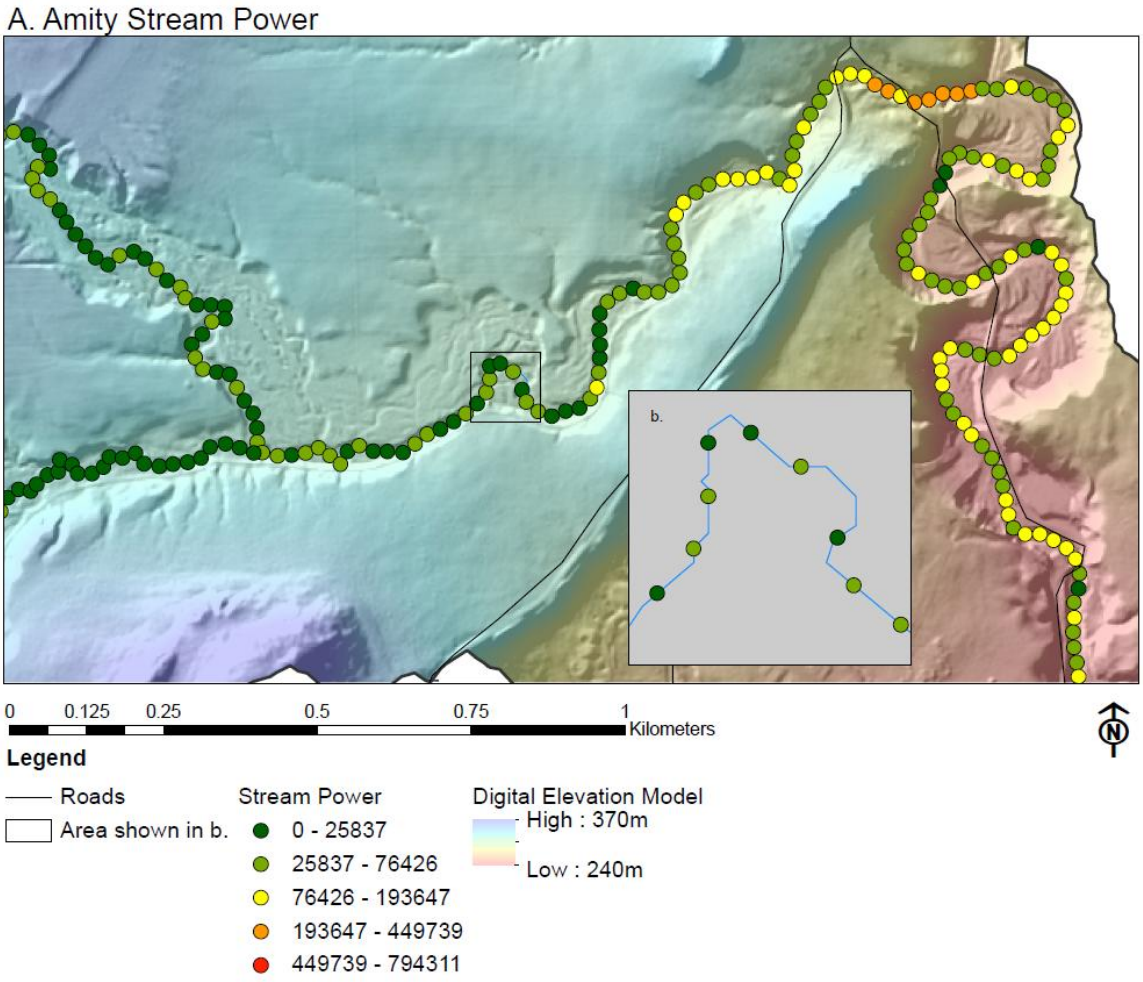

Figure 5. Predictors for Amity Creek Watershed. The area shown in this figure is outlined in Figure 2a. **A.** *SP* in kg/ms^2, shown every 25m. The inset (b.) shows the same data for the area outlined in larger map. Figure continued on following page.

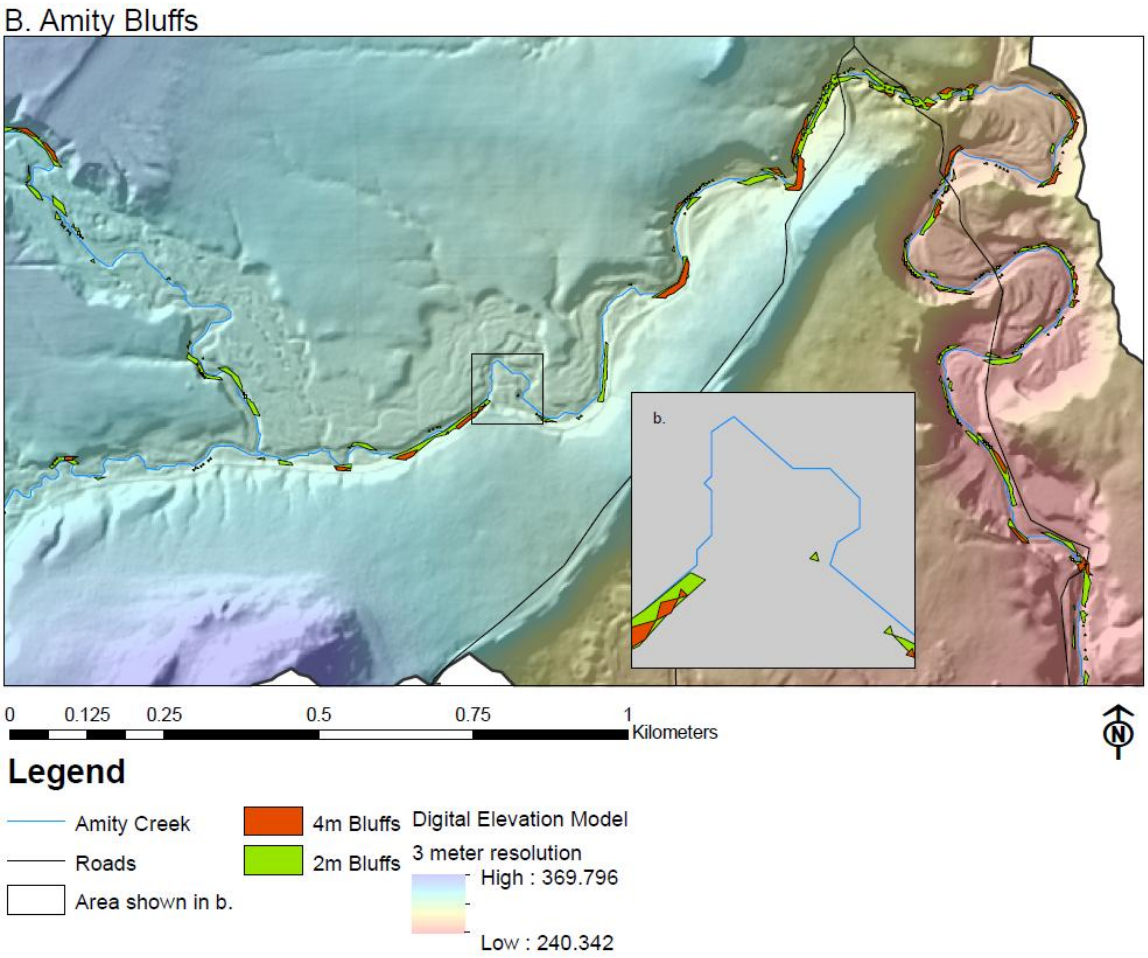

Figure 5, ctd. Predictors for Amity Creek Watershed. The area shown in this figure is outlined in Figure 2a. **B.** 2m and taller bluffs (green) and 4m and taller bluffs (orange) within 14 m-wide channel corridor. The inset (b.) shows the same data for the area outlined in larger map. Figure continued on following page.

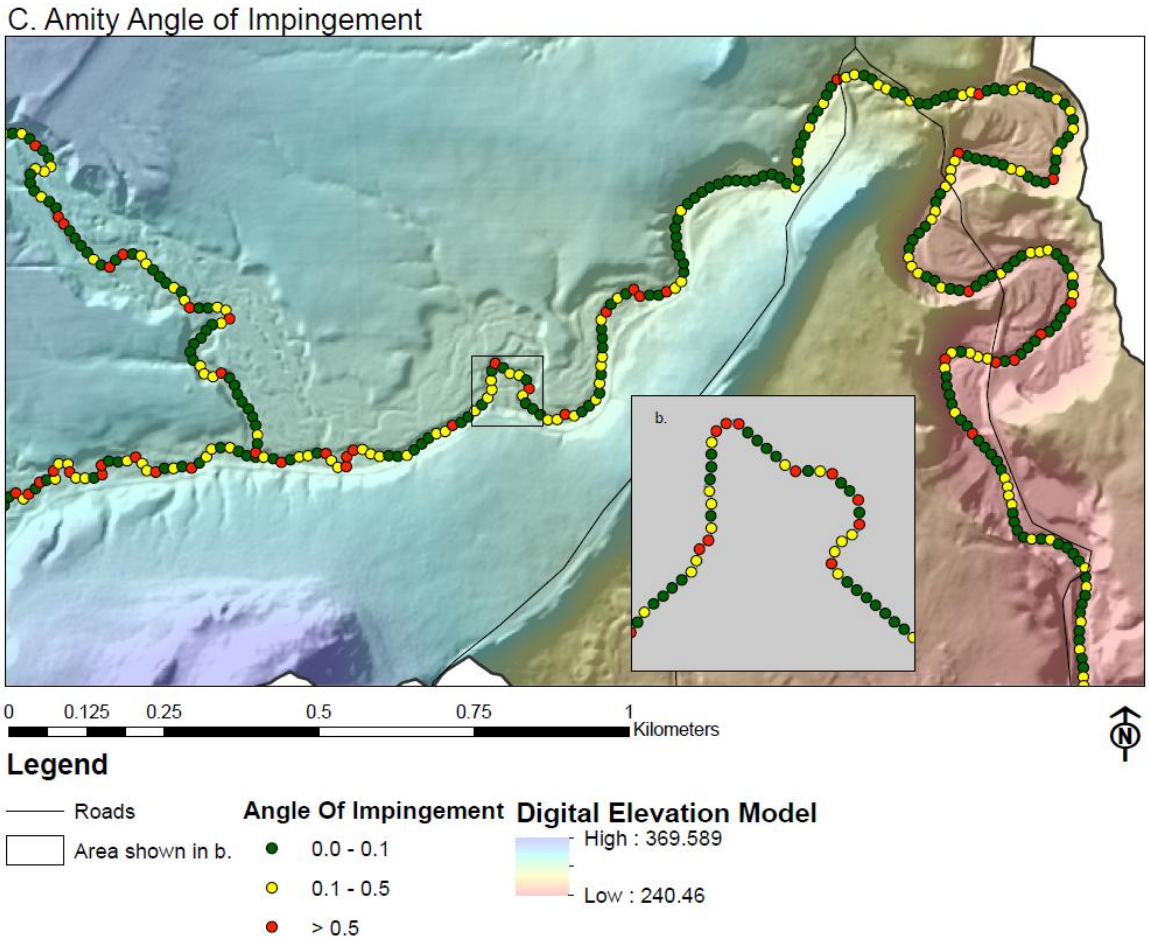

Figure 5, ctd. Predictors for Amity Creek Watershed. The area shown in this figure is outlined in Figure 2a. **C.** Angle of impingement in radians, shown every 15m in large map. The inset (b.) shows angle of impingement every 5m along the stream for the area outlined in larger map. Figure continued on following page.

D. Amity Bedrock Exposure

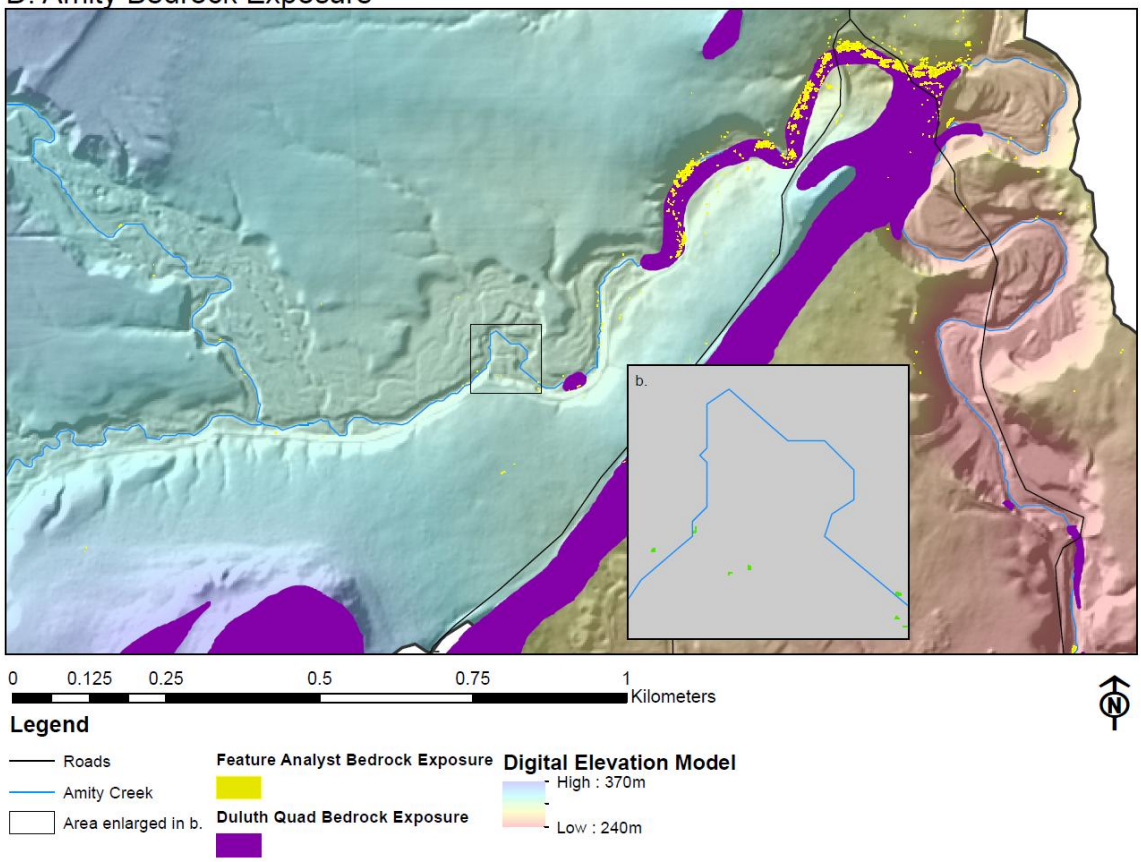

Figure 5, ctd. Predictors for Amity Creek Watershed. The area shown in this figure is outlined in Figure 2a. **D.** Bedrock exposure maps, including Feature Analyst bedrock exposure within a 300 m-wide channel corridor (green), and MGS bedrock outcrops mapped by Hobbs, 2002. The inset (b.) shows the same data for the area outlined in larger map. Figure continued on following page.

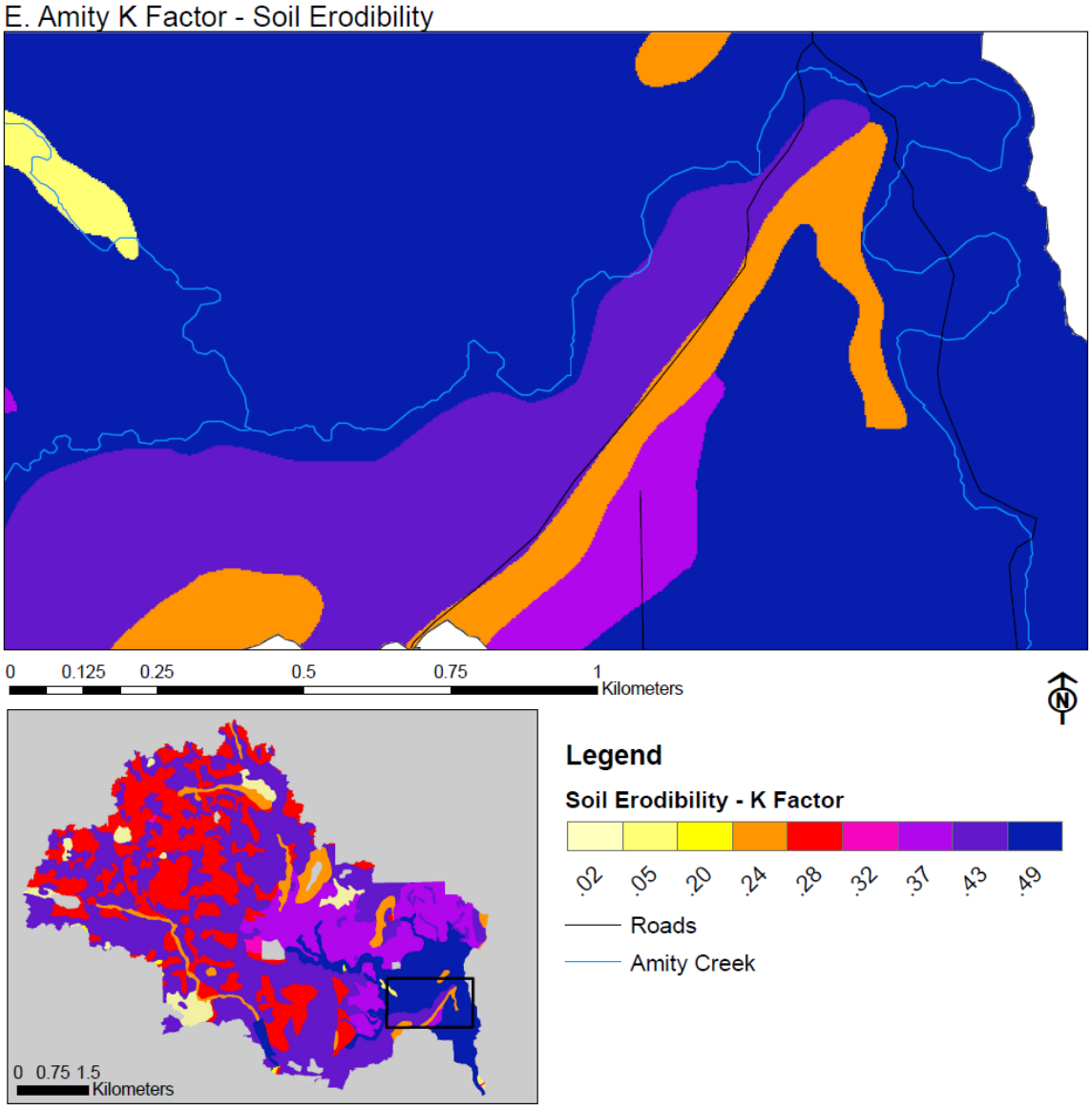

Figure 5, ctd. Predictors for Amity Creek Watershed. **E.** K factor from the Revised Universal Soil Loss Equation, and extracted from SSURGO soils dataset. The area of the watershed shown in the larger map above is outlined in the smaller map at the bottom, which also shows the soils data for the entire watershed.

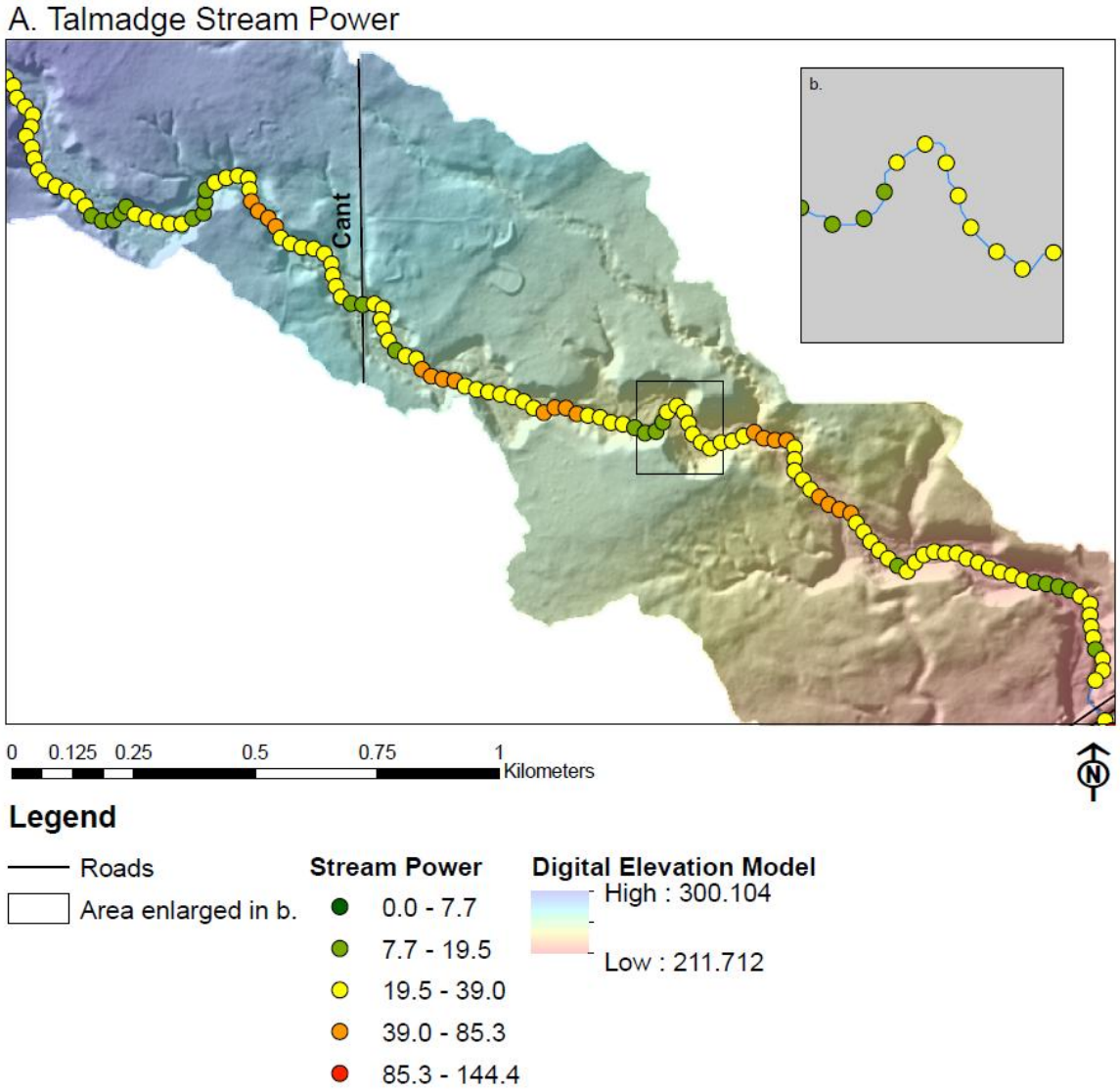

Figure 6. Predictors for the Talmadge River watershed. The area shown in this figure is outlined in Figure 2b. **A.** *SP* in kg/ms^2, shown every 25m. The inset (b.) shows the same data for the area outlined in larger map, but is shown every 5m. Figure continued on following page.

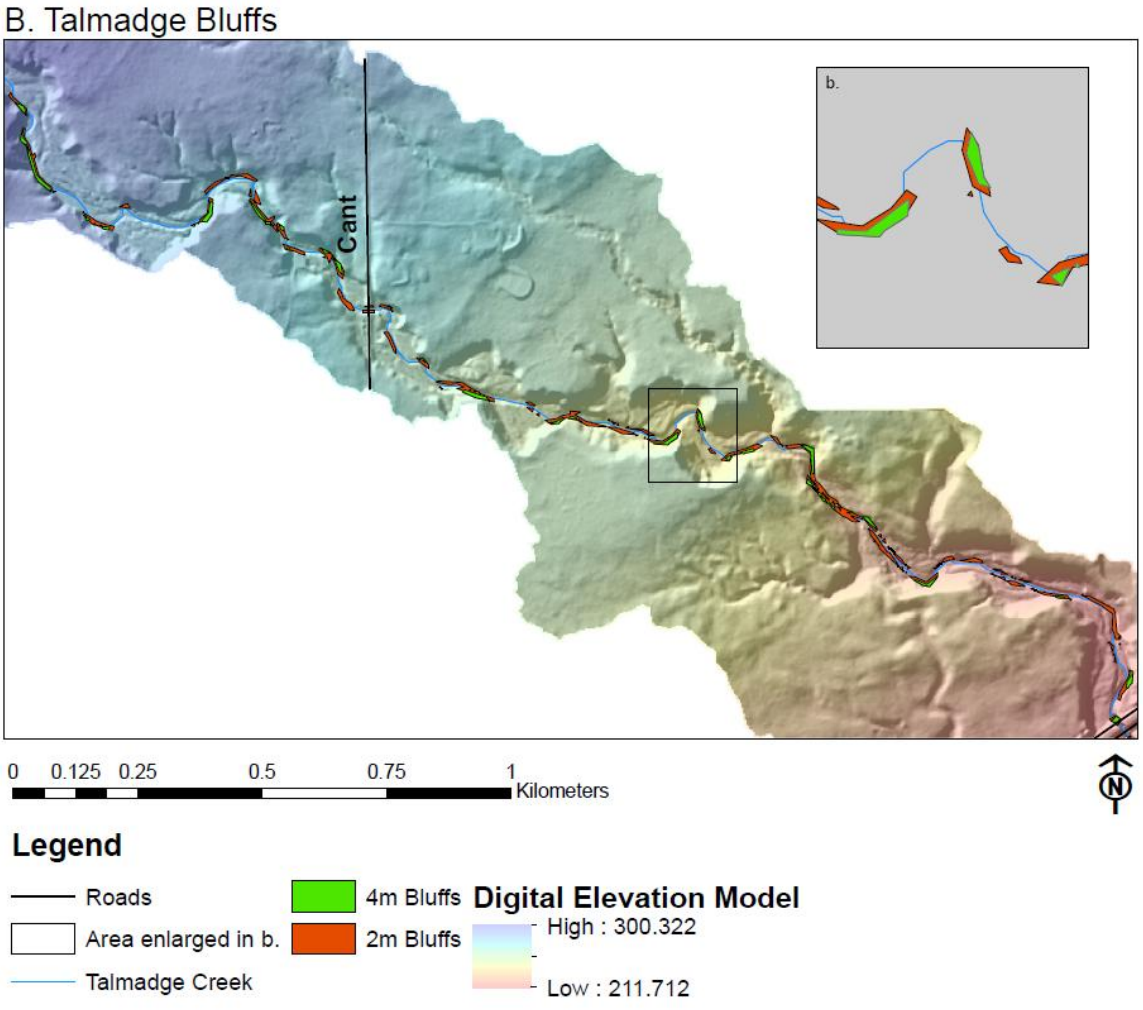

Figure 6, ctd. Predictors for the Talmadge River watershed. The area shown in this figure is outlined in Figure 2b. **B.** 2m and taller bluffs (green) and 4m and taller bluffs (orange) within 14 m-wide channel corridor. Figure continued on following page.

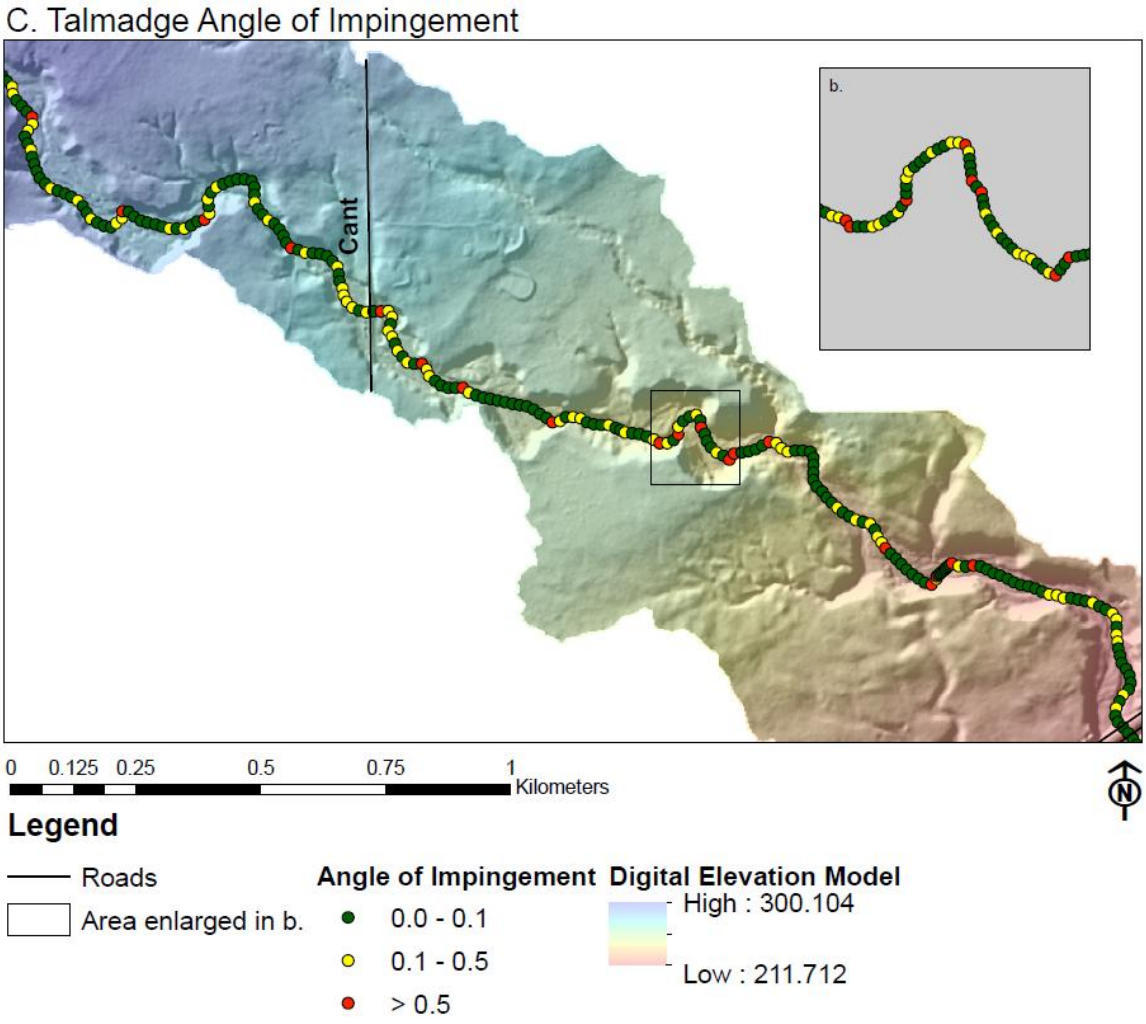

Figure 6, ctd. Predictors for the Talmadge River watershed. The area shown in this figure is outlined in Figure 2b. **C.** Angle of impingement in radians, shown every 15m in large map. The inset (b.) shows angle of impingement every 5m along the stream for the area outlined in larger map. Figure continued on following page.

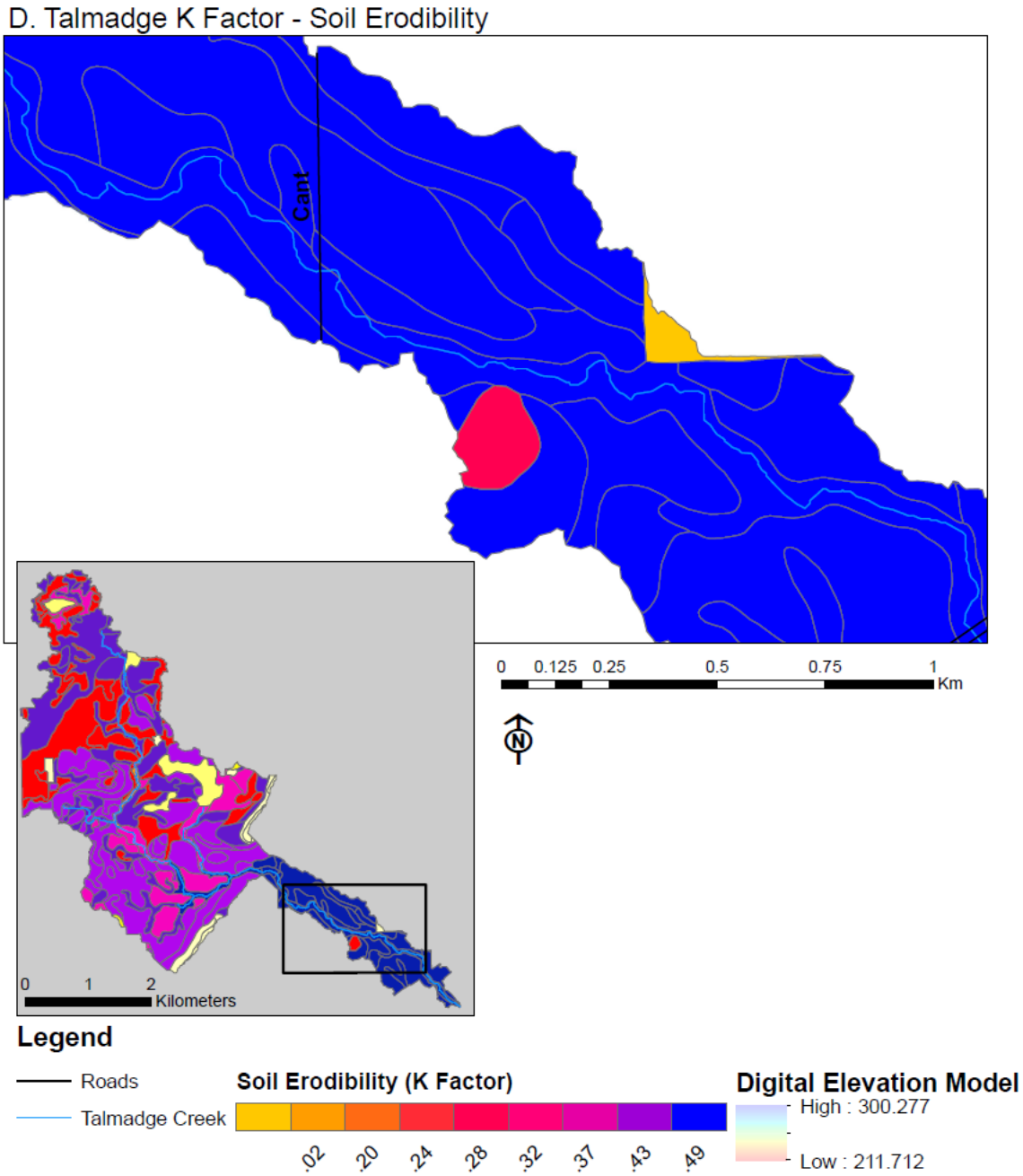

Figure 6, ctd. Predictors for the Talmadge River watershed. **D.** K factor from the Revised Universal Soil Loss Equation, and extracted from SSURGO soils dataset. The small map shows soils data for entire watershed. The area outlined in the smaller watershed map is the area shown in the larger map.

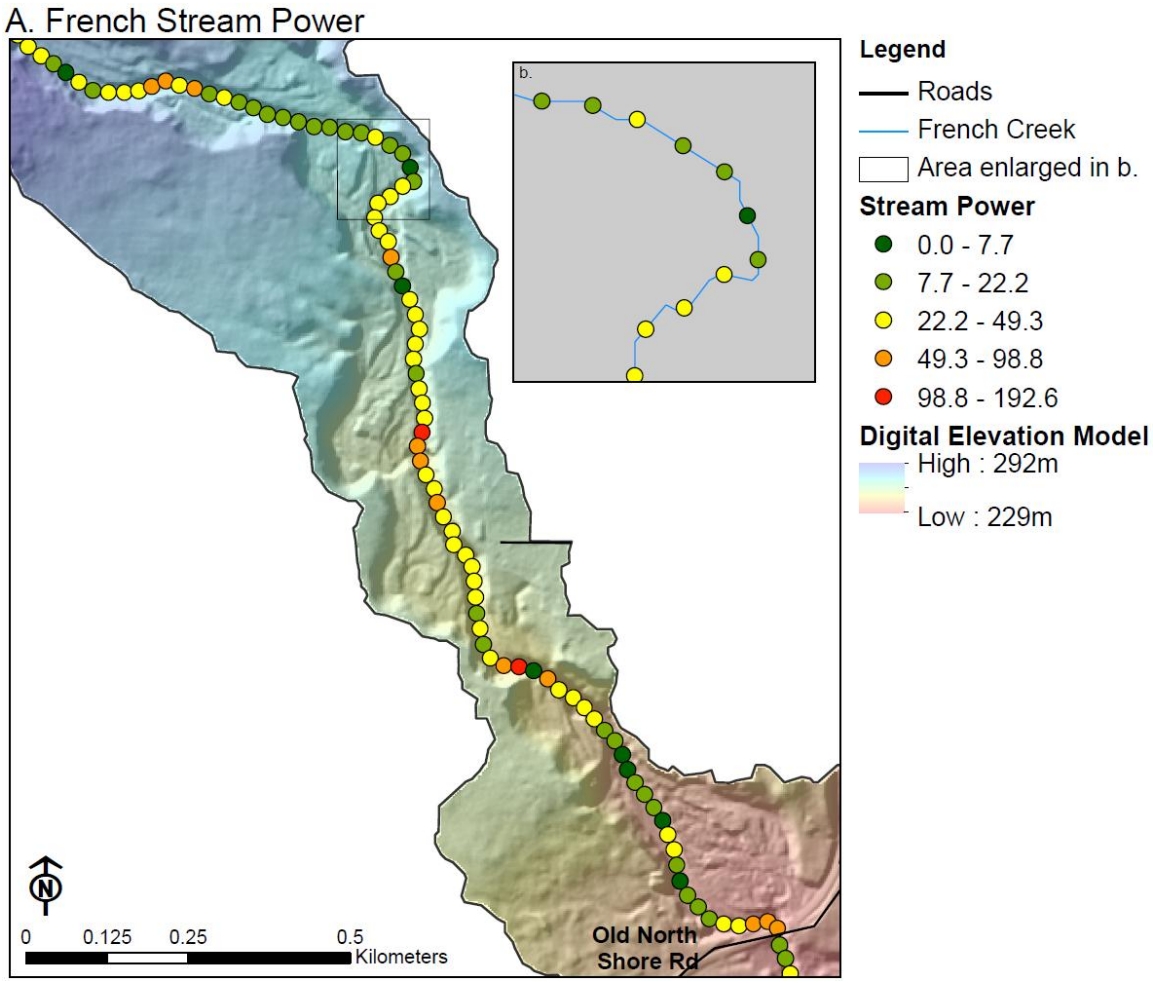

Figure 7. Predictors for the French River watershed. The area shown in this figure is outlined in Figure 2c. **A.** *SP* in kg/ms^2, shown every 25m. The inset (b.) shows the same data for the area outlined in larger map, but is shown every 5m. Figure continued on following page.

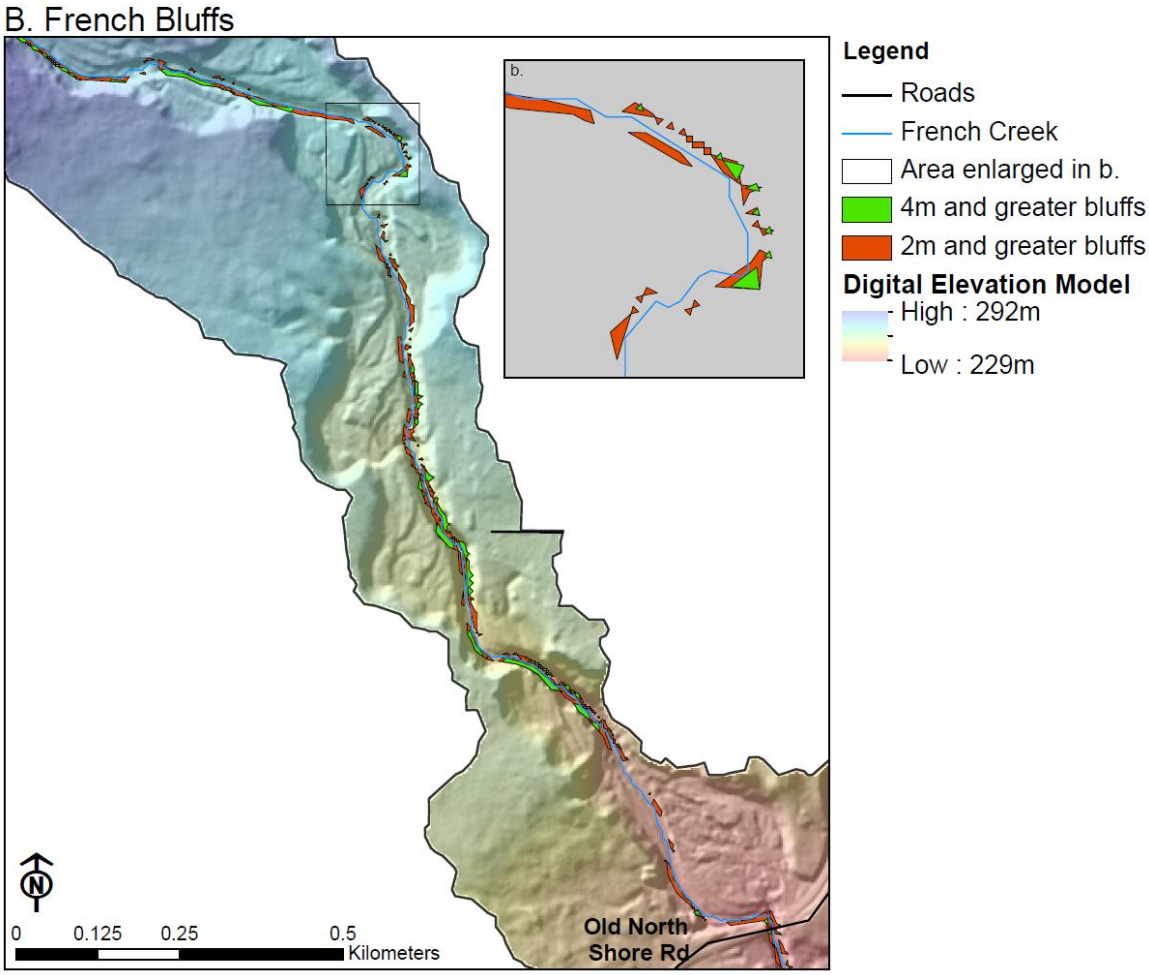

Figure 7, ctd. Predictors for the French River watershed. The area shown in this figure is outlined in Figure 2c. **B.** 2m and taller bluffs (green) and 4m and taller bluffs (orange) within 14 m-wide channel corridor. Figure continued on following page.

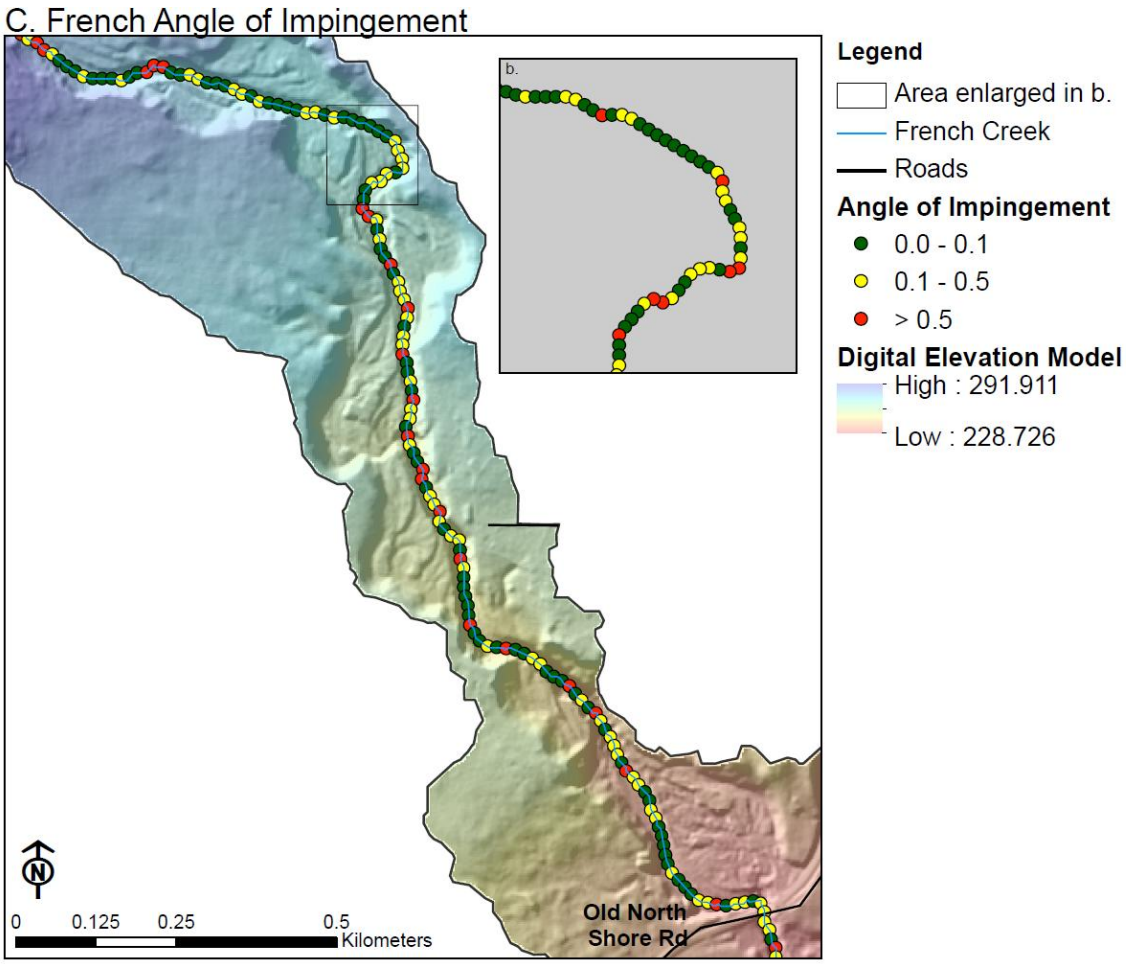

Figure 7, ctd. Predictors for the French River watershed. The area shown in this figure is outlined in Figure 2c. **C.** Angle of impingement in radians, shown every 15m in large map. The inset (b.) shows angle of impingement every 5m along the stream for the area outlined in larger map. Figure continued on following page.

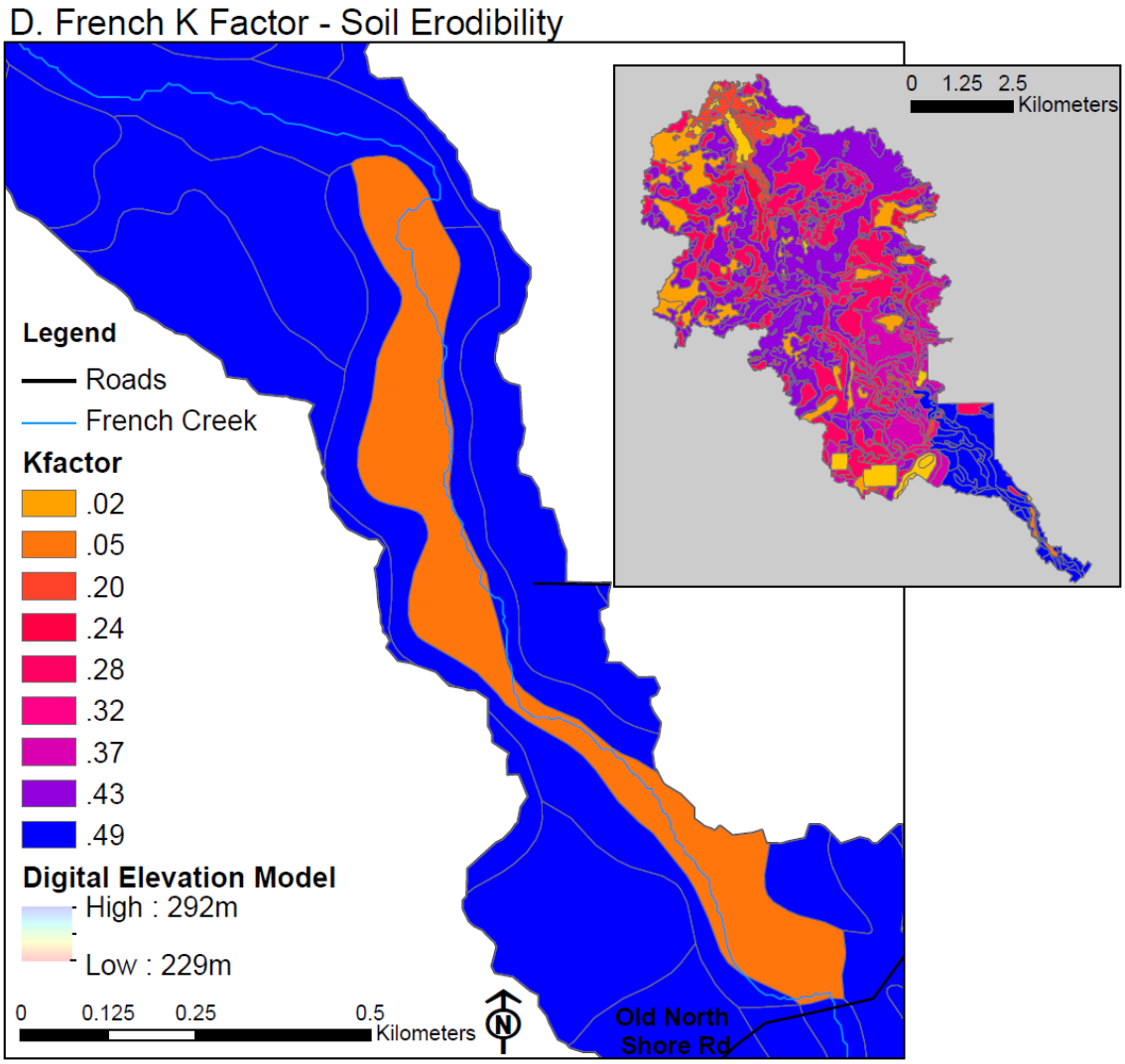

Figure 7, ctd. Predictors for the French River watershed. **D.** K factor from the Revised Universal Soil Loss Equation, and extracted from SSURGO soils dataset. The small map shows soils data for entire watershed. The area outlined in the smaller watershed map is the area shown in the larger map.

Results: Field Surveys

Bank Erosion Hazard Index Surveys

The locations of the BEHI survey points in each watershed are shown in Figure 2. Table 2 shows the scores and ratings for each location. For each watershed, the ratings ranged from very low bank erosion hazard (wetlands or bedrock channel and valley) to very high bank erosion hazard potential. Figure 8 shows a range of BEHI scores from four separate sites on Amity Creek, from a wetland channel with very low erosion hazard (Figure 8a, site 20), to a large eroding bluff that scored extreme erosion hazard on the BEHI survey (Figure 8d, site 28). Images b and c both scored moderate, but one was completed prior to the June 2012 flood and one was completed after the flood.

Field Erosion Index Surveys

We conducted FEI surveys on Amity Creek and the Talmadge River (Figure 9). We collected 341 points along Amity and 137 along the Talmadge. Each point marked a change in erosion, resulting in a continuous dataset along the entire length of stream walked. Figure 9 shows the FEI ratings along Amity Creek and the Talmadge River. Low values, which indicate no erosion (0 - 1), were the most common in both watersheds, followed by moderate values (2 - 5), and very high values (6-7) were rare. These surveys covered a large range of erosion potential along these streams. On Amity, over the length of stream we conducted the surveys on, 62% of the total length experienced some level of erosion (FEI $\geq$ 2). Of the total length surveyed (12.2 km), 19% experienced slumping or complete scour (FEI $\geq$ 4, Figure 9). On the Talmadge, over the length of stream we conducted the surveys on (5.5 km), 38% of the total length experienced some level of erosion (FEI $\geq$ 2), and 8% of the total length surveyed experienced slumping or complete scour (FEI $\geq$ 4, Figure 9). Because we surveyed the lower reaches of the stream where stream power is high, these proportions are not representative of the stream as a whole.

Table 2: BEHI Survey Results

Amity Creek

Site #	Left Bank	Category	Right Bank	Category	Maximum Score	Notes	Timing
0	10.15	Very Low	10.2	Very Low	10.2	Bedrock Substrate	Pre-flood
1	30.8	Moderate	10.2	Very Low	30.8	One Bank is Bedrock	Post-flood
2	10.15	Very Low	10.2	Very Low	10.2	Bedrock Substrate	Pre-flood
3	42.8	High	51.4	Very High	51.4		Post-flood
4	15.75	Low	17.2	Low	17.2		Pre-flood
5	31.2	Moderage	31.4	Moderate	31.4		Post-flood
6	13.7	Low	NA	NA	13.7		Pre-flood
7	26.25	Moderate	28.3	Moderate	28.3		Post-flood
8	36.8	High	38.8	High	38.8		Post-flood
9	24.7	Moderate	31.4	Moderate	31.4		Post-flood
10	26.2	Moderate	13.7	Low	26.2		Pre-flood
11	28.2	Moderate	22.3	Moderate	28.2		Pre-flood
12	10.2	Low	15.7	Low	15.7		Pre-flood
13	13.7	Low	15.7	Low	15.7		Pre-flood
14	43.7	High	14.2	Low	43.7		Pre-flood
15	12.2	Low	25.8	Moderate	25.8		Pre-flood
16	24.7	Moderate	20.3	Low	24.7		Pre-flood
17	22.75	Moderate	55.4	Very High	55.4		Pre-flood
18	15.2	Low	13.2	Low	15.2		Pre-flood
19	22.7	Moderate	27.8	Moderate	27.8		Pre-flood
20	10.15	Very Low	10.2	Very Low	10.2		Pre-flood
21	31.75	Moderate	22.8	Moderate	31.8		Pre-flood
22	13.7	Low	13.7	Low	13.7		Pre-flood
23	22.25	Moderate	22.3	Moderate	22.3		Post-flood
25	13.7	Low	48.6	High	48.6		Post-flood
26	17.7	Low	26.3	Moderate	26.3		Post-flood
27	68.5	Extreme	41.4	High	68.5		Post-flood
28	68.5	Extreme	24.3	Moderate	68.5		Post-flood

Talmadge Creek

Site #	Left Bank	Category	Right Bank	Category	Maximum Score	Notes	
1	10.15	Very Low	10.2	Very Low	10.2	Bedrock Channel	Post-flood
2	42.9	High	32.9	Moderate	42.9		Post-flood
3	34.35	Moderate	56.4	Very High	56.4		Post-flood
4	57.4	Very High	20.7	Moderate	57.4		Post-flood
5	26.3	Moderate	29.3	Moderate	29.3		Post-flood
6	13.75	Low	22.3	Moderate	22.3		Post-flood
7	33.3	Moderate	14.2	Low	33.3		Post-flood
8	12.2	Low	19.2	Low	19.2		Post-flood
9	15.7	Low	17.2	Low	17.2		Post-flood
10	10.15	Very Low	10.2	Very Low	10.2		Post-flood

French Creek

Site #	Left Bank	Category	Right Bank	Category	Maximum Score	Notes	
1	26.75	Moderate	53.9	Very High	53.9		Post-flood
2	10.15	Very Low	10.2	Very Low	10.2	Bedrock Channel	Post-flood
3	17.2	Low	19.2	Low	19.2		Post-flood
4	17.2	Low	14.2	Low	17.2		Post-flood
5	10.15	Very Low	10.2	Very Low	10.2		Post-flood
6	26.7	Moderate	15.7	Low	26.7		Post-flood
7	24.75	Moderate	61.5	Extreme	61.5		Post-flood
8	12.2	Low	12.2	Low	12.2		Post-flood
9	26.2	Moderate	21.3	Moderate	26.2		Post-flood
10	10.15	Very Low	10.2	Very Low	10.2		Post-flood
11	13.7	Low	10.2	Very Low	13.7		Post-flood
12	29.75	Moderate	31.8	Moderate	31.8		Post-flood

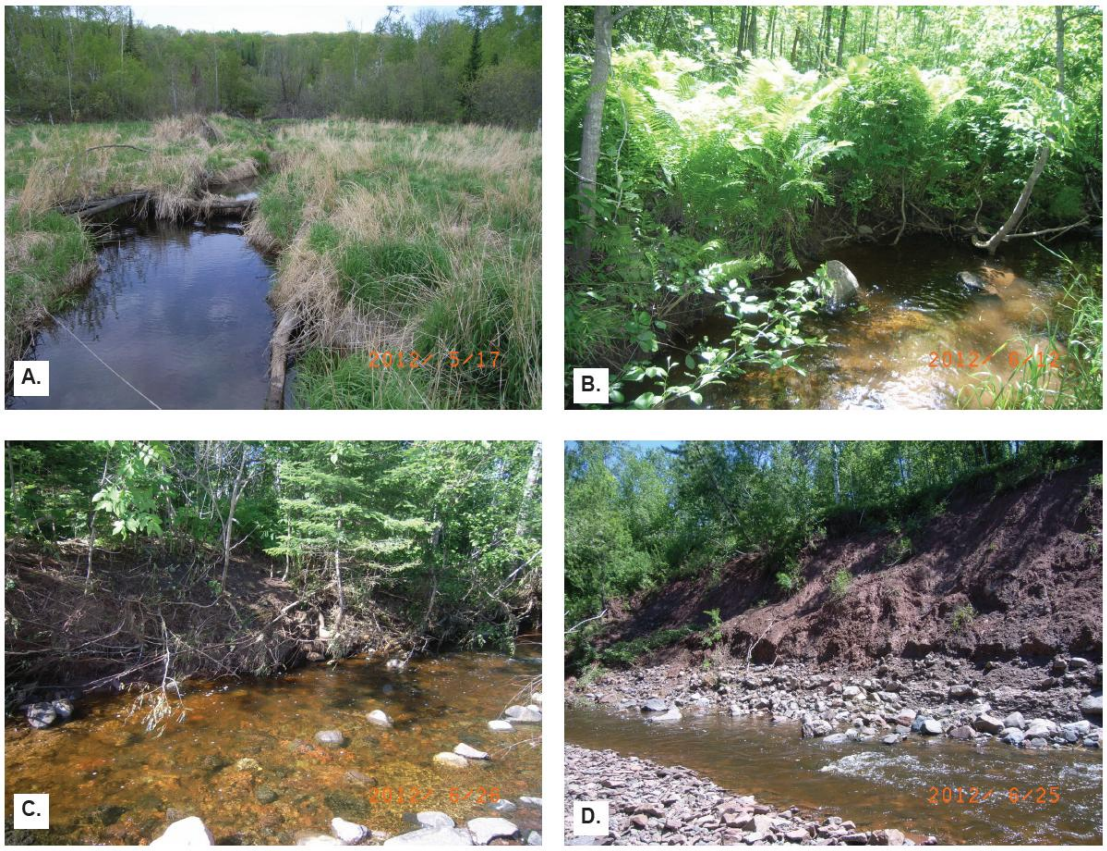

Figure 8. Images of example BEHI site locations with a range of BEHI scores:
Image A. BEHI score of 10.15, Very Low, completed prior to the June 2012 flood (Site #20).
Image B. BEHI score of 31.75, Moderate, completed prior to the flood (Site #21).
Image C. BEHI score of 31.35, Moderate, completed after the flood (Site #9).
Image D. BEHI score of 68.5, Extreme, also completed after the flood (Site #28).

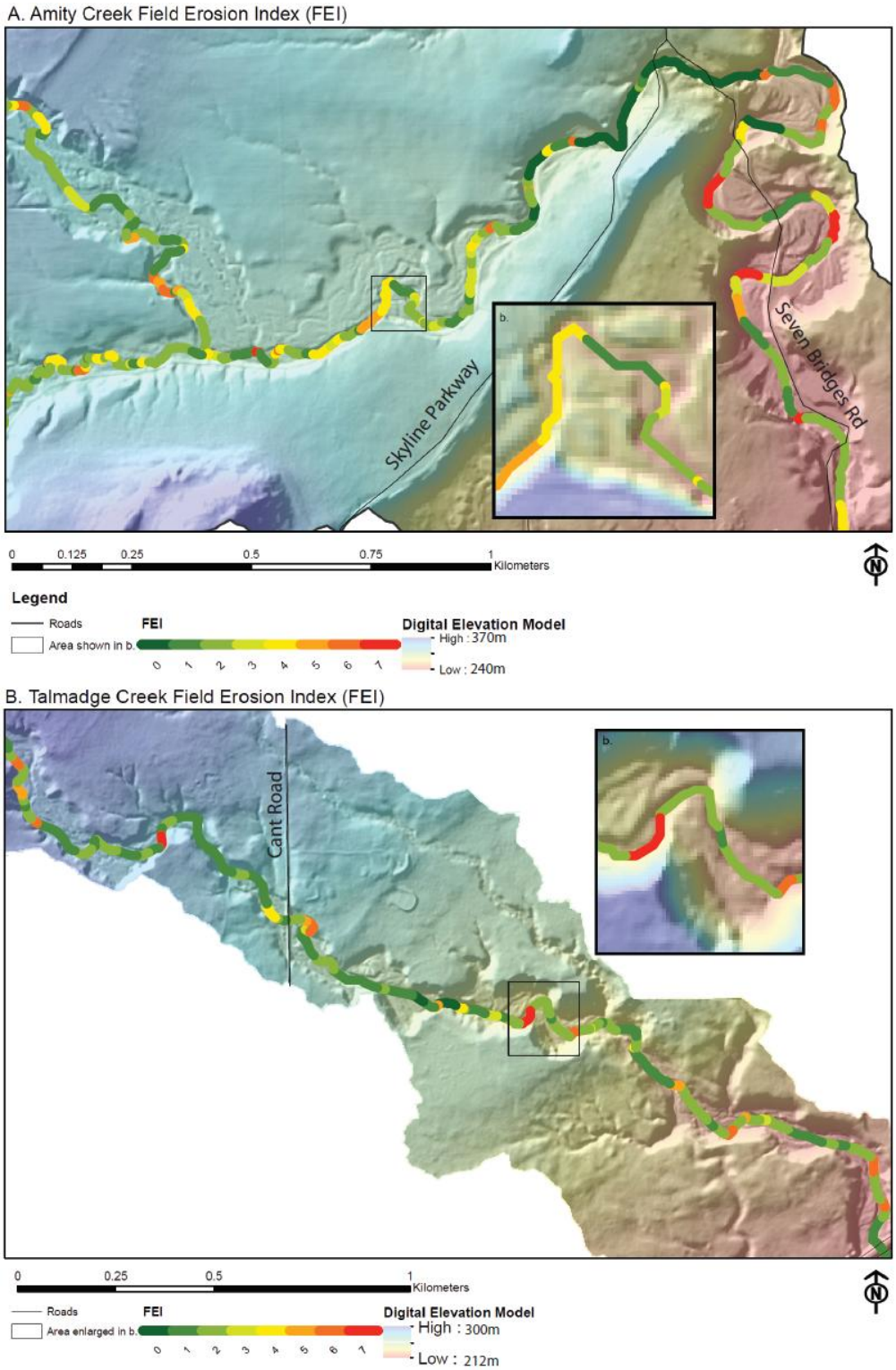

Figure 9. Field Erosion Index data for Amity Creek (A.) and Talmadge River (B.). See Table 1 for definition of each FEI score. Area shown in large maps is outlined in watershed maps shown in Figure 2a and b. Insets (b.) show area outlined in larger map.

Results: GIS Predictors compared to Field Surveys

We compared the results of our GIS predictors to our FEI survey data at points spaced every 25 meters along Amity and every 10 meters along the Talmadge, along the lower channel where the FEI survey data were collected, in order to have a similar total number of points for both rivers (See Methods: Field Surveys). Table 3 and Figure 10 show the number of data points included in the regressions shown in Figure 11 and 12, and the distribution of the data. Figure 11 shows the comparison of GIS predictors to FEI for Amity, and Figure 12 shows the same for the Talmadge.

In each figure respectively, plots A and B show the comparison of average *SP* and average angle of impingement for each FEI value versus FEI, along with standard error bars. Plots B and C show the percent of the points within 7 m of 2 m and taller bluffs (plot B) and 4 m and taller bluffs (plot C). Figure 11E, F, & G (for Amity) show the percent of points within 5 m of bedrock exposure for each FEI score, according to three different bedrock maps. Plot 11E shows the Feature Analyst bedrock map versus FEI. Plot 11F shows the comparison of a manual bedrock exposure map compared to FEI. Plot 11G shows the MGS bedrock exposure map compared to FEI (Hobbs, 2002, Hobbs, 2009). Figure 11 Plot H shows the average K factor values at each FEI score in Amity, along with one standard deviation. Figure 12E shows the percent of points within 5m of bedrock exposure, according to the MGS bedrock map (Hobbs, 2002, Hobbs, 2009) for the Talmadge for each FEI score. Figure 12F shows the average K factor value for each FEI score in the Talmadge, with error bars showing one standard deviation from the mean. Table 4 shows the r^2 values and the p-values for all of the regressions shown in Figure 11 and 12, in addition to the regressions for each predictor and the FEI for each branch of Amity individually. The regressions for *SP*, angle of impingement, and bluff proximity, shown in Table 4 and Figure 11 and 12 do not include data points with FEI=0, but the data for FEI = 0 are shown on the plots. This is because we know that because these points are bedrock they will have low erosion regardless of *SP*, angle of impingement, or bluff proximity. The regressions for K factor do include FEI = 0 data.

Table 3: Number of Points Per FEI Score

	Amity Creek				Talmadge River
FEI	Entire Stream	East Branch	West Branch	Main Stem	Entire Stream
0	48	1	0	47	72
1	134	38	57	39	234
2	181	64	48	69	179
3	31	6	4	21	6
4	37	6	10	21	9
5	17	6	1	10	10
6	24	10	3	11	22
7	12	2	0	10	8
Total	484	133	123	228	540

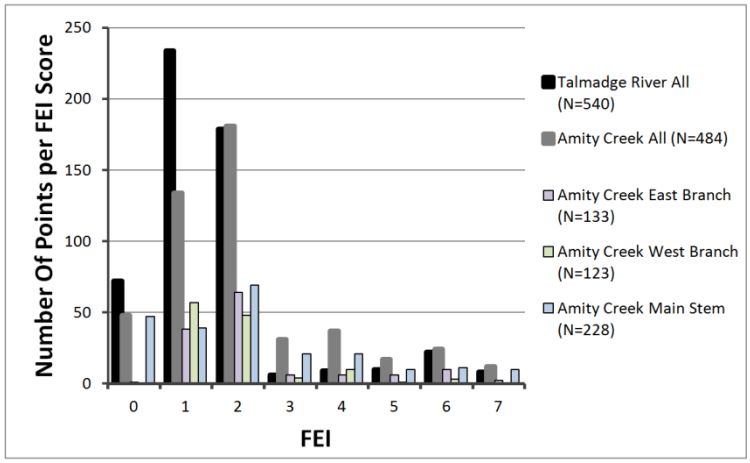

Figure 10. Number of data points for each integer value of FEI score for the entire length surveyed of Amity Creek (grey), for the lengths of the individual branches of Amity surveyed (colored, see legend above), and for the length of the Talmadge River surveyed (black).

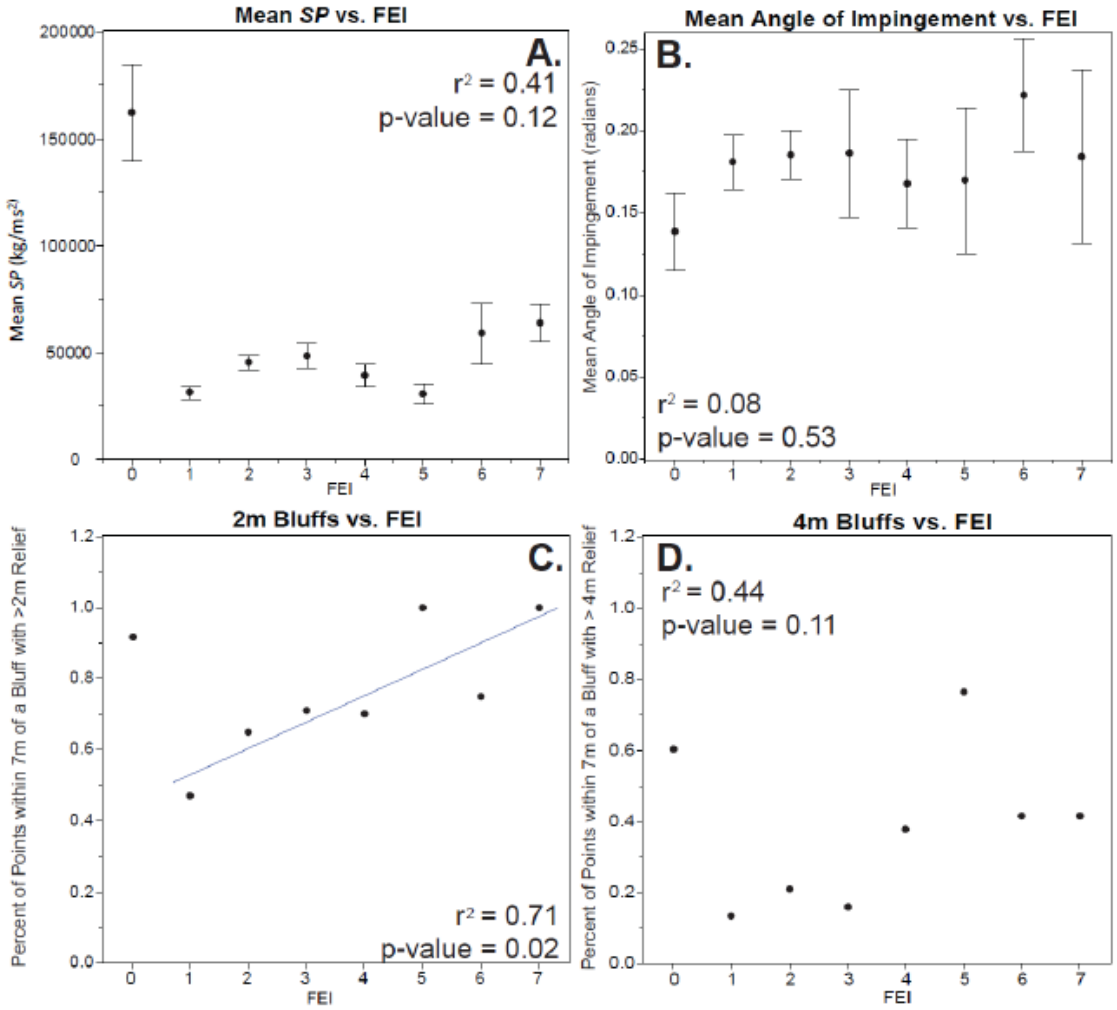

Figure 11: Comparison of GIS predictors & FEI surveys completed on Amity Creek. Data were extracted at points spaced every 25m along the stream network where the Field Erosion Index was surveyed. Plots A and B show the average *SP* and angle of impingement, respectively, along with error bars that represent one standard error from the mean. Plot C and D show the percent of points within each FEI category that are within 7m of a 2m or taller bluff (plot C), or a 4m or taller bluff (plot D). The linear regressions shown here (A, B, C, and D) do **not** include FEI = 0, although FEI = 0 data are shown on these plots. Regression lines are only shown if the regression is significant. Also see Table 4 for r^2 and p-values. Figure 11 continued on following page.

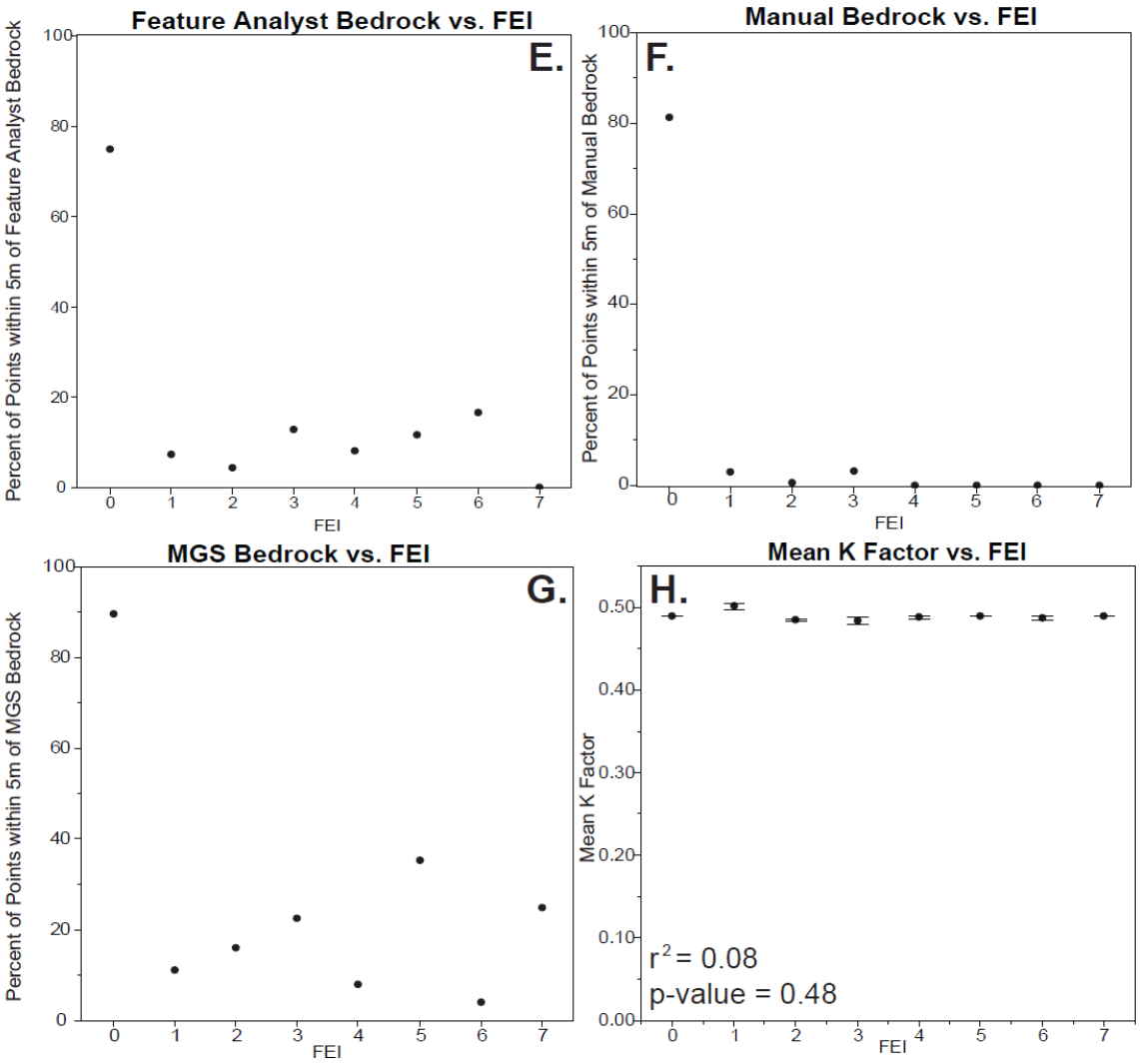

Figure 11, ctd: Comparison of GIS predictors & FEI surveys completed on Amity Creek. Data were extracted at points spaced ever 25m along the stream network where the Field Erosion Index was surveyed. Plots E, F, & G show the percent of points within each FEI category that are within 5m of bedrock exposure, as mapped using Feature Analyst (plot E), manual bedrock exposure map (created using field data, plot F), or bedrock exposure, as mapped on MGS maps by Hobbs (2002) and Hobbs (2009) (plot G). The ideal map would have 100% of the points adjacent to bedrock at FEI = 0, and has 0% of the points adjacent to bedrock for FEI 1 - 7. Plot H shows the average K factor data for each FEI value, and error bars showing 1 standard error. Also see Table 4 for r^2 and p-values.

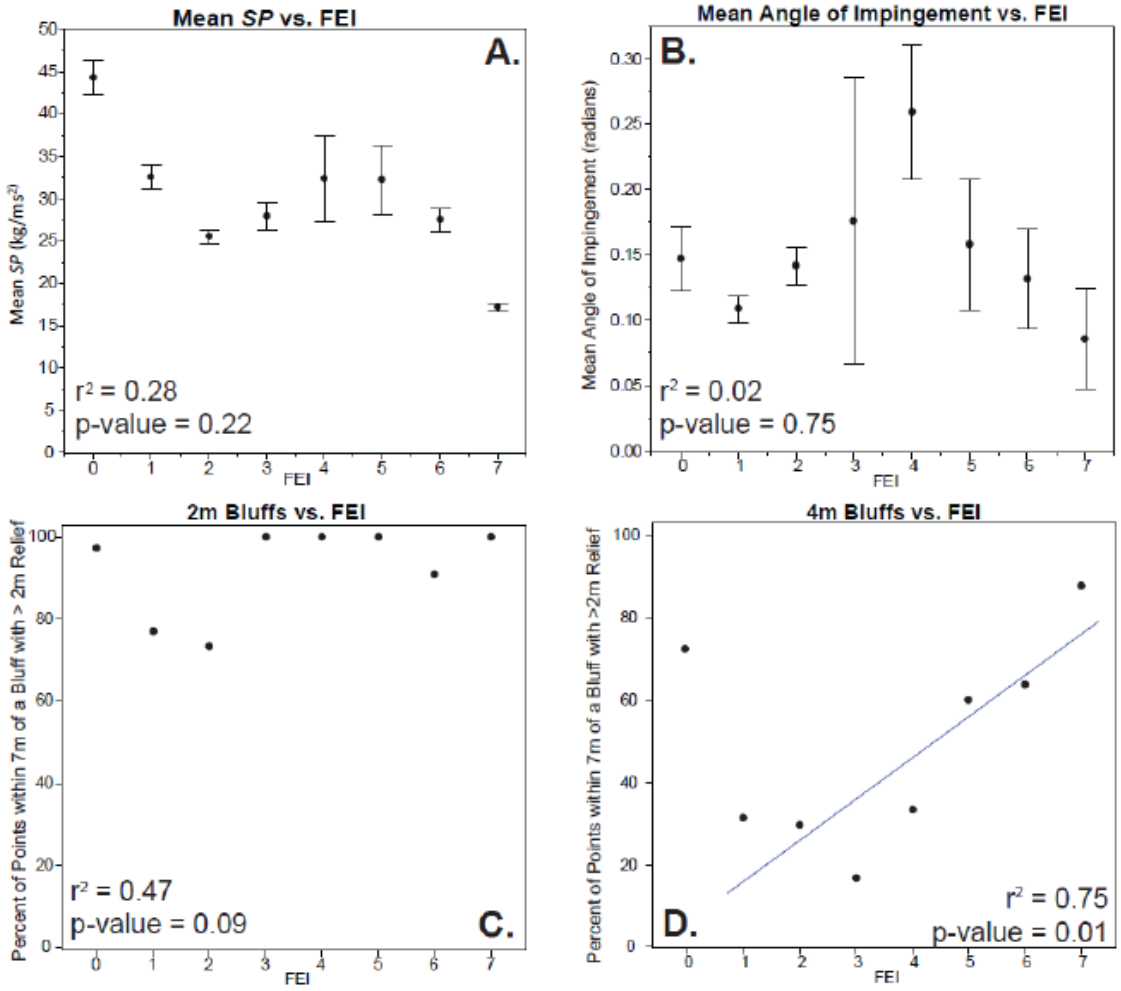

Figure 12: Comparison of GIS Predictors & FEI surveys completed on Talmadge Creek. Data were extracted at points spaced every 10m along stream network where the FEI data were collected. Plots A and B show the average *SP* and Angle of Impingement, respectively, along with error bars that represent one standard error from the mean. Plot C and D show the percent of points within each FEI category that are within 7m of a 2m or taller bluff (plot C), or a 4m or taller bluff (plot D). The linear regressions shown here do **not** include FEI = 0, although FEI = 0 data are shown on these plots. Also see Table 4 for r^2 and p-values. Figure 12 continued on following page.

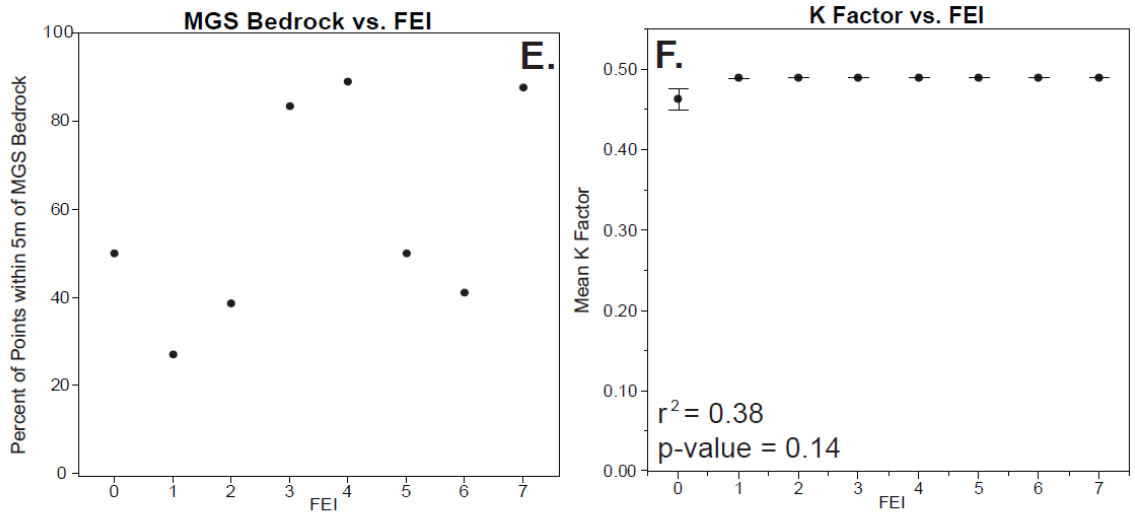

Figure 12, ctd: Comparison of GIS Predictors & FEI surveys completed on Talmadge Creek. Plot E shows the percent of points within each FEI category that are within 5m of bedrock exposure, as mapped on MGS bedrock outcrop maps (Hobbs, 2002, Hobbs, 2008). The ideal map would have 100% of the points adjacent to bedrock at FEI = 0, and has 0% of the points adjacent to bedrock for FEI 1 - 7. Plot F shows the average K factor data for each FEI value, and error bars showing 1 standard error from the mean. Also see Table 4 for r^2 and p-values.

Table 4: Predictor vs. FEI Regression Statistics

FEI	**Entire Stream**		**East Branch**		**West Branch**		**Main Stem**	
Amity Creek	R^2	P-Value	R^2	P-Value	R^2	P-Value	R^2	P-Value
Avg *SP* for each FEI	0.41	0.12	0.12	NS	0.09	NS	0.02	NS
Avg Angle of Impingement per FEI	0.08	NS	0.53	0.07	0.55	NS	0.00	NS
% Pts Near 2m Bluffs	**0.71**	**0.02**	**0.87**	**0.00**	0.18	NS	0.37	0.14
% Pts Near 4m Bluffs	0.44	0.11	**0.77**	**0.01**	0.12	NS	0.08	NS
Avg K factor for each FEI	0.08	NS	0.12	NS	0.50*	0.12	0.17	NS
Number of Points (N)	484		132		123		181	

FEI			**BEHI**		
Talmadge River	R^2	P-Value	**Amity**	R^2	P-Value
Avg *SP* for each FEI	0.28	NS	*SP*	**0.11**	**0.10**
Avg Angle of Impingement per FEI	0.02	NS	Angle of Impingement	0.00	NS
% Pts Near 2m Bluffs	**0.47**	**0.09**	% Pts Near 2m Bluffs	0.10	NS
% Pts Near 4m Bluffs	**0.75**	**0.01**	% Pts Near 4m Bluffs	0.50	0.11
Avg K Factor for each FEI	0.38	0.14	K Factor	0.09	0.15
Number of Points (N)	468		Number of Points (N)	26	

Values in bold indicate a regression significant at 90% level or greater. NS is given if significance is below the 85% level.
NA is given if bedrock regressions were not possible due to limited bedrock exposure in channel.
Correlations that were in the opposite direction than predicted are denoted with a *.
SP, angle of impingement, & bluff regressions were calculated omitting values of FEI = 0.
If applicable, N reflects value with FEI=0 removed.

For Amity Creek, there is a positive correlation between *SP* and FEI which is almost significant ($r^2 = 0.41$, p-value = 0.12). There is not a significant correlation for angle of impingement and FEI. There is a strong significant correlation between the percent of points adjacent to 2 meter and greater bluffs and the FEI ($r^2 = 0.71$, p-value = 0.02). The percent of points adjacent to 4 meter and greater bluffs also correlates with FEI, though this correlation is weaker ($r^2 = 0.44$, p-value = 0.11). There is no correlation between K factor and FEI. We did not report regressions between FEI and bedrock exposure because we would not expect a simple correlation. In Figure 11E, F, and G, we would expect that at FEI = 0, 100% of the points are within 5m of bedrock exposure, because FEI = 0 is defined as a bedrock channel. Likewise, at FEI $\geq$ 1, we would expect 0% of the points to be within 5m of bedrock exposure. Qualitatively, the manual bedrock map is the most significant, because it has a very high percent of points near bedrock at FEI = 0 and nearly zero percent of points near bedrock at FEI $\geq$ 1. Feature Analyst bedrock and MGS bedrock have similar trends, but the percent of points near bedrock for FEI $\geq$ 1is greater than zero for both Feature Analyst bedrock and for MGS bedrock.

We also examined regressions of predictors versus FEI for individual branches on Amity (Table 4). There are no correlations for *SP* in the individual branches or main stem. Like for the entire stream, there are also no significant correlations between angle of impingement and FEI in the main stem or West Branch. However, there is a significant positive correlation between angle of impingement and FEI for the East Branch ($r^2 = 0.53$, p-value = 0.07). There are also significant positive correlations between percent of points adjacent to 2 meter and 4 meter and greater bluffs and FEI in the East Branch, but not in the West Branch or main stem. In the East Branch, the K factor correlates with FEI significantly ($r^2 = 0.57$, p-value = 0.05), but there are no correlations between K factor and FEI in the West Branch or main stem. Bedrock is rarely exposed along the East and West Branches. For the main stem, the three bedrock datasets all showed similar trends but manual bedrock best agreed with the FEI dataset.

For the Talmadge River, the main determinant of FEI estimated erosion was proximity to bluffs, with a particularly strong correlation between 4 meter bluffs ($r^2 = 0.75$, p-value = 0.01, Table 4). There also is a positive correlation between percent of

points adjacent to 2 meter and greater bluffs and FEI ($r^2 = 0.47$, p-value = 0.09). We do not see a significant correlation between *SP*, angle of impingement, or K factor and FEI. In Figure 12E, while we would expect to see a high percent of points near bedrock at FEI = 0, and very low percent of points near bedrock at FEI ≥ 1, we do not see that trend.

Figure 13 shows a comparison of Amity Creek GIS predictors with BEHI survey data. BEHI data are not shown for the Talmadge and French Rivers because there were not enough data for each river (Talmadge: n = 10, French: n = 12). Table 2 shows the BEHI data for all streams surveyed.

BEHI data were collected for both banks at each site. The plots in Figure 13 show the maximum BEHI score at each BEHI site. Plots A, B, and E show the absolute BEHI score, but plots C & D show the percent of the points within 7m of a bluff in each BEHI score category, which range from 1 – 6 (very low to extreme, Table 1). Survey sites that were bedrock channels were excluded from these plots, as we know that these locations have low erosion potential and the erosion potential at those sites is limited by the bedrock and does not depend on *SP*, bluff proximity or angle of impingement. After removing the bedrock points, the Amity plots contain a total of 26 data points. We do not include a regression of bedrock exposure vs. BEHI because only two sites had bedrock exposure, which thus scored very low erosion hazard on the BEHI survey. The limited dataset and nature of the BEHI surveys thus made it ineffective to try to compare bedrock exposure to BEHI score. Table 4 shows the r^2 values and p-values for Predictor versus BEHI regressions for Amity Creek.

There is a weak positive correlation ($r^2 = 0.11$, p-value = 0.096) between *SP* and the BEHI score. There are positive correlations between 2 meter and 4 meter bluff proximity and BEHI scores on Amity. For 2 meter bluffs, this correlation is not significant ($r^2 = 0.10$, p-value = 0.53), but for 4 meter bluffs, this correlation may be significant ($r^2 = 0.50$, p-value = 0.11). We do not see any correlation with angle of impingement or K factor and BEHI scores. Overall, these regressions are in agreement with what we found by comparing predictors to the Field Erosion Index. We would expect slightly better regressions with the percent of points near bluffs, however, the limited size of this dataset probably accounts for the lack of significance.

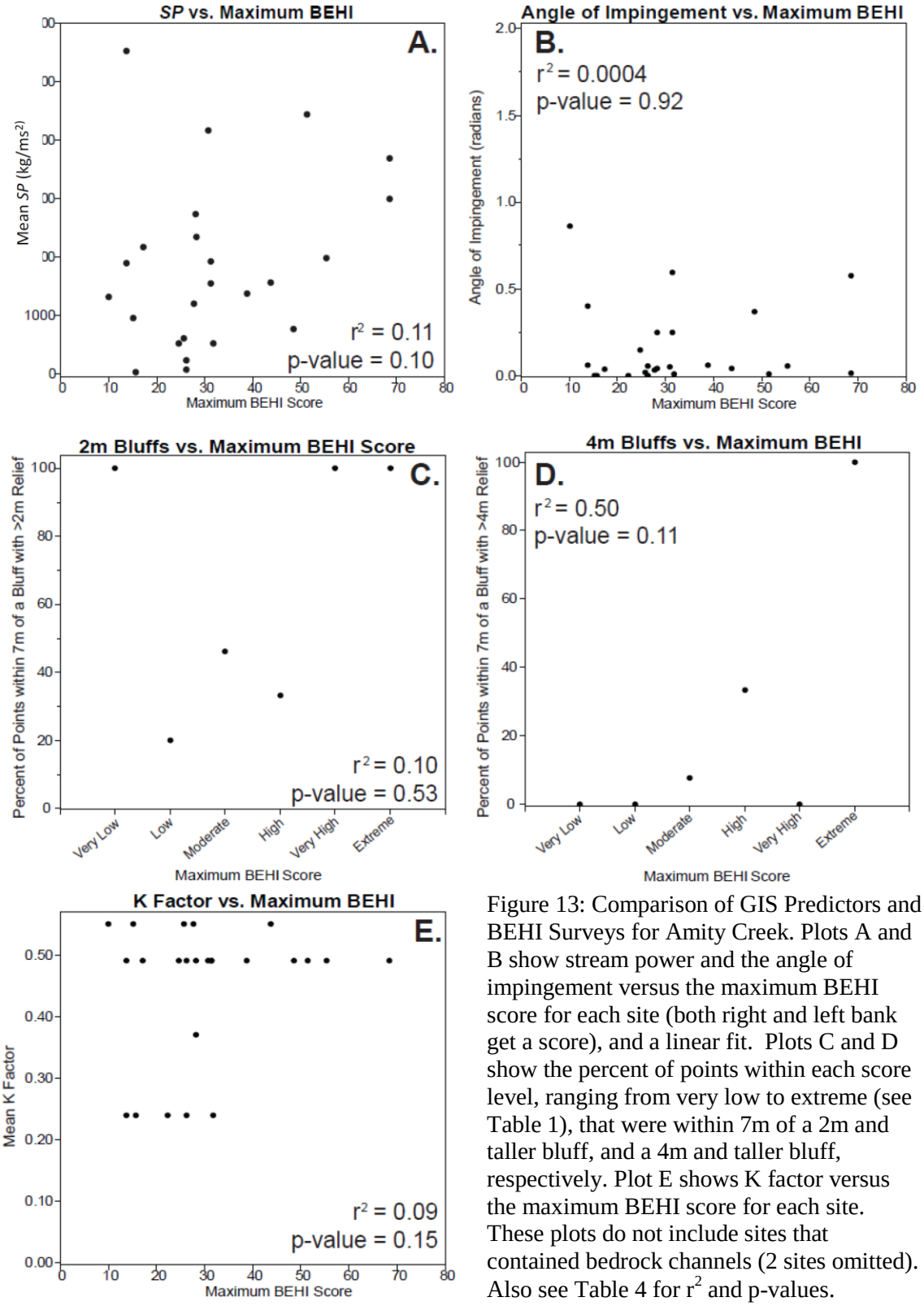

Figure 13: Comparison of GIS Predictors and BEHI Surveys for Amity Creek. Plots A and B show stream power and the angle of impingement versus the maximum BEHI score for each site (both right and left bank get a score), and a linear fit. Plots C and D show the percent of points within each score level, ranging from very low to extreme (see Table 1), that were within 7m of a 2m and taller bluff, and a 4m and taller bluff, respectively. Plot E shows K factor versus the maximum BEHI score for each site. These plots do not include sites that contained bedrock channels (2 sites omitted). Also see Table 4 for r^2 and p-values.

Results: Development of Predictive Model

Logistic Model

The results of the best model for erosion potential for the entire stream are shown in Figure 14, and the distribution of the model output data is shown in Figure 15. Table 5 shows the coefficients (*b*) and the p-values for each predictor in the model. This model had an r^2 value of 0.2149 (Table 6). This model includes the log of *SP*, bedrock exposure, and a bluff index. We used the manual bedrock exposure file, corrected for several errors in which points extracted that had FEI = 0 were not identified as bedrock. The bluff index was created because the individual bluff proximity alone was not a significant predictor in the model. When the 2 meter and 4 meter bluff proximity data were used as individual predictors, the model assigned positive coefficients to them, resulting in a decreased probability for erosion if points were adjacent to bluffs (See Eqn. 3). The bluff index assigns a value of 5 to each point if it is within 7 meters of a 2 meter or taller bluff, and a value of 10 to each point if it is within 7 meters of a 4 meter or taller bluff. Using the bluff index, the model successfully assigns negative coefficients to the bluff index, indicating increased probability for erosion if a point is adjacent to a bluff.

Table 5: Logistic Models for Amity Creek

	Entire Stream Model		**East Branch Model**		**West Branch Model**		**Main Stem Model**	
	Coefficient		Coefficient		Coefficient		Coefficient	
	Value	P-Values	Value	P-Values	Value	P-Values	Value	P-Values
Intercept	4.05	0.002	11.68	NS	11.00	0.0006	1.95	NS
Log *SP*	-1.00	0.001	-0.87	NS	-2.63	0.0006	-0.01	NS
Bluff Index	-0.13	<0.0001	-0.08	0.13	-0.13	0.08	-0.14	0.01
Bedrock - Manual Adjusted	5.36	<0.0001	-8.45*	NS	NA	NA	-2.56*	<0.0001
N		479		133		119		227
Model R^2		0.215		0.035		0.119		0.388

P-values greater than 0.15 are labeled as NS. Coefficients with the incorrect sign are denoted with a *.

NA indicates the predictor was not included in the model (see text).

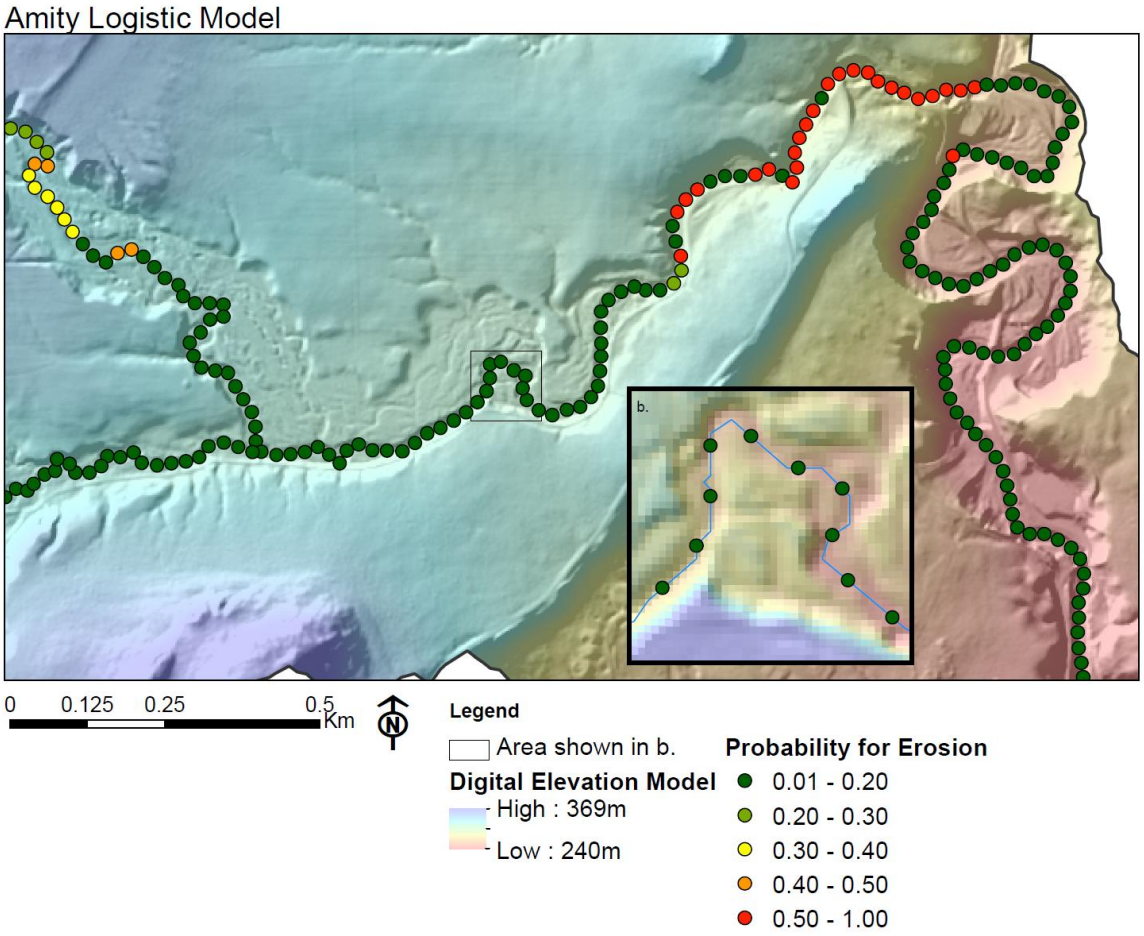

Figure 14: Example output of Logistic Model for Amity Creek. The large map shows the area outlined in Figure 2a. The inset (b.) shows the area outlined in the larger map. The color of each point represents the probability for erosion to occur at that point. The r^2 value for this model is 0.22. Many areas with elevated probability for erosion are also bedrock areas (See Figure 9a).

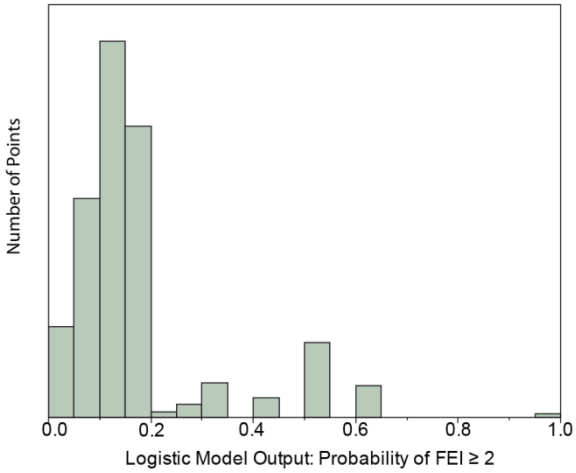

Figure 15. Distribution of the output of the logistic model, probability that FEI ≥ 2.

We used the same three predictors (log of *SP*; manual, adjusted bedrock exposure; and bluff index) to develop models based on the individual branch data. All FEI data (including FEI = 0) was included in the model. The r^2 values for each model, the predictor coefficients, and p-values for each predictor in each model are shown in Table 5. For the East Branch, we could not find a successful model; no predictors were significant in any model runs regardless of which predictors were included. The most successful model generated for the West Branch also used the same predictors as the Entire Stream model except bedrock exposure because the West Branch does not contain bedrock exposure in the channel. The model generated from the three predictors for the main stem had a higher r^2 value, however the bedrock exposure predictor in this model is increasing probability for erosion (coefficient with a negative value), which is incorrect. Furthermore, the *SP* term in this model is not significant, nor is the intercept. For the main stem, we did not find a successful model. All versions of the models on the Main Stem produced coefficients with incorrect sign, did not have significant predictors, and/or had r^2 values of less than 0.01.

Threshold Model

While the logistic model has limited value because it is difficult to actually incorporate our knowledge of how streams work into it, the threshold approach allows us to use our knowledge of how and where North Shore streams erode to develop a predictive model. We developed three versions of the threshold model, which are listed in Table 6 along with their accuracy statistics, as described in the Methods. A map of the results of Model 1, which includes all three predictors, is shown in Figure 16a. For Amity Creek, the percent accuracy for all points for the three models (Models 1, 2, and 3) vary from 70.7 - 72.7%. while percent accuracy for FEI $\geq$ 2 vary from 73.4 - 86% (Table 6). Model 1, which includes all three predictors and is shown in Figure 16, had the highest threshold index, which is a measure of high accuracy of points with FEI $\geq$ 2 and a low rate of over-predicted points (See Methods).

For comparison, we also calculated the statistics described above for the logistic model (Table 6). These calculations were based on 25 m prediction points, resulting in a total number of points of 484. The output of the logistic model is a continuous dataset, so we had to set a threshold in order to compare it to the threshold models. Based on a break in the distribution of the data (Figure 15), we chose a threshold of 0.2. The percent accuracy for all points for the logistic model (35 % accuracy for all points) is lower than any version of the threshold model. In fact, it is less than the percent accuracy for a randomly-generated model, which had 42% percent accuracy for all points. If the logistic model threshold is adjusted up to a higher probability, the accuracy is further decreased. At lower values, the percent accuracy for all points improves, but the percent of points over-predicted also significantly increases.

After developing our threshold model on Amity Creek, we applied it to the Talmadge River (Figure 16b). The percent accuracy for all points range from 64.3 - 66.7% (Table 6), while the percent accuracy for FEI $\geq$ 2 are much lower, ranging from 31.6 - 36.8%. Model 4, which was not completed on Amity, is a model that consists only of *SP* and bluff proximity. This version of the model, which does not include bedrock, was included because MGS bedrock exposure does not have a significant correlation with FEI on the Talmadge River.

Table 6: Threshold Models				
Amity Creek				
Model Details	Model 1	Model 2	Model 3	Logistic Model
Stream Power	>15,000	-	>15,000	-
Bluffs	>2m, within 7m	>2m, within 7m	-	-
Bedrock Exposure	within 5m of Manual	within 5m of Manual	within 5m of Manual	-
Model Statistics*	Model 1	Model 2	Model 3	Logistic Model**
Percent Accuracy for All Points	70.7	71.3	72.7	34.9
Percent Accuracy for FEI ≥ 2	73.4	81.8	86.0	10.4
Percent of Points Over-predicted	12.8	17.5	18.6	10.1
Percent of Points Under-predicted	16.5	11.2	8.7	55.0
Threshold Index	5.7	4.7	4.6	1.0
Total Number of Points	6051	6051	6051	484
Talmadge River				
Model Details	Model 1	Model 2	Model 3	Model 4
Stream Power	>2.7	-	>2.7	>2.7
Bluffs	>2m, within 5m	>2m, within 5m	-	>2m, within 5m
Bedrock Exposure	MGS Map	MGS Map	MGS Map	-
Model Statistics*				
Percent Accuracy for All Points	66.7	65.3	64.3	44.0
Percent Accuracy for FEI ≥ 2	31.6	31.6	36.8	92.1
Percent of Points Over-predicted	7.0	8.4	11.3	53.0
Percent of Points Under-predicted	26.3	26.3	24.3	3.1
Threshold Index	4.5	3.8	3.2	1.7
Total Number of Points	2688	2688	2688	2688

* See Methods: Development of Predictive Model for definitions of each statistic shown here. The thresholds used for each predictor in each model are shown under Model Details. **To calculate these statistics for the logistic, model it was necessary to choose a threshold in the output probabilities. We used a threshold of 0.2 or greater. At prob. ≥ 0.2 and FEI ≥ 2 or at prob. < 0.2 and FEI < 2, a given point was deemed accurate.

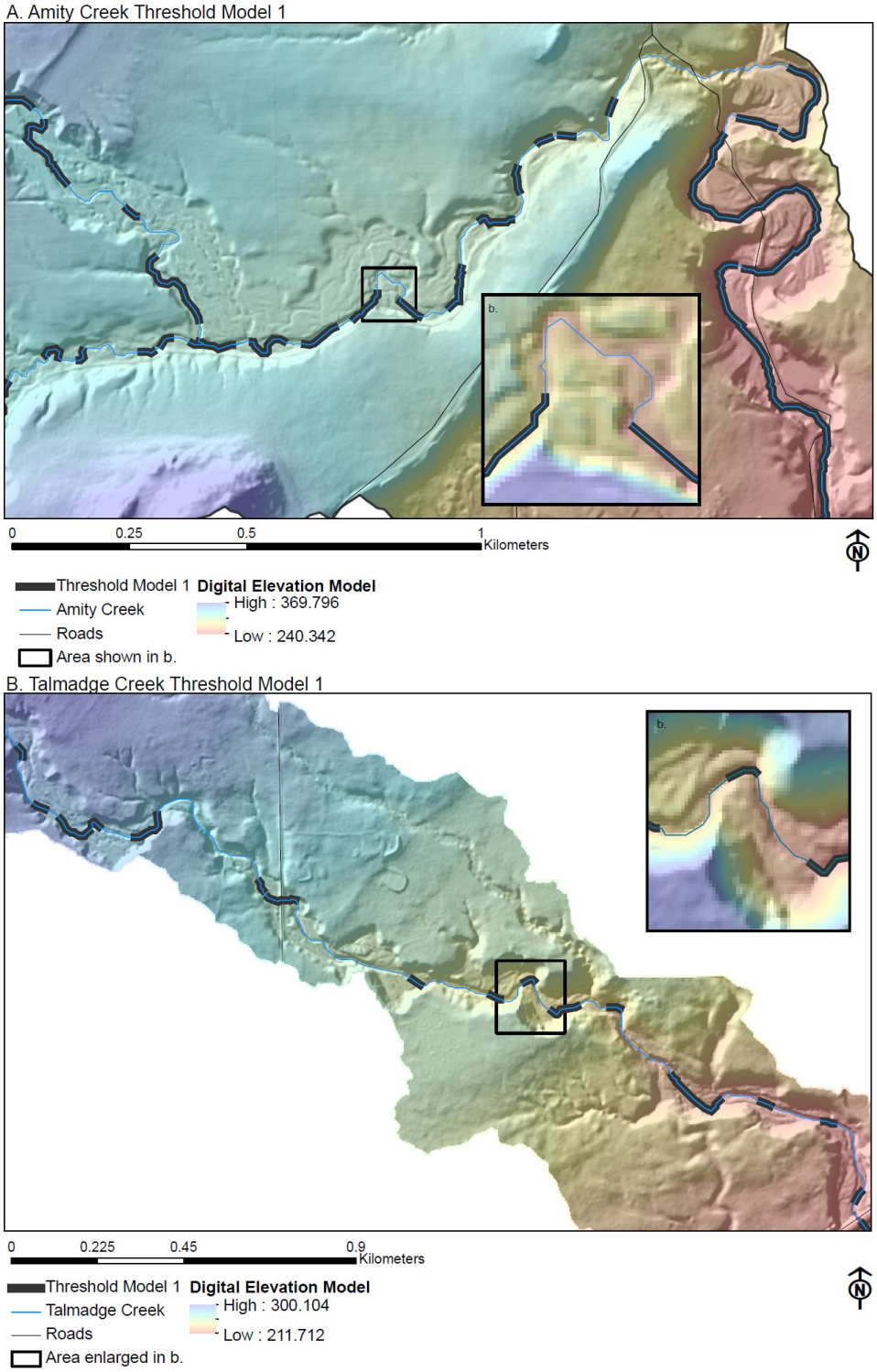

Figure 16. Results of Threshold Model 1 for Amity Creek (A), and Talmadge River (B). Reaches highlighted in grey indicate erosion hotspots. Stream power, 2m bluff proximity, and Manual bedrock exposure were included in Threshold Model 1.

Discussion

Assessment of Predictors

In order to determine the most effective predictors for erosion potential, we decided to focus mainly on the comparison of predictors to the Field Erosion Index surveys, because this dataset had the largest number of data points. While the BEHI surveys generally agreed with the conclusions we drew from the comparison to FEI surveys, the regressions are not as strong, nor as significant, probably due to a limited number of data points. Based on the comparison of GIS predictors and Field Erosion Index Surveys, *SP*, bluff proximity, and bedrock exposure are all potentially useful predictors of erosion potential. Angle of impingement and K factor did not correlate with the field data.

We calculated angle of impingement along the stream network, so by nature it is dependent on accurate network delineation. Small errors in the network delineation may have resulted in increased scatter in our data. However, the most significant caveat of angle of impingement is difficulty determining an appropriate "ruler" to use for the calculation. The angle of impingement is highly dependent on the ruler used, or distance along which the value is calculated. For a given meander, the largest change in angle should be measured every quarter of a wavelength. If the ruler is smaller than a quarter of a wavelength, some amount of change over the meander is still recorded. However, if the ruler is greater than a quarter of a wavelength, the calculation risks missing the curve completely. In other words, if the ruler is longer than the meander itself, it may not calculate any change when there is in fact a meander (Figure 17). For that reason, we chose a small ruler, of 5m, to prevent missing any meanders. However, by doing this, we effectively dampened the signal produced by high amplitude/large wavelength meanders, as measuring the change every 5m along those curves produces only a small change. The bend curvature, or the radius of curvature divided by the channel width, may be more useful but would be difficult to develop an automated system to extract radius of curvature from remote data.

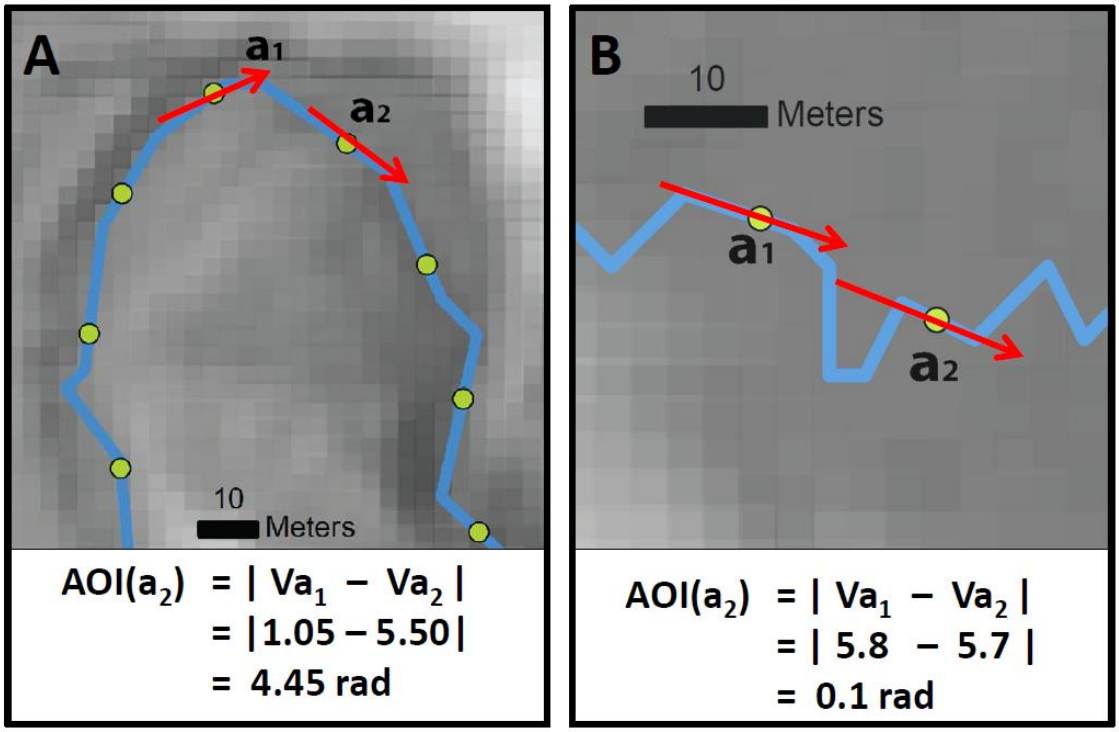

Figure 17. Example calculations of angle of impingement for points a_2. The ruler, or spacing between the points, in both examples is 25m. In A, the ruler is almost a quarter of the wavelength of the meander, resulting in a high angle of impingement. In B, the ruler is much greater than one quarter of the wavelength, resulting in a very low angle of impingement despite the tight meander between the points of interest. In order to record change in angle over the meander shown in B, the ruler used must be shorter. In streams with variable meander wavelength, one ruler length is not suitable for the entire stream and this calculation becomes difficult to automate.

We know that around tight bends, direct hydraulic action on the cut bank due to secondary circulation results in an increase in shear stress, but we did not observe correlations between angle of impingement and FEI for Amity (entire stream), for Amity's West Branch, or for Amity's main stem. We did see a weak positive correlation (r^2= 0.53, p-value = 0.07) on Amity's East Branch. Each segment of Amity Creek (Main Stem, East Branch, West Branch) has a distinct average meander size, and the 5m ruler may be suitable for the meander wavelength on Amity's East Branch, but not on the rest of Amity Creek. Angle of impingement may be a useful predictor in streams with

uniform meander wavelength, but has significant limitations due to difficulties identifying the most useful ruler to use in streams with variable meander wavelength.

Likewise, overall we did not see a correlation between the K factor extracted from the SSURGO soils dataset and our FEI surveys. We know that substrate material is very important for erosion potential in North Shore streams. The two major substrate types are bedrock, which has very low erodibility, and clay-rich glacial deposits, which have higher erodibility. The large polygons in the SSURGO dataset contain aggregated depth to bedrock data that are not representative of the depth to bedrock in the channel itself, and therefore are not useful for this study. The K factor values refer only to the soil/sediment itself, not bedrock. Within the K factor dataset, there is very little variation within the watershed. We extracted K factor values of the dominant component for each polygon, but the dominant component may represent as little as 51% of an entire polygon. The polygons are large, and by lumping together significant fine-scale variation, site-specific K factor values, like site-specific depth to bedrock data, are lost.

While the angle of impingement and K factor predictors did not prove useful, *SP*, bluff proximity, and bedrock exposure did show correlations with our FEI surveys. *SP* had a weak positive correlation with the FEI surveys for Amity. The stream power-based index depended only on the upstream area and slope of the channel. We assumed that erodibility was constant in this calculation because we accounted for the substrate erodibility in our bedrock identification and soil erodiblity analyses. However, the erodibility of the substrate is not constant throughout these watersheds. There are generally two major types of substrate with distinct erodibility characteristics in these watersheds: bedrock, which is not erodible at all at the timescale of interest, and clay-rich glacial deposits, including glacial till and glaciolacustrine deposits, which are more erodible relative to bedrock at the timescale of interest. If a reach has high *SP*, it may not necessarily have high erosion potential if the substrate is bedrock. Thus, it is very important when assessing erosion potential remotely to know the locations of bedrock channels. For this reason, we eliminated the known bedrock reaches (FEI = 0) from the *SP* regressions.

Despite removing these reaches, we still have a weak correlation between *SP* and FEI. For North Shore streams, the stream power-based erosion index may not be as valuable as it is in other watersheds where erosion potential spikes at knickpoints with greater slope relative to the rest of the watershed (e.g. Gran et al. 2007; Finlayson et al., 2002; Snyder et al., 2000). These types of studies focus on long-term erosion, and especially in bedrock streams. In North Shore streams, slope gradually increases towards the outlet. Streams generally flow through transport-limited reaches in the upper parts of watersheds. As the slope increases towards the outlet, streams transition to detachment-limited step pool, cascade, and bedrock reaches closer to the outlet, where the stream has incised further due to the drop in base level after the last glaciation. Erosional hotspots require both high stream power and erodible sediments, and this only occurs in the transition zone, where the streams have not incised down to bedrock yet. The weak correlation may also be due to additional scatter in the dataset introduced by the type and extent of erosion caused by a 500-year flood and an annual or biannual flood versus long-term erosion rates, which is also discussed in more detail below.

The delineation of steep bluffs adjacent to the stream is a very simple calculation that had a significant positive correlation with FEI surveys and BEHI surveys in both Amity Creek and the Talmadge River. We would expect this result, because our FEI data is at least partly dependent on the presence of bluffs. For example, we would not expect slumps (FEI = 4, 5) to occur along a reach unless a steep valley wall is present *to* slump. While areas that were completely scoured (FEI = 6, 7) in the flood do not depend on the presence of a bluff to be scoured, complete scour often occurred on bluffs adjacent to the stream. The major limitation of this analysis, like the stream power-based erosion index, is the presence of different substrate materials. If a bluff is made of bedrock, erosion potential should be very low, while a bluff consisting of glacial sediments should have erosion potential that is quite high. This analysis is definitely most useful with either prior knowledge of the watershed or bedrock outcrop maps. Even so, if prior knowledge is not available, this analysis may still be a useful way to identify field locations to investigate further.

To be useful predictors of erosion, both *SP* and bluff delineation depend on knowing the exact locations of bedrock exposure, because high *SP* and steep bluffs only influence sediment input if the channel is not bedrock. For many North Shore streams, bedrock exposure data are unavailable or the only available data are from MGS geological maps. The scale of these maps is 1:24,000 scale and the polygons are very generalized and do not match our more detailed bedrock exposure field data.

The ability to map bedrock exposure remotely may be the key to successful erosion potential prediction over a large area. Previous authors have used feature extraction tools for ArcMap to map landforms using texture, reflectance, elevation and intensity patterns from different datasets. This is a common practice to map land use trends such as forest, logged areas, urban areas, etc. We attempted to use that technique to map bedrock exposure along the channel corridor in Amity Creek using the Feature Analyst tool. We found that while the manual bedrock exposure map did a better job, Feature Analyst bedrock correlated well with the FEI scores.

The Feature Analyst bedrock exposure map was generated using remote data, but we used field data as well as the MGS outcrop maps (Hobbs, 2002; Hobbs, 2009) to identify outcrops on the air photos for our initial bedrock training map. Therefore, this map was not generated strictly from remote data and prior knowledge of outcrop exposure was necessary. The high-resolution air photo that we used for this exercise was taken in spring during leaf-off, and contains extensive shadows which complicated the process of visually identifying outcrop by both user and the program. In this photo, leaf-off deciduous forest was nearly indistinguishable from bedrock outcrop. In addition to the difficulties seeing the bedrock outcrop in the air photo, in some areas along Amity bedrock outcrops along the creek are overlain by thick layers of clay till that may or may not have high erosion potential. These areas are probably impossible to delineate from air photos as the bedrock outcrops are nearly vertical and are underneath surficial sediments that mask them from above.

To improve the predictive power of this method, it may be useful to make use of other air photos taken at different times. The City of Duluth had 4-band air photos with 3-inch resolution collected with the LiDAR data in spring 2011. These photos, which were

unavailable at the time of this research, show the potential to allow identification of bedrock outcrops strictly from the photo without prior knowledge of the location of bedrock outcrops. However, even the best photos may still pose challenges in certain areas due to the nature of North Shore watersheds, which are highly forested with narrow, incised creeks often located in confined valleys. These characteristics create shadows and mask the creek with dense forest. Furthermore, these high-resolution air photos are very large and difficult to analyze due to computing limitations.

We mapped bedrock exposure using Feature Analyst for Amity Creek only due to limited time and resources. This exercise was limited by the computing power of our machines and the huge size of the datasets we were working on. For example, the size of the air photo of 300-meter corridors along the stream network for the entire watershed was 3.3 GB. We also did not have access to high-resolution air photos for the other two watersheds of interest. Further efforts to complete this exercise using these additional datasets may prove more useful.

This tool did help us create a map of bedrock outcrop for Amity Creek, but the Feature Analyst bedrock did not match the FEI data as well as our manual bedrock exposure and FEI. We also used the MGS map as another comparison. At FEI ≥ 1, the MGS bedrock data showed up to 40% of points near bedrock, indicating the dataset is inaccurate. The resolution of the MGS dataset is not adequate to use for this purpose. For the Talmadge River, the only bedrock exposure dataset available was the MGS bedrock exposure map. On the Talmadge, we did not find a good correlation between the MGS bedrock exposure and FEI either. Prior knowledge of outcrop exposure in the watershed could greatly improve erosion potential predictions. If future maps of surficial and bedrock geology included higher-resolution bedrock-exposure data, it may be more useful for prediction of erosion potential.

Assessment of Field Surveys

Bank Erosion Hazard Index surveys are commonly used by watershed managers to assess erosion hazard during a typical annual flood (e.g. Clar et al., 1999; Hansen et al., 2010; Van Eps et al., 2004). These surveys depend on the ability to identify bankfull

height, which is the stage of the stream at which it is spilling onto the floodplain, and is typically defined as a 1 - 2 year flood (Williams, 1978). This is the stage of the river that has been shown to complete the most geomorphic change over time due to the combination of relatively high frequency and magnitude (Wolman and Miller, 1960). It is possible to identify bankfull using banks and bent vegetation indicators, but it is not always easy and often requires assessment of long lengths of the stream if there are no indicators directly at the site. In addition, the process of bankfull identification is inherently subjective. The assessment of percent vegetation cover, root density, root depth, and the measurement of bank angle (due to the natural variability of bank angles) are all also subjective. To reduce subjectivity error associated with multiple observers, I completed all of these surveys myself.

To complicate matters further, many of the bankfull indicators on these streams were eliminated by the 500-year flood that the field area experienced in June 2012. In Amity Creek, 11 surveys were completed after the flood, and 17 surveys were completed prior to the flood. All of the BEHI surveys on the Talmadge and French Rivers were completed after the flood. This no doubt introduced additional error into the BEHI measurements on all streams. Despite the subjectivity and change in conditions mid-field season, relative erosion hazard as assessed with these surveys, from very low erosion potential areas compared to very extreme erosion potential areas, should still be valid.

More significant than the inherent error with these BEHI surveys, which would be very difficult to eliminate, is the limited number of data points collected, especially along the Talmadge and French Rivers. This inadequate number of surveys collected was due to field help, weather, and time constraints, and the addition of the Field Erosion Index Surveys following the flood. The inadequate number of datapoints collected, along with the inherent error in those points is at least partially responsible for the limited statistical significance of the predictors versus BEHI data regressions. For that reason, for our central comparison, we concentrated on the Field Erosion Index survey data.

The Field Erosion Index was developed in response to the flood event that the Duluth area experienced in June 2012. This storm provided an opportunity to record evidence of large-scale geomorphic change in response to a 500-year flood. We assumed

that virtually all areas that would erode in a typical annual flood would definitely erode during the 500-year event. In other words, if our erosion potential model is robust, we would assume that all areas predicted to have high erosion potential should erode in a 500-year event, which may not be true for an annual event.

However, there may be a fundamental difference between erosion due to an annual flood and erosion due to an extreme event like a 500-year flood event. The additional discharge may initiate erosion in areas that would not erode in a typical annual event, and unpredictable variables like movement or buildup of debris could exacerbate erosion in some areas. This may be one of the reasons that our correlations between *SP*, bluff proximity and angle of impingement for Amity and/or the Talmadge are not very strong. For example, in the Talmadge River watershed there were sites with high FEI values with relatively low *SP* and angle of impingement. If these areas were influenced by additional fine-scale variation during the 500-year flood event, such as a log jam that directed the thalweg into a bank during the peak flow in an area that does not typically have a high angle of impingement or high *SP*, the FEI score would be very high despite relatively low predictor values for *SP* values and angle of impingement. However, the extent of this influence, especially in the Talmadge watershed, is unclear.

Logistic Model

The statistical model developed for Amity Creek using predictor data and the Field Erosion Index dataset was not as robust as hoped for with the highest r^2 value of just 0.2149, indicating very low predictive power. The highest probabilities for erosion often fall in areas where bedrock is exposed (Figure 14 - model results, Figure 9 - FEI results). This is due to the fact that the areas in the watershed with high *SP* tend to also be areas that have bluffs and/or bedrock exposure. Bluffs along the channel indicate a confined valley, which could restrict meandering and result in increased slope and increased *SP* in that area. Furthermore, increased incision rates due to local areas of high *SP* can result in incision down to the bedrock. In areas where the stream flows through bedrock reaches, *SP* tends to be high due to high slopes controlled by the bedrock geology, as well as confined bedrock valleys. Additionally, bedrock is typically only

exposed in reaches near the outlet, where drainage area is large, which also increases *SP*. Even though our model includes a bedrock term, it seems the *SP* and bluff terms "overpower" it resulting in a prediction of high probability for erosion even in areas that are bedrock. However, if bedrock points are removed from the model all together, the predictive power of the model drops substantially, to $r^2 = 0.08$.

In addition to the predictors identified above, we also attempted to use several other variables in our model. Because we know that angle of impingement may not be important unless the *SP* is high, and that the ruler over which we measure angle of impingement is very important, we used angle of impingement calculated over 5 meters, 10 meters, 20 meters, and 30 meters in our model. We also tried to scale the various angle of impingement calculations by the *SP* in an attempt to account for meander size variability from upstream reaches to reaches near the outlet. However, the angle of impingement was not significant in any versions of our model for the entire dataset or for individual branches, so it was left out of the model reported here. While there is a general trend of increasing meander amplitude towards the outlet, individual bend sizes are highly variable, so simply scaling the ruler for angle of impingement is ineffective. Measuring the angle of impingement for each meander bend individually with an appropriate may be more useful but would be time-intensive, especially for large watersheds.

We also substituted the Feature Analyst and the MGS bedrock exposure data for the manual bedrock exposure data in our model, but these both decreased the predictive power of the model significantly. This demonstrates, again, how necessary an accurate map of bedrock exposure is for identifying erosion hotspots.

We attempted to develop models particular to the individual branches of Amity. The East Branch and the main stem were impossible to develop models for. When applied to the West Branch, the bluff index and log *SP* predictors were still significant predictors; however the r^2 for the model dropped to 0.12. The range of values for each predictor can be significantly reduced for each individual branch compared to the entire stream dataset. This may be one reason for the differing predictive power of the variables on the different segments of stream. Furthermore, the lack of bedrock outcrop in the West

Branch may reduce the complications in predicting erosion due to bedrock's low erodibility, making it an easier segment to model.

Overall, a model with an r^2 value of only 0.2 has very limited predictive ability, and in fact the predictions are incorrect. While the predictors identified in this study generally do correlate with erosion potential, it appears that developing a statistical model to quantitatively predict erosion potential is not possible with our datasets. Due to the limitations of this model and the lack of accurate bedrock exposure data for the Talmadge, we did not apply the model to the Talmadge River.

Threshold Model

An alternative approach to developing a predictive model is using our understanding of the physical processes occurring in the streams to define thresholds above which reaches may be more prone to erode. Erosion is a threshold-dependent process in which a critical shear stress must be reached in order to entrain sediment and transport it downstream. Therefore, a threshold-based model may be more useful than a statistical model. We used the three predictors that we determined were statistically significant to develop our model on Amity Creek (Figure 16a), and results of the threshold model were significantly better than results of the logistic model (Table 6).

While this model is based on the actual processes occurring in bank erosion in Amity Creek, the selection of thresholds can be somewhat arbitrary. For example, it was difficult to determine an appropriate *SP* threshold to use in the model. In order to fit our data, we chose a value that maximized the percent accuracy of points with FEI ≥ 2 while minimizing the percent of points over-predicted. In reality, the *SP* threshold required to entrain sediment is dependent on site characteristics like roughness, grain size, vegetation, planform geometry, etc, and can vary throughout the watershed. Regardless of the limitations of this type of model, it was more successful than the logistic model. The most accurate version of the threshold model for Amity Creek, Model 3, included *SP* and bedrock exposure, and successfully predicted 73% of points spaced every 2 meters along the stream (Figure 16a).

We applied this model to the Talmadge with more limited success. While percent accuracy for all points was just a little lower than the accuracy for all points for Amity Creek, the percent accuracy for points with FEI ≥ 2 was significantly less than for Amity (31.6 - 36.8% on Talmadge compared to 73 - 86% on Amity). One potential reason for this is differences in the extent of erosion experienced by the two watersheds during the June 2012 flood event that our FEI is based on. For the Talmadge River, 38% of the points extracted every 2 m had FEI ≥ 2, while on Amity, 62% of the points had FEI ≥ 2. However, we did scale the *SP* threshold to the Talmadge River in order to account for the difference in size between the two watersheds. The lower accuracy on the Talmadge is likely attributable in part to the limited resolution of the bedrock exposure data available on the Talmadge. We used the MGS bedrock exposure maps, but they do not seem to be at a high-enough resolution for this scale of project. In fact, the correlation between MGS bedrock exposure and the FEI on the Talmadge is poor, and the trend is opposite from what is expected (Figure 12E).

Issue of Scale in Predicting Erosion Potential

Spatial Scales

Anecdotal evidence collected while completing field surveys indicates that fine-scale variability such as changes in vegetation patterns and movement and buildup of large and small woody debris may play a significant role in where erosion occurs during a given event. These fine-scale variables may have a significant influence on erosion potential, especially in large-scale flooding events, but also in annual floods. One of the major caveats of this study is the inability to predict these fine-scale variables using remote data. The absence of LWD in an erosion potential model may result in some areas with high erosion potential going undetected for a given event. Large woody debris can be mobile, so individual areas with elevated erosion potential associated with LWD may change through time.

The role of woody debris in streams has been studied extensively in mountain streams (e.g. Keller & Swanson, 1979; Curran & Wohl, 2003; Montgomery & Abbe 2006; Oswald & Wohl, 2008; Wohl & Cadol, 2011). Large wood can enter the stream

through bank failure, mass wasting, blowdown, or collapse due to ice loading. Due to the small size of North Shore streams, in an annual flood, channel-spanning LWD is likely to remain at or near the input site, while smaller LWD typically moves during each flood (Merten et al., 2010). Woody debris is ecologically valuable as it can increase channel and floodplain roughness, armor the banks, form dams and slows flow, and provide habitat for organisms. Debris dams can cause scouring under the dam and just downstream, or in areas where the flow is directed into a bank. Deposition often occurs in the slow waters upstream from the dam (e.g. Keller and Swanson, 1979). In some cases log jams can result in stream avulsions (e.g. Montgomery & Abbe, 2006, O'Connor et al., 2003). Log jams created in a large event like this are likely to persist for a long time, until another large event when they are mobilized again (Abbe & Montgomery, 1996; Oswald & Wohl, 2008).

During our field erosion surveys, we observed many debris jams that spanned the river (Figure 18a & b). Because of the magnitude of the 2012 flood, LWD recruitment into the stream would have been quite high, and LWD would have been more mobile than in an annual flood. This additional mobility allowed LWD to be transported downstream, where it was caught and formed large debris dams. We noticed that these debris dams were often associated with areas of significant erosion and deposition. In addition, small-scale changes in riparian vegetation type and density may also influence erosion hotspots. Vegetation patchiness can influence bank strength, infiltration, and bank loading. For example, during our field studies we noticed that bank erosion was common in areas where there were patches of coniferous forest with limited understory. These localized features may be very important variables in predicting erosion potential, especially at an event scale, but are difficult to incorporate into an erosion potential model that incorporates only remote data. However, Feature Analyst pattern analysis may be useful to identify vegetation patches in the riparian zone using LiDAR and high resolution air photos. Using Feature Analyst to map vegetation patchiness requires additional technique development, and would not be able to identify LWD unless very recent photos were available.

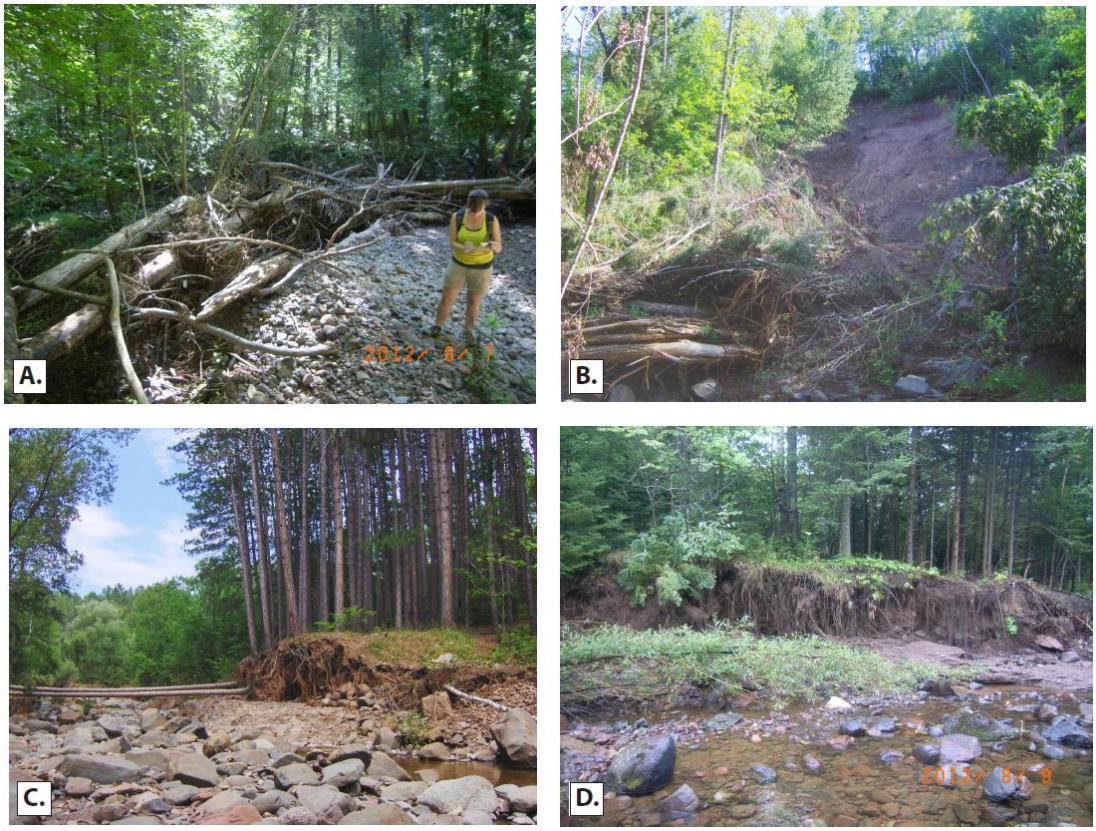

Figure 18: Examples of erosion potentially linked to fine-scale features undetectable by remote datasets. Images A and B are examples of debris jams observed along Amity Creek during FEI surveys. The cobble bar in the foreground in image A was deposited behind the large debris jam in the background. Image B shows a slump that resulted in a debris dam that may have directed flow against the exposed bluff. Images C and D show examples of coniferous forests that may have influenced erosion due to loading and lack of understory vegetation to stabilize banks.

Temporal Scales

In order to identify areas with high erosion potential to target for management techniques, we must also consider the timescale of interest. Because we are interested in areas that contribute significantly to the total sediment input, we are interested in erosion during the effective discharge. As discussed above, the effective discharge in a graded river generally occurs at a recurrence interval of 1-2 years (Knighton, 1998). The BEHI method of assessing erosion hazard is based on bankfull (which is established by the effective discharge) measurements, and therefore should be highly applicable for comparison with our predictions. Our FEI surveys were based on observations of erosion

caused by a single 500-year flood event. The discharge during this event was much greater in magnitude than a 1- or 2-year flood. Fundamentally the variables that affect erosion are the same (erodibility, stream power, radius of curvature, storage, vegetation, etc), but the relative importance of each variable may be different in a 1- or 2- year flood and a 500-year flood. For example, in North Shore streams, angle of impingement may be the best erosion potential predictor for an annual flood when flow stays within its banks, but in a 500-year flood, the flow may cut off major meanders, therefore the angle of impingement calculated for the pre-flood stream network would not represent the flow path during the flood. Additionally, small-scale spatial variation in the watersheds (e.g. vegetation patchiness, and LWD) may not be equally significant in annual floods and 500-year floods.

Furthermore, the important variables for identifying erosion hotpots that facilitate long-term channel evolution may not be the same as variables that influence erosion in any given event. Stream power, for example, should remain constant and predict locations where incision is occurring at any given time. On the other hand, locations of channel-spanning LWD or locations of tight bends may predict erosion in a single event, but may change through time. The FEI dataset, which we used to design our model, consists of data from just a single event. Because it was a very extreme event, we would assume it includes the erosion hotspots that would facilitate long-term channel evolution, but it also includes areas that only eroded in that event and may not erode repeatedly through time. These areas add scatter to the dataset. A more robust comparison would involve the comparison of erosion predictions to channel migration rate or long-term incision rate data. We attempted to calculate migration rates in Amity using historic air photos, but this was not possible due to the forested nature of the watershed. Dense forest in the watershed makes it very difficult to accurately georeference historic air photos, and makes it difficult to see the stream network itself in many areas.

Conclusions: Applications of this Project and Future Work

Three successful predictors for erosion hotspots in North Shore streams were identified based on analyses done on three rivers: the stream power-based erosion index,

bluff proximity, and bedrock exposure. In North Shore streams, *SP* tends to increase towards the outlet, due to the concave-down nature of North Shore stream long profiles. This is a general trend that can be used to locate sensitive reaches in a watershed on a very broad scale. *SP* and bluff proximity are simple analyses that, in conjunction with bedrock exposure data, could allow watershed managers to identify areas that are more susceptible to erosion. Identifying a way to delineate bedrock exposure is imperative, but also perhaps the most difficult analysis. If high-resolution bedrock exposure data are available, then *SP* and bluff delineation can be combined to create a threshold-based erosion hotspot prediction model. This type of model was around 70% accurate where high-resolution bedrock datasets were available. These would be helpful as first-round analyses to locate potential field sites, especially in watersheds where managers already have background knowledge of watershed characteristics such as vegetation patterns, land use, and surficial geology.

The combination of these analyses into a statistical erosion potential model was largely unsuccessful. The intricately-linked nature of the predictors resulted in areas with bedrock exposure being predicted to have the highest erosion potential, as they are also areas with high *SP* and nearby bluffs. In these watersheds slope and area increase towards the outlet, resulting in very high *SP* values in areas near the outlet which overwhelms the other predictor variables. In addition, the limitations of the field dataset and discrepancy between erosion in a 500-year event compared to a 1-2 year event adds additional scatter in our datasets that limits the development of a highly-predictive logistic model.

Perhaps the most significant limitation of our study was the absence of publicly-available remote datasets that include detailed bedrock exposure for the North Shore. SSURGO data proved to have inadequate resolution to predict reach-scale hotspots, and creating bedrock exposure maps using air photos and LiDAR data for the entire North Shore was impractical due to a lack of availability of high-resolution air photos and limited computing power. Other major limitations of our project included an inability to predict fine-scale variation of vegetation and LWD, which both influence erosion potential for a single event, using remote data. It may be possible to use Feature Analyst to identify vegetation patches in the riparian zone, in a similar way to how we mapped

bedrock exposure, which could improve future studies. Another limitation was a discrepancy between our predictors, which aim to predict erosion hotspots that contribute to significant geomorphic change over time and turbidity issues in North Shore streams, and our main field dataset, which was based on erosion caused by a 500-year flood event.

This study and the methods described herein would benefit greatly from future research. First, a comparison of predictors with a more rigorous BEHI survey dataset would help distinguish between long-term erosion hotspots and sites that just eroded due to the magnitude of the 500-year event. This could improve the correlations shown in Figures 11 and 12. A long-term erosion dataset, which could be estimated by calculating of migration rates along the stream through time, would likely be very helpful for distinguishing between sites that experience repeated erosion and sites that eroded in a single event. However, this may not be possible due to limitations in historic air photos. Overall, more/improved field data, including more BEHI surveys and a long-term erosional dataset, to use for comparison would contribute to a better understanding of the relative importance of controls on erosion in North Shore streams.

Our work illustrates the importance of knowing where bedrock is exposed in the channel in North Shore streams for predicting erosion. In most North Shore streams, this is not available at a high enough resolution or at all, so prior knowledge of the watershed is necessary. While our goal was to identify erosional hotspots for all of the watersheds shown in Figure 1, we did not apply our model to those watersheds due to the lack of high-resolution bedrock exposure data available for those areas. We describe a method that could be applied to those watersheds to identify bedrock exposure remotely using air photos and LiDAR data, but to be effective, this method needs to be refined and tested.

References

Abbe T. B. and Montgomery D. R. (1996). Large woody debris jams, channel hydraulics and habitat formation in large rivers. *Regulated Rivers Research & Management*, 12(23), 201-221.

Abernathy B. and Rutherfurd I. D. (2000). The effect of riparian tree roots on the mass-stability of riverbanks. *Earth Surface Processes and Landforms,* 25(9), 921-937.

American Society of Civil Engineers (ASCE) Task Committee on Hydraulics, Bank Mechanics, and Modeling of River Width Adjustment. (1998). River width adjustment: I. Processes and mechanisms. *Journal of Hydrualic Engineering* 124, 881 – 902.

Barrett J. C., Grossman G. D., and Rosenfeld, J. (1992). Turbidity-induced changes in reactive distance of rainbow trout. *Transactions of the American Fisheries Society,* 121, 437-443.

Begin Z. B. (1981). Stream curvature and bank erosion: A model based on the momentum equation. *The Journal of Geology*, 89, 497-504.

Brown T. N., Host G. E., and Johnson L. B. (2011). Lake Superior Streams Sediment Assessment, Report. Natural Resources Research Institute, University of Minnesota Duluth. 34 p.

Clar M., Outen D., and Gemmill E. (1999). "Integrated Stream Stability Assessment and Water Quality Modeling for A Watershed Study." ASCE 26th Annual Conference on Water Resource Planning and Management, Annual Conference on Environmental Engineering.

Crouse A. B. (2013). Land Use/Land Cover and Hydrologic Effects on North Shore Tributary Water Quality. (Masters Thesis) University of Minnesota Duluth. 118 p.

Curran J. H. and Wohl E. E. (2003). Large woody debris and flow resistance in step-pool channels, Cascade Range, Washington. *Geomorphology,* 51(1), 141-157.

Czuba C. R., Fallon J. D., and Kessler E. W. (2012). Floods of June 2012 in Northeastern Minnesota. USGS Scientific Investigations Report 2012-5283. 52 p.

Day, R. and Axten, G. (1989). ”Surficial Stability of Compacted Clay Slopes.” *Journal of Geotechnical Engineering*, 115(4), 577–580.

Detenbeck N. E., Elonen C. M., Taylor D. L., Anderson L. E., Jicha T. M., and Batterman S. L. (2003). Effects of hydrogeomorphic region, catchment storage and mature forest on baseflow and snowmelt stream water quality in second-order Lake Superior Basin tributaries. *Freshwater Biology,* 48, 912 – 927.

Detenbeck N. E., Elonen C. M., Taylor D. L., Anderson L. E., Jicha T M., and Batterman S. L. (2004). Region, landscape, and scale effects on Lake Superior tributary water quality. *Journal of the American Water Resources Association,* June, 705 -720.

Easson G., and Yarbrough L. D. (2002). The effects of riparian vegetation on bank stability. *Environmental & Engineering Geoscience*, 8(4), 247-260.

Farrand W. R. (1969). The Quaternary history of Lake Superior. In *Proceedings of the 12th Conference on Great Lakes Research.* p. 181-197.

Finlayson D. P., Montgomery D. R., and Hallet B. (2002). Spatial coincidence of rapid inferred erosion with young metamorphic massifs in the Himalayas. *Geology*, 30, 219 – 222.

Fitzpatrick F.A., Peppler M.C., DePhilip M.M. and Lee K.E. (2006). Geomorphic Characteristics and Classification of Duluth-Area Streams, Minnesota. USGS Scientific Investigations Report 2006-5029.

Furbish D. J. (1988). River-bend curvature and migration: How are they related? *Geology*, 16(8), 752-755.

Furbish D. J. (1991). Spatial autoregressive structure in meander evolution.*Geological Society of America Bulletin*, 103(12), 1576-1589.

Gatto L. W. (1995). Soil Freeze-Thaw Effects on Bank Erodibility and Stability (No. CRREL-SR-95-24). US Army Corps of Engineers Cold Regions Research and Engineering Lab Special Report, 17 p.

Gran K. B., Hansen B., and Nieber J. (2007). Little Fork River channel stability and geomorphic assessment. Final Report to the MPCA Impaired Waters and Stormwater Program, 109 p.

Hansen B., Dutton D., Nieber J., and Gorham A., (2010). Poplar River sediment source assessment, Final Project Report to Minnesota Pollution Control Agency, University of Minnesota, 149 p.

Hickin E. J. (1984). Vegetation and river channel dynamics. *Canadian Geographer* 28, 111 – 126.

Hobbs H. C. (2002). Surficial Geology of the French River and Lakewood Quadrangles, St. Louis County, Minnesota. University of Minnesota and Minnesota Geological Survey Miscellaneous Map Series MAP M-127.

Hobbs H. C. (2009). Surficial geology of the Duluth Quadrangle, St. Louis County, Minnesota. University of Minnesota and Minnesota Geological Survey Miscellaneous Map Series Map M-187.

Hooke J. M. (1979). An analysis of the processes of river bank erosion. *Journal of* Hydrology, 42, 39 -62.

Huttner P. (2012). "Duluth "Mega Flood" sets new records; Quieter, drier forecast ahead" *Updraft with meteorologist Paul Huttner*. June 21, 2012. Minnesota Public Radio News. Accessed 12/18/2012. <http://minnesota.publicradio.org/collections/special/columns/updraft/archive/2012/06/duluth_mega_flood_records_quie.shtml>.

JMP, Version 10. SAS Institute Inc., Cary, NC, 1989-2013.

Keller E. A. and Swanson F. J. (1979). Effects of large organic material on channel form and fluvial processes. *Earth Surface Processes*, 4(4), 361-380.

Knighton A. D. (1973). Riverbank erosion in relation to streamflow conditions, River Bollin-Dean, Cheshire. *East Midland Geographer*, 6, 416 – 426.

Knighton A. D. (1974). Variation in width-discharge relation and some implications for hydraulic geometry. *Geological Society of America Bulletin*, 85(7), 1069-1076.

Knighton D. *Fluvial forms and processes*. New York, NY: John Wiley & Sons, Inc., 1998. 383 p.

Lauer J. W. (2006). Channel Planform Statistics, An ArcMAP Project. Part of the National Center for Earth-surface dynamics stream restoration toolbox, available at http://www.nced.umn.edu/content/tools-and-data.

Lecce S. A. (1997). Nonlinear downstream changes in stream power on Wisconsin's Blue River. *Annals of the Association of American Geographers*, *87*(3), 471-486.

Leopold L. B. and Maddock T. Jr. (1953). The Hydraulic geometry of stream channels and some physiographic implications. U.S. Geological Survey Professional Paper 252.

Leopold L. B. and Wolman M. G. (1957). River channel patterns: braided, meandering, and straight (pp. 37-86). Washington, DC: US Government Printing Office.

MPCA (Minnesota Pollution Control Agency), (2012). Minnesota's Impaired Waters and TMDLs, Impaired Waters List. <http://www.pca.state.mn.us/index.php/water/water-types-and-programs/minnesotas-impaired-waters-and-tmdls/impaired-waters-list.html Accessed 4/11/2013> Accessed 4/11/2012.

Merten, E., Finlay, J., Johnson, L., Newman, R., Stefan, H., & Vondracek, B. (2010). Factors influencing wood mobilization in streams. *Water Resources Research*, *46*(10).

Montgomery D. R. and Abbe T. B. (2006). Influence of logjam-formed hard points on the formation of valley-bottom landforms in an old-growth forest valley, Queets River, Washington, USA. *Quaternary Research*, 65(1), 147-155.

Montgomery D. R. and Buffington J. M. (1998). Channel processes, classification, and response. *River ecology and management*, 112, 1250-1263.

Montgomery D. R. and Gran K. B. (2001). Downstream variations in the width of bedrock channels. *Water Resources Research*, 37, 1841 – 1846.

Nanson G. C. and Hickin E. J. (1986). A statistical analysis of bank erosion and channel migration in western Canada. *Geological Society of America Bulletin,* 97, 497 – 504.

Neitzel G. (in prep) Monitoring event-scale stream bluff erosion with repeat terrestrial laser scanning: Amity Creek, Duluth, MN. (Masters Thesis) University of Minnesota, Duluth.

Nieber J. L., Wilson B. N., Ulrich J. S., Hansen B. J., and Canelon D. J. (2008) Assessment of streambank and bluff erosion in the Knife River watershed, Final Report to Minnesota Pollution Control Agency, University of Minnesota, 58 p.

O'Connor J. E., Jones M. A., and Haluska T. L. (2003). Flood plain and channel dynamics of the Quinault and Queets Rivers, Washington, USA. *Geomorphology*, 51(1), 31-59.

Oswald E. B., and Wohl E. (2008). Wood-mediated geomorphic effects of a jökulhlaup in the Wind River Mountains, Wyoming. *Geomorphology*, 100(3), 549-562.

Passalacqua P., Do Trung T., Foufoula-Georgiou E., Sapiro G., and Dietrich W. E. (2010a). A geometric framework for channel network extraction from LiDAR: nonlinear diffusion and geodesic paths, *Journal of Geophysical Research* 115, F01002, doi:10.1029/2009JF001254.

Passalacqua P., Tarolli P., and Foufoula-Georgiou E. (2010b). Testing space-scale methodologies for automatic geomorphic feature extraction from LiDAR in a complex mountainous landscape, *Water Resources Research*, 46(11), 17 p.

Pfankuch D. J. (1975). Stream reach inventory and channel stability evaluation: A watershed management procedure. U.S. Department of Agriculture, Forest Service. R1-75-002. Government Printing Office.

Renard K. G., Foster G. R., Weesies G. A., and Porter J. P. (1991). RUSLE Revised universal soil loss equation. *Journal of Soil and Water Conservation*, 46, 30–33.

Sigler J.W., Bjornn T. C., and Everest F. H. (1984). Effects of chronic turbidity on density and growth of steelheads and coho salmon. *Transactions of the American Fisheries Society*, 113, 142-150.

Simon A., Langendoen E. J., Collison A., and Layzell A. (2003, June). Incorporating bank-toe erosion by hydraulic shear into a bank-stability model: Missouri River, Eastern Montana. In *World Water and Environmental Resources Congress and Related Symposia*. American Society of Civil Engineers, Philadelphia, Pennsylvania. 70 – 76.

Sims P. K., and Morey G. B. (1972). "*Geology of Minnesota: a centennial volume*." Minnesota Geological Survey. 632 p.

Sklar L., and Dietrich W. E. (1998). River longitudinal profiles and bedrock incision models; stream power and the influence of sediment supply, *in*Tinkler, K. J., and Wohl, E. E., editors, *Rivers Over Rock: Fluvial Processes in Bedrock Channels:* Amercian Geophysical Union, Geophysical Monograph 107, Washington, D. C., 237–260.

Snyder N. P., Whipple K. X., Tucker G. E., and Merritts, D. J. (2000). Landscape response to tectonic forcing: Digital elevation model analysis of stream profiles in the Mendocino triple junction region, northern California. *Geological Society of America Bulletin*, 112(8), 1250-1263.

Stock J. D., and Montgomery D. R. (1999). Geologic constraints on bedrock river incision using the stream power law. *Journal of Geophysical Research: Solid Earth (1978–2012)*, 104(B3), 4983-4993.

Sweka J. A., and Hartman K. J. (2001). Effects of turbidity on prey consumption and growth in brook trout and implications for bioenergetics modeling. *Canadian Journal of Fisheries and Aquatic Sciences*, 58, 386-393.

Talling P. J. and Sowter M. J. (1998). Erosion, deposition and basin-wide variations in stream power and bed shear stress. *Basin Research*, 10(1), 87-108.

Thorne C. R. and Tovey N. K. (1981). Stability of composite river banks. *Earth Surface Processes and Landforms*, 6(5), 469-484.

Van Eps M. A., Formica S. J., Morris T. L., Beck J. M., and Cotter A. S. (2004). Using a Bank Erosion Hazard Index (BEHI) to estimate annual sediment loads from streambank erosion in the West Fork White River Watershed. In *Arkansas Watershed Advisory Group Conference Proceedings*, 7 p.

Verry E. S. (1987). The effect of aspen harvest and growth on water yield in Minnesota. *Forest hydrology and watershed management*, 167, 553-562.

Arnborg L., Walker H. J., and Peippo J. (1966). Water discharge in the Colville River, 1962. *Geografiska Annaler. Series A. Physical Geography*, 195-210.

Weithman A. S. and Anderson R. O. (1977). Survival, growth, and prey of Esocidae in experimental systems. *Transactions of the American Fisheries Society*, 106, 424-430.

Whipple K X. and Tucker G E. (1999). Dynamics of the stream-power river incision model: Implications for height limits of mountain ranges, landscape response timescales, and research needs. *Journal of Geophysical Research*, 104, 17661 – 17674.

Wright H. E. (1971). Retreat of the Laurentide ice sheet from 14,000 to 9000 years ago. *Quaternary Research*, 1(3), 316-330.

Williams G. P. (1978). Bank-full discharge of rivers. *Water Resources Research*, 14(6), 1141-1154.

Wohl E. and Cadol D. (2011). Neighborhood matters: Patterns and controls on wood distribution in old-growth forest streams of the Colorado Front Range, USA. *Geomorphology*, 125(1), 132-146.

Wolman M. G., and Miller J. P. (1960). Magnitude and frequency of forces in geomorphic processes. *The Journal of Geology*, 54-74.

Wynn T. and Mostaghimi S. (2006). The Effects of vegetation and soil type on streambank erosion, Southwestern Virginia, USA. *Journal of the American Water Resources Association*, 42(1), 69-82.

Zeitler P. K., Meltzer A. S., Koons P. O., Craw D., Hallet B., Chamberlain C. P., Kidd, W. S. F., Park S. K., Seeber L., Bishop, M., and Shroder, J. (2001). Erosion, Himalayan geodynamics, and the geomorphology of metamorphism. *GSA Today*, 11(1), 4-9.

Appendices:

A. GIS Procedures

The following are the detailed procedures that we used to delineate stream networks and calculate the GIS predictors used in this study. All of these procedures were completed using ESRI's ArcMap 10.0.

Hydrologic Conditioning of LiDAR Data & Network Delineation

We first cropped the 3-meter DEM to a rectangular area that included the entire watershed based on knowledge of the watershed from 1:24,000 USGS maps. We then delineated the basin using the Spatial Analyst Hydrology toolbox in ArcMap:

a. Fill – creates a new DEM with filled depressions, which allows flow vectors to continue downslope and not "dead end" in depressions.

b. Flow Direction – Creates a raster with each pixel containing values that represent the steepest downslope direction for that pixel, or the flow vector.

c. Flow Accumulation – Creates a raster with pixel values that represent the number of pixels upslope that flow into that pixel. This is the most rudimentary flow network.

d. Greater Than – This assigns a threshold in the accumulation raster, above which value of accumulation the pixel is deemed the stream network.

e. Conditional – This eliminates the data in all of the raster except in the stream network itself.

f. Stream to Feature – This converts the raster network to a vector stream network.

Once the stream network was delineated, we compared the network produced to USGS 1:24K stream networks, air photos and 3m DEM and hillshade itself to identify areas where the network is not correct. These are usually digital dams, or areas where a culvert or bridge creates a barrier to the flow. The process of correcting for these digital dams is called hydrologic conditioning. In order to remove the digital dams, we first created a shapefile (a dam-break shapefile) for each digital dam. In the dam-break shapefiles, we used the editor to draw a short line where we wanted to force the river to flow, across the digital dam. To determine the exact location of the line, we used the info button and identified the lowest point at the top of the dam, and the lowest point at the bottom of the dam, and connected those two points with the line. We recorded the elevation of the lowest point on the line, which is the elevation that we later assigned to the entire line.

Next we converted the dam-break shapefile to a raster. To do this, we used the Feature to Raster tool under in the Conversion Toolbox (making sure to set the processing extent, snap raster, and cell size to match the original DEM). Then, we reclassified the dam-break raster data. We used Reclassify (under 3D Analyst Tools) to assign new values to the raster as follows:

Old Values	*New Values*
No Data	0
0	1

Lastly, we re-assigned the new elevation data to the dam-break raster using the Con tool in the Spatial Analyst toolbox using the following inputs:

- Input- Reclassified dam-break raster
- Expression - if "value" = 0
- True- use 3-m DEM
- False – The elevation at the bottom of the dam-break line

The output from this last step was a DEM that is the same as the original DEM, except the values for the pixels in the dam-break raster across the digital dam have been replaced with the new elevation values. We repeated this process for each individual digital dam identified.

After creating this new DEM with pixels replaced crossing each digital dam, we then delineated the basin once again using the Hydrology Toolbox, using the new DEM. Once again, we compared the resultant stream network to the DEM, hillshade, and USGS 24K streams to check if it is accurate. In several cases, we had to go back and repeat the process because additional errors were identified. It is an iterative process, and it may be necessary to repeat the process multiple times depending on the purpose the network will be used for. We did not correct for errors that were in the very flat upland reaches of stream as they did not affect the main network and had low erosion potential. After a satisfactory stream network was delineated, the conditioned DEM, and flow direction/accumulation rasters produced from it, were used for all of the following analyses described here. Finally, we delineated the watershed by using the Watershed tool in the Hydrology toolbox and converting the resultant raster to a polygon.

Note: There are several methods that can be used to burn digital dams. For this project, this manual method was the most efficient. Alternatively, there is also a built-in function in ArcMap that is designed to allow automated stream burning: Spatial Analyst > Interpolation > Topo to Raster. We found that this tool was clunky and often crashed on the high resolution 3-meter DEMs. It may be effective with smaller datasets or increased computing power.

Creating Prediction Point File

We created a file with points spaced every 25m along the stream network and calculated each of our predictor variables at these points. This interval can easily be changed depending on the desired resolution. In order to create this point file, we exported the stream network to a new file, and then used the Split tool to split segments "Into Equal Parts". The Split tool lists the length of the segment selected, so we simply calculated the number of equal parts needed to break the selected segment into 25m segments. We repeated this for all segments. (*Note*: To split a stream segment into more than 100 reaches in Arc 10.0, you will need to download Service Pack 2. With the service pack, you are able to split a given segment into up to 1000 segments.) Next, we converted this stream file, with 25m stream segments, to a point file using Feature to Point. By checking the "Inside" option, this assigns all points to the line itself, ensuring that all points fall directly on the stream network. The output of this step created what we call the **predpts** file, which we used to extract data and sample rasters for calculation in the following analyses.

Stream Power-based Erosion Index (SP)

The stream power-based erosion index (*SP*) was calculated according to equation (2) above. In order to calculate *SP* in Microsoft excel at each of our **predpts**, we first extracted the drainage area (referred to here as accumulation) and the slope from the DEM. To do this, we first clipped the accumulation raster (created with the flow accumulation command while delineating the watershed) to the watershed boundary. Then, we "enlarged" the river. We did this to ensure that the data extracted was the accumulation in the stream itself (the maximum accumulation), not some value adjacent to the stream. To enlarge the river, we used the Focal Statistics tool in the Spatial Analyst toolbox, with the Maximum statistic and a 10 cell x 10 cell rectangle. The output of this analysis is an accumulation raster with the stream enlarged to be 10 cells wide.

Next, we extracted the data itself using the Sample tool in Spatial Analyst. Our input rasters were the DEM itself, and the accumulation raster with the enlarged river. The input point feature was the **predpts** file. We then exported the data as a comma-delimited text file, and opened it in Excel. Using the elevation data in the exported table, we calculated the slope at each point over 100 meters, and then calculated *SP* at each point according to Equation (2). We then imported the data back into ArcMap (using the Add XY Data tool) and checked to make sure the results were logical.

Angle of Impingement

We used the Planform Statistics tool (Lauer, 2006) to calculate angle of impingement. This tool can be downloaded directly from the National Center for Earth Surface Dynamics website (http://www.nced.umn.edu/content/stream-restoration-toolbox). Directions to install the extension and add the buttons to the toolbar in ArcMap are provided in a powerpoint on the website.

First, we prepared stream "bank" lines that we input into the Planform Statistics tool. We only have centerlines for our streams, but the inputs necessary for Planform Statistics are right bank and left bank lines. To approximate bank lines, we used the buffer tool to create right and left bank lines. We created a buffer 4m wide (2m on each side of the centerline, with flat ends), and then converted it to a line file (Polygon to Line tool in the Data Management toolbox). We then edited the line file to produce one file with two single-segment streambank lines, pointing downstream, that each parallel the stream centerline, and do not include any segments perpendicular to the stream centerline. Lastly, we exported each segment to its own shapefile, a right bank line and a left bank line. We prepared separate bank lines for each branch/tributary of the stream, and then compiled the data for all tributaries into one excel file at the end.

Next, we used the Planform Statistics centerline interpolation tool (the icon with the stream line with dots down the middle: ) and followed directions, inputting 5m for the distance between points (the ruler discussed above), and100,000 for the maximum number of points to find. We chose 5m because this ruler yielded the most success, but this may vary depending on the curvature of the stream. Occasionally at 5m, the calculation got "stuck" on sharp curves and did not complete the entire stream. If it did this, we edited the bank lines, removed the part that was completed, ran the program again on the remaining portion of the line, and merged the data together at the end in

Excel (see below). At shorter lengths, the program made significant errors (e.g. assigned points out into space), so some adjustment of the distance between the points may be necessary. After the calculation itself is complete, the tool asks for a file name and location to save a text file with the output data.

We then opened the text file created in Excel and merged multiple branches and segments together. In this text file, the D_theta column in the output is the angle of impingement calculated over the interval you chose (5m). Here, we calculated the angle of impingement values for other ruler lengths (multiples of 5), by using the theta values given for the points (which are 5m apart) and finding the absolute values of the change between points.

We then imported the data back into ArcMap using the Add XY Data tool in order to visually check the calculation and qualitatively identify which ruler length is the most effective. We found that the most helpful display was to use Quantities – graduated colors and classify the data into 3 groups: 0 – 0.1, 0.1 – 0.5, and > 0.5.

Note: For *SP* and angle of impingement, we buffered the point data and then converted the buffer layers to rasters. This will created files that we could Sample and export to a single Excel file, with all the analyses compiled in one location.

Delineating Bluffs

We calculated relief over a moving window in the watershed, and then applied a threshold to identify bluffs with greater than 2m of relief. In order to do this, we used the Focal Statistics tool in Spatial Analyst, with the 3-meter conditioned DEM as the input, with a 4 cell by 4 cell square window, and the Range statistic. Then we used the Greater Than tool (Spatial Analyst) to distinguish between areas with more than 2m of relief and less than 2m of relief. In order to only identify areas with greater than 2m of relief, we used the Con tool.

We are only interested in bluffs that are adjacent to the stream itself. In order to identify bluffs adjacent to the stream, we buffered the stream centerline, and then eliminated all of the bluffs that were not within that buffer. First we created a 7m buffer of the stream centerline. Next we used the Clip function under Raster Processing in the Data Management Toolbox to clip the output from the Con tool using the 7m stream buffer as the Output Extent. This only works if you check the box that says "Use input features for clipping geometry". The output of this analysis is a raster file that includes only bluffs with relief greater than 2m, which are within 7m of the stream centerline. This raster can then be converted to a polygon using the Raster to Feature tool.

Next, we identified which of the predpts were adjacent to a bluff. We used Select by Location, choosing features from the predpts file, with the Bluff polygon file as the source layer. We used the "within a certain distance" spatial selection method, with a distance of 7m. This selects all predpts within 7m of a bluff. The selection can then be exported to a new shapefile that only contains predpts within 7m of a bluff. We then buffered these points, converted it to a raster, and sampled it to produce a binomial dataset indicating which points are adjacent to bluffs. This was then compiled in an Excel file with the *SP* and angle of impingement analyses.

Soils

We used the SSURGO soils database to extract the K factor (soil erodibility) from the Revised Universal Soil Loss Equation for the watershed. To do this, we first downloaded and installed the Soil Data Viewer (publicly available at http://soils.usda.gov/sdv/download.html). The Soil Data Viewer allows the user to choose data from the SSURGO database and display it in ArcMap, and provides options for how to display the data. After adding the SSURGO data (clipped to the watershed of interest) to ArcMap, we used the Soil Data Viewer to display K factor - whole soil (Under Soil Erosion Factors) data for the watershed. Under Rating Options, we chose to the dominant component for all layers. We exported the map produced to a new shapefile, which we then converted to a raster. In order to do that we first created a new field in the attribute table, in which we used to Field Calculator to turn the K factor values into integers: " [KfactRF] * 100 ". Next, we used Polygon to Raster (Conversion Tools) to convert the shapefile to a raster, using the new field we created as the Field. Under Environments, we chose the DEM for the Processing Extent, Snap Raster, and for Cell Size. The output of this analysis was a raster that we used to sample the K Factor data at our predpts.

Bedrock Exposure

We used the Feature Analyst extension to map bedrock exposure. We do not provide detailed methods for mapping bedrock exposure remotely here because the method was not straightforward in our study. More time and effort should be put towards further work mapping bedrock exposure remotely. If bedrock exposure data are available, vector files can be converted to raster datasets and sampled to provide bedrock exposure data in the following steps.

Analysis of Predictors in Excel

We used the raster layers produced in the above analyses to sample at the predpts and extract data for further analysis in Excel.

B. Modified Bank Erosion Hazard Data Sheet and Calculation

Modified BEHI Surveys were conducted for this study. Figure A1 shows the field sheet that was used to collect data in the field. The following attributes were collected or calculated for each bank (left and right) at each BEHI site:

- Bank Height / Bankfull Height Ratio. We measured bank height as the height of the bank from the average depth. We used bankfull indicators such as bent vegetation and bankfull benches to determine bankfull height.
- Root Depth, given as the average root depth as a percent of bankfull height.
- Root Density is the average root density by volume for the entire bank.
- Percent Cover is the average percent surface protection above bankfull height.
- Bank Angle is the angle of the bank, measured above bankfull height.
- Valley Confinement is given a score based on a valley wall that is presently interacting with the stream (3), a valley wall within the active floodplain but not interacting with the stream (2), or no valley within the active floodplain.

- Valley Wall Height / Bankfull Height. If a valley wall was presently interacting with the stream, the site was given a score for the valley wall height / bankfull height ratio.

Each of the above attributes has an associated score based on the measurements observed (shown in Figure A1). These scores were then totaled to calculate the BEHI score for each bank at each site. The maximum score for each site is the score that was used in the regressions in Figure 13.

River: Site #: Date:

Bank Height		Bankfull Height	Surface Protection		Root Dept (% of BFH)		Root Density (%)		Bank Angle (%)		Valley Wall Height	
Left	Right		Left	Right	Left	Right	Left	Right	Left	Right	Left	Right
											0	0

						Average
BF Width						
	downstream (higher elev)		upstream (smaller elev)		Total Change	
Distance					0	
Stadia Rod Elevation					0	

Slope: radians degrees

Valley Walls	Left	Right
Distance top:		
Distance Bottom		
elev. Top		
elev. Bottom		

BEHI Scores	Very low	Low	Moderate	High	Very high	Extreme	Value L	Value R	Score L	Score R
BH/BFH	1.0-1.1	1.11-1.19	1.2-1.5	1.6-2.0	2.1-2.8	>2.8				
	1.45	**2.95**	**4.95**	**6.95**	**8.5**	**10**				
Root	90-100	50-89	30-49	15-29	5-14	< 5				
depth	**1.45**	**2.95**	**4.95**	**6.95**	**8.5**	**10**				
Root	80-100	55-79	30-54	15-29	5-14	< 5				
density	**1.45**	**2.95**	**4.95**	**6.95**	**8.5**	**10**				
Cover	80-100	55-79	30-54	15-29	10-14	< 10				
	1.45	**2.95**	**4.95**	**6.95**	**8.5**	**10**				
Bank	0-20	21-60	61-80	81-90	91-119	> 119				
angle	**1.45**	**2.95**	**4.95**	**6.95**	**8.5**	**10**				
valley	**1**		**2**			**3**				
confinement	**1.45**		**4.95**			**10**				
VWH/BFH	1.0-1.1	1.11-1.19	1.2-1.5	1.6-2.0	2.1-2.8	>2.8				
	1.45	**2.95**	**4.95**	**6.95**	**8.5**	**10**				

Only Add VWH/BFH if Valley Wall is interacting with Stream (# 3)

TotalScore 0 0

Category

Valley Walls	LB	RB
valley confinement		
valley wall height	0	0
Terraces	LB	RB
yes or no?		
height?		

Valley Confinement

1 No valley/not within floodplain
2 Valley wall in floodplain
3 Valley wall interacting with stream

Vegetation:

Stream type and substrate for banks:

substrate

erosion

Figure A1. Data sheet used to collect BEHI survey data in the Field. Chart labeled BEHI Scores shows the score values for a given attribute measurement. Those scores are then totaled to calculate the BEHI score for a given bank at a given site.